Analysis and Optimization of MAC Protocols for Wireless Networks

by

Feng Shu

Submitted in total fulfilment of
the requirements for the degree of

Doctor of Philosophy

Department of Electrical and Electronic Engineering
The University of Melbourne
Australia

June, 2007

Produced on acid-free paper

Abstract

Analysis and Optimization of MAC Protocols for Wireless Networks

by **Feng Shu**

Emerging wireless technologies target a wide range of new applications that cannot be easily supported by legacy wireless networks. An important class of such applications is high bandwidth multimedia services. To cater for the diverse requirements of multimedia services, the data rates and complexity of supporting wireless technologies are being significantly increased. On the other hand, low-rate, low-power data collection applications have been predicted to have a critical impact on our understanding of the physical world. The technologies of the wireless networks to support these low-rate applications are being simplified as much as possible to meet the stringent requirement of low energy consumption.

Medium access control (MAC) plays a vital role in satisfying the varied quality of service (QoS) requirements in wireless networks. Many MAC solutions have been proposed for these networks, and performance evaluation, optimization and enhancement of these MAC protocols is needed. In this thesis, we focus on the analysis and optimization of MAC protocols for some recently emerged wireless technologies targeted at low-rate and multimedia applications.

Firstly, we develop analytical models for the recently ratified IEEE 802.15.4 standard, and these models provide useful insights on the dynamic behaviors and optimized performance of the standard under various system parameters and traffic conditions.

Secondly, we propose a new energy optimization framework to choose optimal duty cycles for wireless sensor networks where energy consumption is of primary concern. Our optimization algorithms interact with the underlying MAC protocol and energy models, and minimize the expectation of the overall energy consumption per unit time. We then evaluate a simple "selected and transmit" MAC scheme and

the IEEE 802.15.4 MAC under the energy optimization framework.

Finally, we propose a simple yet efficient MAC protocol for wireless multimedia cellular networks which support a wide range of services (e.g., voice calls, video/audio streaming, video-conferencing, multimedia messaging service, *etc.*). Our MAC protocol is designed to meet diverse QoS requirements specified in terms of transmission rate, delay bound and maximum tolerable bit error rate. The proposed protocol uses a joint packet reservation and packet scheduling mechanism with optimal channel access to accommodate multimedia traffic types.

This is to certify that

(i) the thesis comprises only my original work,

(ii) due acknowledgement has been made in the text to all other material used,

(iii) the thesis is less than 100,000 words in length, exclusive of table, maps, bibliographies, appendices and footnotes.

Signature_____

Date_____

Acknowledgments

I would like to acknowledge the help and support of many people during my PhD study. Firstly, I would like to thank my parents and my dear wife Dr. Wei Chen. It is their unstinting love that makes me become an optimistic and persevering person.

I feel grateful for the constant and valuable support that I have received from my supervisors and friends, Professor Moshe Zukerman and Dr. Taka Sakurai. It was their sincere encouragement and friendship that made the past three years a fruitful and unforgettable time to me.

I also would like to thank the University of Melbourne to provide me financial supports through MIFRS for tuition fee and the PORES scholarship for my post-graduate visit to the University of Stuttgart, Germany. I also appreciate that the Victoria Research Laboratory, National ICT Australia (NICTA) Ltd., has supported my living allowance and many domestic and overseas conference trips.

Thanks also go to Dr. Hai L. Vu, Dr. Gangxiang Shen, Dr. Iradj Oveysi, Dr. Mansoor Shafi, Dr. Lachlan Andrew, Professor Stephen Hanly, Professor Siew Chee Kheong, Professor Marcel Neuts, and Mr. Marc Necker for many useful discussions, and Professor King-Tim Ko and Professor Eric Wing-Ming Wong for their assistance to organize research presentations for me at the City University of Hong Kong. A special thank goes to Professor Paul J. Kühn for inviting me to visit IKR at the University of Stuttgart and sharing with me his vision about the development of telecommunications.

As a NICTA student, I have spent all my three years of PhD candidature at the ARC Special Research Center for Ultra-Broadband Information Networks (CUBIN). I would like to thank everyone in CUBIN for creating such a friendly and stimulating research environment.

Contents

List of Figures

List of Tables

Acronyms

1G First Generation

2G Second Generation

3G Third Generation

3GPP Third Generation Partnership Project

ABR Available Bit Rate

AMPS American Mobile Phone System

BEB Binary Exponential Backoff

BER Bit Error Rate

BF Beacon Frame

BI Beacon Interval

BS Base Station

BTMA Busy Tone Multiple Access

CA Contention Access

CAP Contention Access Period

CBR Constant Bit Rate

CCA Clear Channel Assessment

CDMA Code Division Multiple Access

CF Contention Free

CFP Contention Free Period

C-PRMA Centralized PRMA

CSMA Carrier Sense Multiple Access

CSMA-CA Carrier Sense Multiple Access with Collision Avoidance

CSMA-CD Carrier Sense Multiple Access with Collision Detection

CSMA-RI Carrier Sense Multiple Access with Reservations by Interruptions

CTS Clear-To-Send

DBTMA Dual Busy Tone Multiple Access

DCF Distributed Coordination Function

DMAC Data Gathering Medium Access Control

DSMA Digital Sense Multiple Access

EDGE Enhanced Data Rates for GSM Evolution

FDMA Frequency Division Multiple Access

FFD Full Function Device

FRMA Frame Reservation Multiple Access

GSM Global System for Mobile Communications

HSPA High-speed Packet Access

JPPS Joint PRMA and Packet Scheduling

LR-WPAN Low-rate Wireless Personal Area Network

MAC Medium Access Control

MAI Multiple Access Interference

MC Multicode

MDPRMA-BB Multidimensional PRMA with Prioritized Bayesian Broadcast

MEMS Microelectromechanical Systems

MIMO Multiple-input Multiple-output

NACK Non-acknowlegement

NIP Node Idle Period

NSP Node Sleep Period

OFDM Orthogonal Frequency Division Multiplexing

O-QPSK Offset Quadrature Phase Shift Keying

OSD One Shot Data

OSI Open Systems Interconnection

OVSF Orthogonal Variable Spreading Factor

PACT Power Aware Clustered TDMA

PAN Personal Area Network

PHY Physical

PN Pseudorandom Noise

PRMA Packet Reservation Multiple Access

QoS Quality of Service

RFD Reduced Function Device

RI-BTMA Receiver-initiated BTMA

RTS Request-To-Send

SD Superframe Duration

SMACS Self-organization Medium Access Control for Sensor Networks

SMS Short Messaging Service

STEM Sparse Topology and Energy Management

TD-CDMA Time Division CDMA

TDD Time-division Duplex

TDMA Time Division Multiple Access

TRMAC Traffic-adaptive MAC

UBR Unspecified Bit Rate

UTRA UMTS Terrestrial Radio Access

UMTS Universal Mobile Telecommunication System

VBR Variable Bit Rate

WAN Wide Area Network

WISPER Wireless Multimedia Access Control Protocol with BER Scheduling

WLAN Wireless Local Area Network

WMAN Wireless Metropolitan Area Network

WPAN Wireless Personal Area Network

WSN Wireless Sensor Network

WWAN Wireless Wide Area Network

UWB Ultra-wideband

VoIP voice over Internet Protocol

Z-MAC Zebra MAC

Chapter 1

Introduction

1.1 Overview

The last decade has witnessed an explosive growth in wireless networking technologies. The advances in wireless technologies are driven by developments in physical layer techniques such as multiple antennas (e.g., multiple-input multiple-output (MIMO) [8]), advanced modulation techniques (e.g., orthogonal frequency-division multiplexing (OFDM) [9]), highly efficient coding schemes (e.g., Turbo codes [10]), and so on. The overall system performance of a wireless network, however, is not only determined by physical layer technologies but also the upper layer communication protocols such as medium access control (MAC).

The radio channel is a broadcast medium by nature. When multiple devices attempt to transmit simultaneously on a single wireless channel, data can be garbled and then discarded, resulting in wastage of the scarce spectrum resources and the potential to make the quality of service (QoS) unacceptable. As a part of the data link layer, the MAC sublayer is located between the physical and networking layers in the Open Systems Interconnection (OSI) reference model [11] (see Figure 1.1). MAC protocols that allow devices to deliver data in an orderly and efficient manner are one of the key factors in determining network capacity and are thus of paramount importance. In this thesis, we focus on MAC protocols for wireless networks.

Substantial research efforts have been directed to MAC protocols in the past forty years. The existing MAC protocols can be classified into the following five categories [12].

1. Fixed assignment protocols, in which a fixed portion of channel resource is allocated to each user. Examples of fixed assignment protocols include time

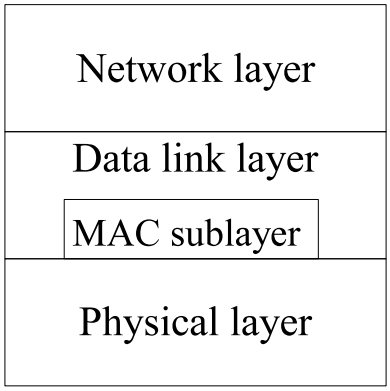

Figure 1.1: MAC in the OSI protocol stack.

division multiple access (TDMA), frequency division multiple access (FDMA) and code division multiple access (CDMA).

2. Random access protocols, in which devices contend for the use of the channel, allowing the possibility of collisions. Protocols like ALOHA [13], carrier sense multiple access (CSMA) [14], and group random access [15] fall into this category.

3. Centrally controlled demand assignment protocols, where explicit control information is exchanged to meet user capacity demands. Typical examples of this type include polling [16] and split-channel reservation multiple access (SRMA) [17].

4. Demand assignment protocols with distributed control, in which channel capacity is allocated to users in a distributed manner. Examples of this category include reservation ALOHA [18].

5. Adaptive strategies and mixed modes, which include the hybrid access methods and those that are adaptive to varying needs (e.g., [19]).

As we will describe later in this section, this thesis is concerned with certain wireless technologies that employ MAC protocols belonging to categories 2 and 3. To help understand the context of these wireless technologies, it will be useful to introduce a classification of wireless networks according to geographical coverage area. The first type of wireless networks are wireless wide area networks (WWANs)

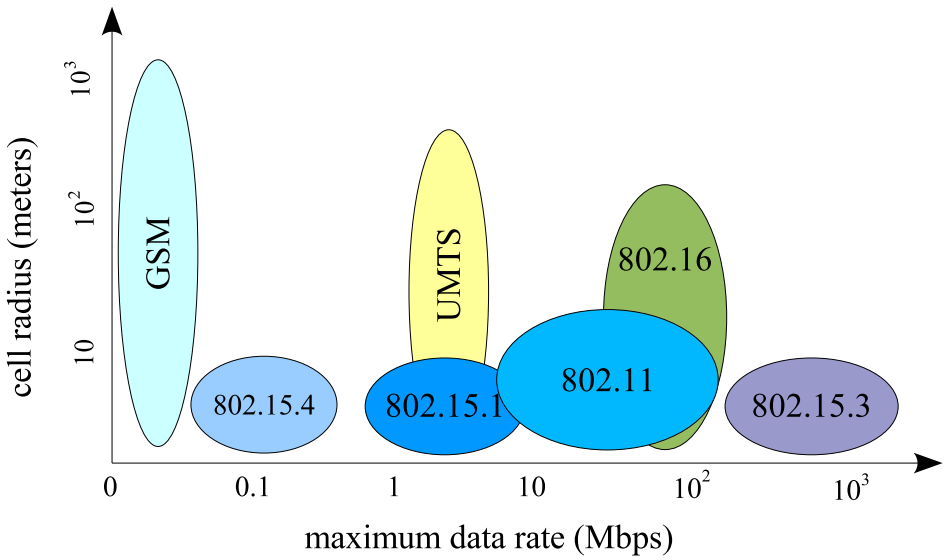

Figure 1.2: Comparison of different wireless technologies in terms of maximum achievable data rates and cell coverage.

which typically span a very large area such as a state, a country or even a continent. Examples of WWANs include mobile cellular networks and satellite networks.

In recent years, wireless metropolitan area networks (WMANs) have been proposed to provide broadband wireless access over long distances ranging from several blocks of buildings to entire cities. Such networks are anticipated as a promising technology to become an alternative for the "last-mile" connectivity for broadband networks [20]. The standards that have been developed for WMANs include the IEEE 802.16 [21, 22] and the ETSI HiperMAN [23].

In contrast to WWANs and WMANs, wireless local area networks (WLANs) supply network access to a group of users in close proximity such as in a home or an office building. Various WLAN standards have been developed [24–27]. Among those standards, the IEEE 802.11 family (also known as WiFi) that provides data rates of up to 54 Mb/s has achieved significant market success.

The last type of wireless networks are wireless personal area networks (WPANs) which typically operate within the radio range of a few meters [28]. The IEEE 802.15 working group [29] focuses on the development of WPAN standards including IEEE 802.15.1 which forms the basis for Bluetooth [30, 31], IEEE 802.15.3 for high data rate ultra-wideband (UWB) networks, and IEEE 802.15.4 for low-rate WPANs (LR-

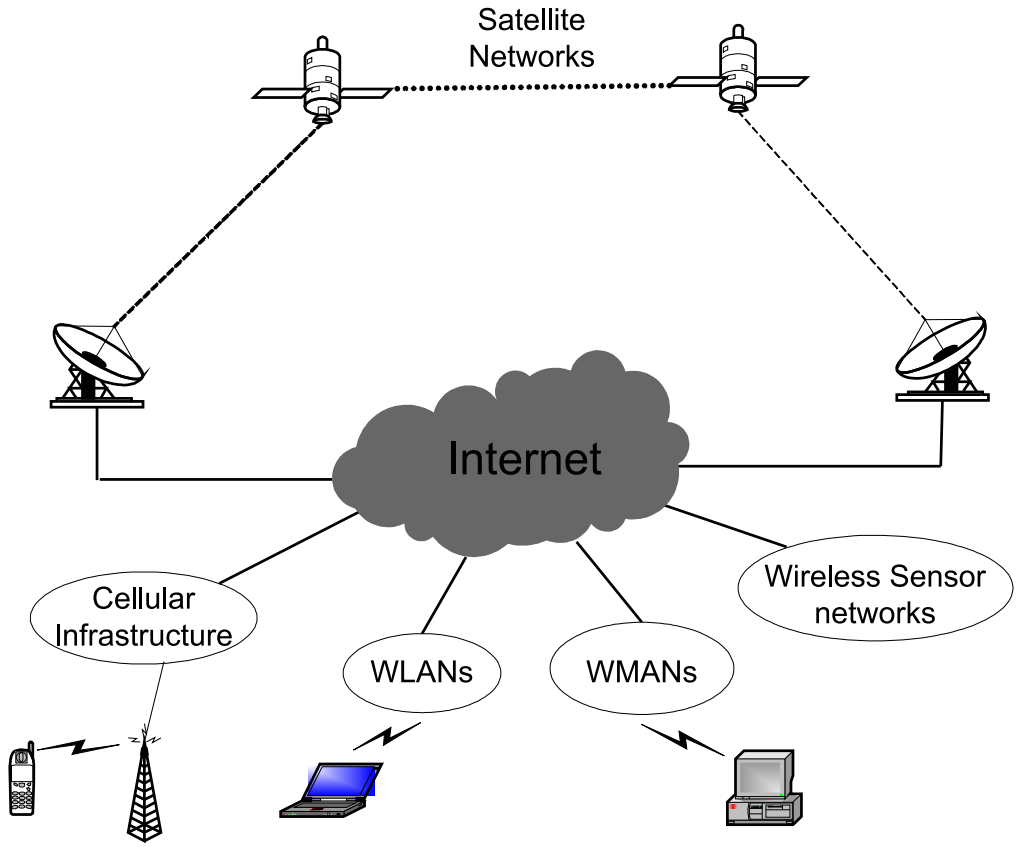

Figure 1.3: An integrated global wireless network.

WPANs) including wireless sensor networks.

Figure 1.2 illustrates a comparison of various wireless technologies according to the maximum achievable data rates and the cell radii. In a future integrated global wireless network, as depicted in Figure 1.3, the different wireless networks would seamlessly be interconnected with the Internet and other fixed networks, providing truly ubiquitous network access.

In this thesis, the performance of MAC protocols for certain wireless sensor and cellular networks is investigated. We conduct performance analysis, optimization and enhancement of MAC protocols using a variety of methodologies including applied probability theory, optimization theory, asymptotic analysis and computer simulation studies.

One of the objectives of the thesis is to investigate the random access mechanism included in the IEEE 802.15.4 MAC. The IEEE 802.15.4 standard has been recently ratified in response to the rapid development of LR-WPANs. There are a number

of salient energy saving features proposed in the IEEE 802.15.4 MAC and it is important to understand its performance under various network scenarios. We first analyze a generalized CSMA with collision avoidance (CSMA-CA) protocol under saturation and then extend our analysis to nonsaturation traffic conditions. Analytical models based on applied probability and fixed point theories are developed to conduct throughput analysis. We also optimize system parameters and conduct asymptotic analysis under saturation conditions. Furthermore, we present a packet delivery analysis of the IEEE 802.15.4 MAC using a nonstationary Markov chain approach under a realistic one-shot data traffic scenario.

We also develop energy optimization techniques for general wireless sensor networks (WSNs). A multitude of applications that require only low-data-rate and short-range communications have been identified for WSNs. These applications include environmental and industrial monitoring, security surveillance, home automation, military applications, and so on [32,33]. Unlike most of the traditional wireless networks where high bandwidth utilization and low transmission delay are usually the most important performance metrics, WSNs are deployed and desirably exist for as long as possible without requiring replacement of the usually battery-powered sensors. Therefore, energy efficiency has become the primary challenge in the MAC design. In this thesis, we propose a new framework to minimize energy consumption by optimally choosing duty cycles for WSNs. We also consider a simple MAC protocol called "selected and transmit" (S&T), in which a sensor node chooses a transmission slot uniformly in a sensor active period without using carrier sensing.

Finally, we propose a new centrally controlled demand assignment MAC protocol for wireless cellular networks. Mobile cellular networks, as one of the most important wireless technologies, provide subscribers "anywhere, anytime" access, and have had a profound influence on our daily lives. Compared to the existing second generation (2G) mobile networks, the third generation (3G) networks (e.g., the universal mobile telecommunication system (UMTS) [34]) offer much higher data rates up to 2 Mb/s. In addition to the traditional voice calls, 3G cellular systems support a wider range of services [35] such as video/audio streaming, video-conferencing, multimedia messaging service, *etc.* The existing voice-based MAC protocols would

perform unsatisfactorily in a multimedia network environment where diverse QoS requirements such as transmission rate, delay bound and maximum tolerable bit error rate (BER) need to be satisfied for various traffic types. Therefore, a highly flexible and efficient MAC protocol is needed for future multimedia cellular networks. We address these needs by developing a joint packet reservation and packet scheduling MAC protocol with optimal channel access to accommodate multimedia traffic types. Computer simulation is used for performance comparisons between our proposed scheme and other existing protocols.

The remainder of this chapter is organized as follows. In Section 1.2, we define the basic network concepts and the research scope. The thesis structure is then presented in Section 1.3. Finally, we summarize the main contributions of the thesis in Section 1.4.

1.2 Concepts and Scope of Research

A wireless network, in its simplest form, is a collection of devices with wireless adapters that provide information exchange by using electromagnetic waves. Radio, microwave, infrared and visible light can be used for wireless communication [11, Chapter 2]. Throughout this thesis, we restrict our attention to radio wireless networks, and "radio" and "wireless" are used interchangeably.

The wireless devices are referred to as *nodes*, and the information that is exchanged between nodes are called *messages*. A message is represented by a finite string of bits. A *packet* is an assembled data unit which includes control bits such as source and destination addresses used to facilitate the delivery through the network. A long message can be fragmented into many small packets for transmission. Here, we use "message" and "packet" interchangeably. When a node has one or more packets in its buffer to be transmitted, we call this node a *backlogged* node.

The way in which the nodes are interconnected is referred to as *network topology*. Wireless networks are typically laid out in *centralized* (also known as *star*) and *ad hoc* topologies [36, Chapter 11]. Ad hoc wireless networks can be further divided into two categories. In a fully connected network, each node can communicate

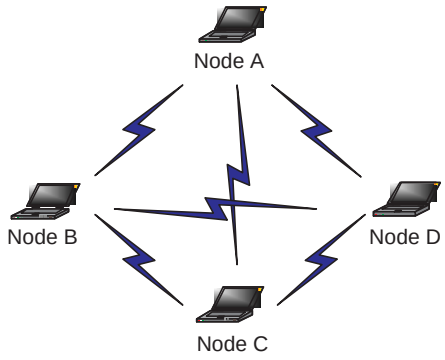

(a) Ad hoc networks: fully connected.

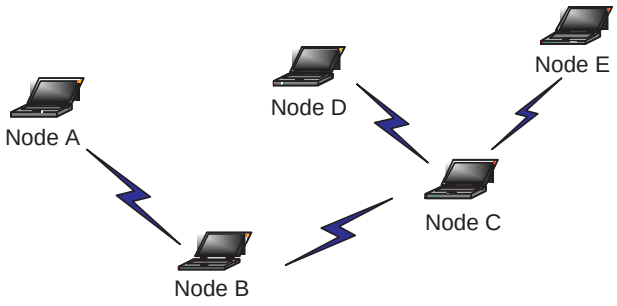

(b) Ad hoc networks: multihop.

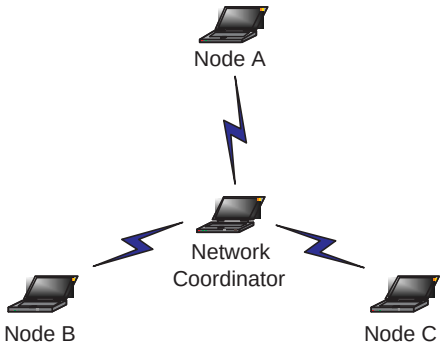

(c) Centralized networks.

Figure 1.4: Wireless Network Topologies.

directly with any other node in the network, while in multi-hop networks, a source node can communicate with a destination node via multiple intermediate nodes. Figures 1.4(a) and 1.4(b) illustrate a fully connected ad hoc network and a multihop network, respectively. In centralized networks, as depicted in Figure 1.4(c), one node is appointed as the *network coordinator* or *base station*, and it centrally controls, among other things, the channel access of the other nodes in the network. Any communication between one node to another goes through the network coordinator. In centralized networks, data transmission from nodes to the network coordinator is termed *uplink* transmission, and data transmission from the network coordinator to nodes is called *downlink* transmission. We focus on the MAC performance on the uplink of centralized wireless networks in this thesis.

Researchers have developed technologies that exploit multiple frequency chan-

nels [37] and radio transceivers with directional antennas [38] to increase channel capacity. However, the use of multiple channels and directional antennas may not always be appropriate due to reasons of additional cost and complexity. Unless stated otherwise, we assume a single radio channel to allocate resources among competing nodes that are equipped with omnidirectional antennas. Under the above assumptions, if only one node attempts to transmit a packet on the channel and the packet is successfully received by the receiver node, this transmission is called a *success*. If two or more nodes transmit at the same time, their packets become interference noise to each other, and we call this transmission a *collision*.

Under the *capture effect*, it is possible that a packet can be successfully retrieved even when it is involved in a collision [39]. This is because the received packets may arrive with different power levels due to the *near-far* effect [40], and the packet with higher power level could survive the collision. The capture effect is not assumed throughout this thesis,.

1.3 Thesis Outline

In this section, we introduce the thesis structure. This thesis consists of six chapters. **Chapter 1: Introduction** overviews the recent development of wireless technologies, defines the basic wireless network concepts and the scope of research, and gives an introduction to the thesis.

Chapter 2: Analysis of an Energy Conserving CSMA-CA Protocol gives a literature survey of CSMA protocols, and then focuses on a generalized CSMA-CA protocol that captures the most important energy conserving features of the IEEE 802.15.4 MAC. We analyze the protocol under both saturation and nonsaturation traffic conditions.

Chapter 3: Analysis of IEEE 802.15.4 Packet Delivery introduces the IEEE 802.15.4 MAC protocol in detail and reviews the related body of literature on performance evaluation of the standard. We then propose a non-stationary three-dimensional Markov chain model to analyze the packet delivery performance of the

IEEE 802.15.4 MAC under a realistic one-shot data traffic scenario.

Chapter 4: Energy Optimization for Wireless Sensor Networks emphasizes the importance of energy efficiency in wireless sensor networks and then introduces a wide range of energy saving techniques used in existing sensor network MAC protocols. We then consider a simple S&T MAC scheme, and present an energy optimization framework for general wireless sensor networks.

Chapter 5: Joint PRMA and Packet Scheduling for Multimedia Cellular Networks overviews the evolution of mobile cellular systems in the last thirty years, and introduces an efficient MAC protocol for wireless multimedia cellular networks where a mixture of traffic sources such as voice, video, audio and data exists.

Chapter 6: Conclusion summarizes the main results of this thesis.

1.4 Contributions

This thesis has four main contributions. Firstly, we develop a new analytical model for performance analysis of an energy conserving CSMA-CA protocol under both saturation and nonsaturation traffic conditions. Our new model is based on a new analytical perspective involving a one-dimensional Markov chain and a simple fixed-point formulation. Although we focus on throughput analyses, our analytic framework is flexible enough to yield other performance metrics such as packet delay statistics.

Secondly, we propose a new analytical approach that is based on a non-stationary Markov chain to accurately predict the packet delivery statistics of the IEEE 802.15.4 MAC protocol. We then evaluate the MAC layer of the standard under a realistic bursty traffic condition that would appear in many IEEE 802.15.4 networks with spatially correlated nodes. Furthermore, an alternative backoff strategy with a large initial backoff window and decreasing backoff windows for subsequent backoffs is considered to improve the packet delivery performance of the IEEE 802.15.4 MAC.

Thirdly, we introduce a new energy optimization framework which chooses op-

timal duty cycles for sensor networks while at the same time, meeting a range of QoS constraints. Our optimization algorithms interact with the underlying MAC protocol and energy models, and minimize the expectation of the overall energy consumption per unit time. The S&T and IEEE 802.15.4 MAC schemes are then evaluated under the energy optimization framework.

Finally, we propose a simple yet efficient MAC solution for uplink transmissions in multimedia cellular CDMA networks. The techniques of packet reservation and packet scheduling are combined to maximize the system throughput, and minimize computational complexity and signaling overhead at the same time. In the proposed MAC protocol, real-time and non-real-time traffic are given different priorities, and an optimal channel access method is proposed for active terminals to send transmission requests through channel contention.

In the following, we list our research papers that present the contributions of this thesis.

Research Papers

1. F. Shu, T. Sakurai, M. Zukerman and H. Vu, "Packet Loss Analysis of the IEEE 802.15.4 MAC without Acknowledgements", *IEEE Communications Letters*, vol. 11, no. 1, January, 2007, pp. 79-81.

2. F. Shu, T. Sakurai, "Analysis of an Energy Conserving CSMA-CA", In Proceedings of *IEEE Global Communications Conference (GLOBECOM)*, 2007.

3. F. Shu, T. Sakurai, H. Vu and M. Zukerman, "A Framework to Minimize Energy Consumption for Wireless Sensor Networks", In Proceedings of *IEEE Global Communications Conference (GLOBECOM)*, 2006, San Francisco, California.

4. F. Shu, T. Sakurai, H. Vu and M. Zukerman, "Does a WSN MAC Based on Uniform Access without Re-attempts Have Merits?", In Proceeding of *IEEE Region 10 International Conference (TENCON)*, 2006, Hong Kong.

5. F. Shu, T. Sakurai, H. Vu and M. Zukerman, "Optimizing the IEEE 802.15.4

MAC", In Proceeding of *IEEE Region 10 International Conference (TENCON)*, 2006, Hong Kong.

6. F. Shu, T. Sakurai, M. Zukerman and M. Shafi, "A Joint PRMA and Packet Scheduling MAC Protocol for Multimedia Wideband CDMA Cellular Networks" In Proceedings of *IEEE International Symposium on Personal Indoor and Mobile Radio Communications (PIMRC)*, vol. 4, pp. 2216-2220, Sept., 2005, Berlin, Germany.

Chapter 2

Analysis of an Energy Conserving CSMA-CA Protocol

2.1 Introduction

The ALOHA protocol [13,41] appears to have been one of the first MAC mechanisms for radio broadcast communications [14]. Developed by Abramson *et al.* at the University of Hawaii in the early 1970's, the protocol was used as a means of random access for a wireless single-hop network, which interconnected a host computer with other nodes located on different islands. In this original ALOHA protocol (also known as pure ALOHA), a node is allowed to immediately transmit whenever it has a backlogged packet. The pure ALOHA protocol can be enhanced by introduing slots, where each slot equals a packet transmission time. In this slotted ALOHA protocol, when a packet is generated, it can only be transmitted at the boundary of the next time slot. It has been shown that the maximum channel throughput of the slotted ALOHA is double that of its predecessor [42].

The ALOHA protocols do not exploit the information of channel activity, and nodes transmit packets independently of one another. By listening to the channel before transmission, the data throughput may be improved. Carrier sense multiple access (CSMA) mechanisms are a class of MAC protocols for contention-based data transmission. In CSMA protocols, nodes monitor the channel status and act accordingly before they commence transmission. There exist many CSMA variants proposed for various system environments. In the context of wireless channels, CSMA with collision avoidance (CSMA-CA) protocols are often used, and they have been widely adopted in many network technologies, notably IEEE 802.11 [25], AppleTalk [43] and more recently, IEEE 802.15.4 [1].

One of the major challenges for wireless communication is energy efficiency, since wireless devices usually have limited power. In wireless networks with small-scale battery-powered nodes, such as sensor networks, it becomes overwhelmingly important to minimize energy consumption. Many energy conserving algorithms have been proposed in the MAC sublayer. In the recently ratified IEEE 802.15.4 standard [1], for instance, the CSMA-CA protocol incorporates some new energy conserving features that particularly address the energy efficiency issue.

In [44] and [45], the authors developed models to analyze the saturation throughput of the IEEE 802.15.4 CSMA-CA. In this chapter, we conduct accurate performance analysis of a generalized IEEE 802.15.4 CSMA-CA under a much wider range of scenarios. We capture the most important aspects of the energy conserving CSMA-CA mechanism of the IEEE 802.15.4 MAC and present a new analytical model for both saturation and nonsaturation traffic conditions. Our approach distinguishes itself from other models in that it is based on a new analytical perspective involving a simple one-dimensional Markov chain. Furthermore, we demonstrate that our model can be readily extended to nonsaturated traffic without compromising accuracy. The accuracy of our analysis is verified with simulation. While we focus on throughput as the performance metric, our analytic framework is flexible enough to yield other performance metrics such as packet delay statistics.

The remainder of this chapter is organized as follows. In Section 2.2, we present an overview of the CSMA variants and analytical techniques to analyze CSMA protocols. In Section 2.3, the new features of the energy conserving CSMA-CA are briefly described. Analytical results of the saturated and nonsaturation traffic conditions are presented in Section 2.4 and 2.5, respectively. We present numerical results and discussion in Section 2.6. Finally, we summarize the work in Section 2.7.

2.2 The CSMA Protocol Family

2.2.1 Basic CSMA Variants

Unlike ALOHA, CSMA protocols allow nodes to listen to the channel before they transmit. The behaviors following the channel listening depend on the type of CSMA protocol. In this subsection, we introduce the three basic CSMA variants.

To start with, we introduce the simplest carrier sense protocol, in which a backlogged node continuously senses until the channel is sensed idle, and then immediately transmits a packet. If the transmitted packet suffers a collision, the node will wait a randomly chosen time period before it resumes channel sensing. Because a node will transmit with a probability of one as soon as the channel is idle, this protocol is named the *1*-persistent CSMA protocol.

In the less "greedy" p-persistent CSMA scheme, when the channel is found idle, a backlogged node transmits its packet with probability p; conversely, it defers the transmission to the next slot with probability $1-p$. After the deferral, if the channel in the next slot is still idle, it transmits the packet with probability p. This process repeats until the packet is sent. If the channel is busy, a backlogged node follows the procedures as in the *1*-persistent CSMA protocol, i.e., immediately sensing the channel again in the next slot. It is clear that *1*-persistent CSMA is a special case of p-persistent CSMA with $p = 1$.

The last basic CSMA variant is called nonpersistent CSMA. In this protocol, when the channel is found busy, instead of immediately sensing again, a node waits a random time period and then it restarts the process. As soon as the channel is found idle, the node immediately transmits the packet.

It has been demonstrated that the throughput performance of CSMA is significantly better than that of ALOHA [14]. For different CSMA variants, the persistent CSMA protocols typically outperform nonpersistent CSMA in throughput under low traffic load. At high traffic load levels, however, nonpersistent CSMA protocols tends to have superior performance. Comparable performance can also be achieved by persistent CSMA protocols with an appropriately chosen transmission probability p.

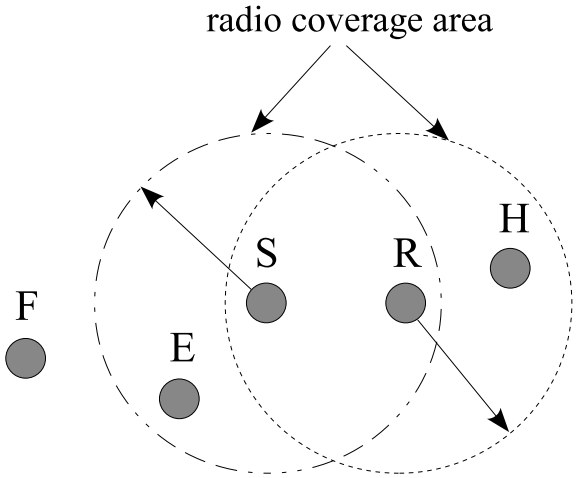

Figure 2.1: Hidden/exposed node problems.

The performance of CSMA can be seriously degraded by the so called hidden/exposed node problems of wireless networks [46, 47]. In the hidden node problem, a node is located in the radio range of the receiving node but out of the radio range of the sending node. In Figure 2.1, for instance, when node S is transmitting to node R, since H is outside of the radio range of S, it senses the medium to be idle. If node H starts transmitting to R, it will cause interference to the transmission of S. The exposed node problem, as discussed by Karn in [47], occurs when a node (e.g., node E in Figure 2.1) is located in the radio range of a sending node but not the receiving node, and thus it senses a busy channel and is falsely prevented from transmitting to other nodes (e.g., node F in Figure 2.1).

2.2.2 CSMA with Collision Detection

A further improvement of CSMA can be accomplished by using the information of channel activity when transmissions are ongoing. In CSMA with collision detection (CSMA-CD), nodes keep monitoring the channel while transmitting. As soon as a collision is detected, they immediately abort the current packet transmissions.

Prior to packet transmission, the operation of CSMA-CD is the same as that of CSMA. When a packet is being transmitted, a node continuously monitors the channel status by listening to the medium. If the received signal is different from what it sends, the node concludes that a collision has occurred, and immediately

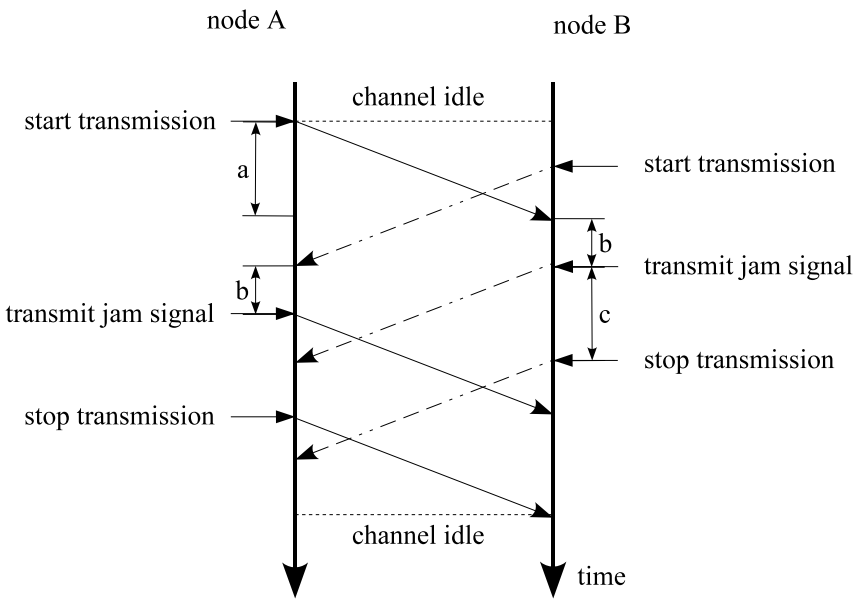

Figure 2.2: Time diagram for CSMA-CD, where a denotes the propagation delay, b denotes the time to detection a collision and c the duration of a jam signal.

stops transmitting the rest of the packet. After that, the node transmits a predefined jam signal to explicitly notify other nodes of the collision. A random backoff procedure is then initiated to schedule packet retransmission in future time slots.

Figure 2.2 illustrates the detailed operation of CSMA-CD. Suppose that node A detects a clear channel and commences a packet transmission. Node B can only detect the transmission after a seconds later due to propagation delay, so it also starts a transmission before it senses the signal of A. After the transmission, node B monitors the channel and eventually detects the collision after b seconds. It then transmits a jam signal of c seconds and aborts the transmission of the current packet.

The CSMA-CD mechanism is adopted in IEEE 802.3, which was developed for local area computer networks in the middle of the 1980s. The truncated binary exponential backoff (BEB) algorithm is the recommended random backoff algorithm in the IEEE 802.3 standard. In this algorithm, a backlogged node transmits the packet in the next available slot. If a collision occurs, it performs a random backoff, the length of which (measured in slots) is chosen from the range of $[0, 1]$. At the end of the backoff, the node transmits the packet in the next slot. If the retransmission ends up with a collision again, the node performs another random backoff with a

doubled backoff window size (i.e., the backoff length is chosen from the range of $[0, 3]$. In response to the ith collisions, the node backs off randomly in the range of $[0, 2^i - 1]$. After ten repeated collisions, the backoff window size remains at 2^{10} for future retransmissions. If a packet has not been successfully transmitted after 16 attempts, it is discarded.

2.2.3 CSMA with Collision Avoidance

As seen in CSMA-CD, collisions can be readily detected during ongoing packet transmissions in cable networks by sensing the voltage levels. It is however, very difficult to detect collisions in radio communications when packets are being sent. The reasons for the difficulty are two-fold. Firstly, the sending node's own radio signal dominates all other signals in its vicinity [36, Chapter 11, page 533], and thus it requires a full duplex radio to allow simultaneous transmission and reception, which increases the cost of the node significantly. Furthermore, the fundamental assumption that nodes can hear each other in the collision detection mechanism is not necessarily valid in wireless networks due to the hidden/exposed node problems. Therefore, CSMA-CD is usually inappropriate for wireless networks.

Instead, CSMA-CA is used on wireless channels. In a typical CSMA-CA protocol, a node first executes a random backoff during which channel sensing is applied to ensure that the channel is idle. At the end of the backoff, the node transmits the packet. If the destination node successfully receives the packet, it sends back a positive acknowledgement. If no acknowledgement is received within a specified time interval, the sending node assumes that a collision has occurred and performs a retransmission after another random backoff to avoid repeated collisions. In this way, collisions can be detected using acknowledgements.

The WLAN standard IEEE 802.11 specifies a CSMA-CA mechanism for contention-based channel access in the distributed coordination function (DCF) [25]. In the IEEE 802.11 CSMA-CA, a backlogged node starts with a random backoff and the backoff time is uniformly distributed in the range of $[0, CW - 1]$, where CW denotes the contention window. The contention window for the first attempt is initialized to be equal to the minimum contention window, W_{min}. The node performs channel

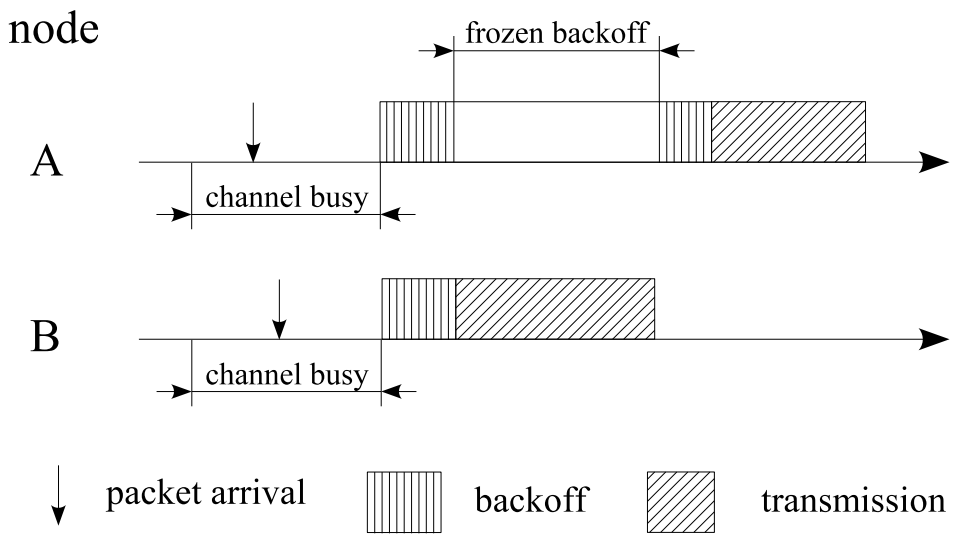

(a) Basic access method.

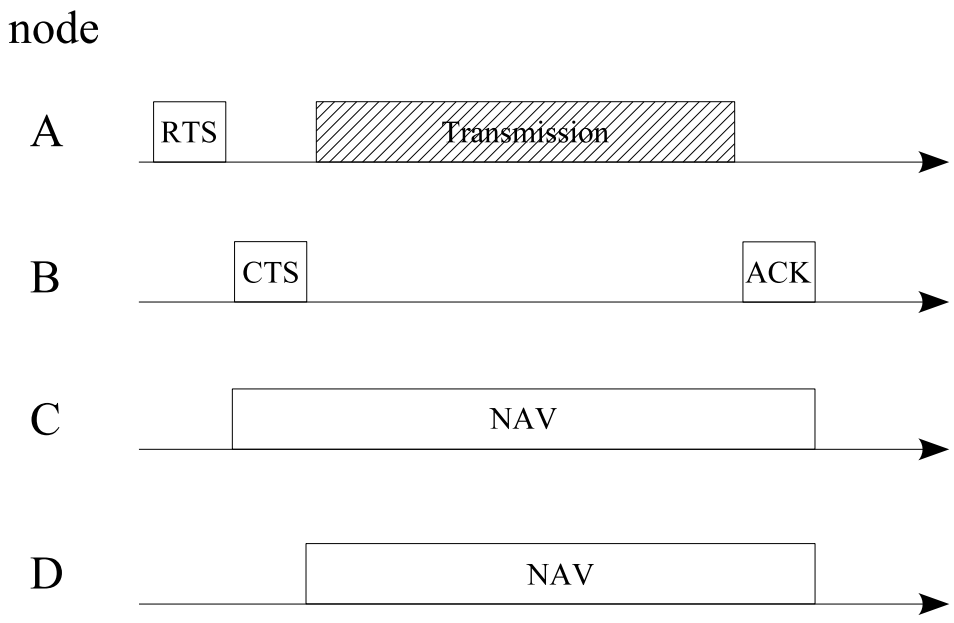

(b) RTS/CTS method. Node C hears the RTS packet and node D hears the CTS packet.

Figure 2.3: Access methods of IEEE 802.11 DCF.

sensing at the beginning of every slot, and its backoff time counter is decremented by one on every idle slot. Upon detecting busy slots, the backoff time counter is frozen and not reactivated until next idle slot. At the end of the backoff, the node transmits the packet. If two or more nodes transmit at the same time, a collision results. If a node is involved in a collision, it waits a random time using a similar BEB backoff strategy as in IEEE 802.3 and retransmits the packet later.

The scheme described above is based on a two-way handshaking and known as the basic access method of DCF. There is another access method called Request-To-Send/Clear-To-Send (RTS/CTS) access method which is based on a four-way handshaking mechanism. In the RTS/CTS access method, a node sends a short RTS message to the intended receiver node, and the receiver responds with a CTS message if the transmission request is granted. The transmission duration is included in the RTS/CTS packets. Thus, all other nodes that hear either the RTS or CTS packet are aware of the transmission. These nodes then update their network allocation vector (NAV) and defer their transmissions until the end of the transmission. Therefore, only the RTS packets are subject to contention, and they are transmitted using the backoff rules in the basic access method. The RTS/CTS scheme can alleviate the hidden terminal problem in wireless networks [48] and achieve a higher efficiency, especially for long data frames. Figure 2.3 illustrates the two access methods of the IEEE 802.11 DCF.

As mentioned in Section 2.1, the IEEE 802.15.4 includes a different CSMA-CA algorithm, which will be described in detail in Chapter 3. In this work, we capture the energy conserving features of the IEEE 802.15.4 CSMA-CA, and analyze a generalized energy conserving CSMA-CA mechanism under a wide range of network traffic conditions.

2.2.4 Reservation-based CSMA Variants

It is well-known that contention-based access methods, including CSMA, work well under light traffic load, but the system performance can degrade due to collisions under heavy traffic load. Reservation techniques can be used to enhance the performance of CSMA.

In [49], Chen and Li proposed a reservation CSMA-CD protocol which is a hybrid of CSMA-CD and the broadcast recognizing access method [50]. In this protocol, four system states (i.e., contention, collision, transmission and scheduling) are defined. Initially, the channel is in the contention state where each node can contend for transmission. A backlogged node, say node i, detects the channel to be idle and starts transmission. The subsequent state transitions depend on whether the transmission is a success. If node i is involved in a collision, the channel enters the collision state, and the colliding nodes stop transmitting and perform random backoffs. The channel then returns to the contention state at the end of the collision period. If node i transmits without collisions, the channel is in the transmission state. The channel then enters the scheduling state after the packet is successfully transmitted. In the scheduling state, every other node except node i is allocated a scheduling slot for transmission according to their identification numbers. The channel goes back to the contention state after the scheduling state is finished. The authors also considered a modified version of the above procedure, in which the channel switches to scheduling state after the collision state for collision resolution.

Foh and Zukerman [51] introduced a CSMA with reservations by interruptions (CSMA-RI) protocol to reduce collisions in CSMA-CD networks. In CSMA-RI, a backlogged node is allowed to interrupt a successful transmission to reserve capacity by broadcasting a predefined short signal. Upon detecting an interruption signal, the currently transmitting node immediately retransmits the small interrupted portion. If two or more nodes send interruption signals at the same time, a collision occurs and a collision resolution (e.g., truncated BEB) can be used to retransmit the interruption signals. It has been demonstrated that CSMA-RI always outperforms the CSMA-CD protocol [51].

2.2.5 CSMA with Control Channel

As mentioned earlier, collisions can be caused by the hidden node problem in radio networks, which leads to a deterioration in performance. Provided that there is a central node in the range of all other nodes in the network, the hidden node problem can be eliminated by using separate control channels. Such techniques have been

adopted in a few CSMA variants.

Tobagi and Kleinrock [46] proposed an approach called busy-tone multiple access (BTMA) where the total system bandwidth is divided into two channels. The first channel is called a message channel for transmitting data messages. The second channel is a busy-tone channel. As long as the central node senses signal on the incoming message channel, it broadcasts a sine wave which serves as a busy-tone signal on the busy-tone channel. Prior to transmissions, the other nodes can sense the busy-tone channel to determine the status of the message channel. The authors presented a detailed analysis of the nonpersistent BTMA scheme where BTMA is applied to nonpersistent CSMA.

In [52], Wu and Li developed the receiver-initiated BTMA (RI-BTMA) protocol for packet radio networks. As in BTMA, the total bandwidth is divided into two channels, one for data transmission and the other for busy tone. Packets in RI-BTMA include a preamble portion and a data portion. A backlogged node first senses the busy-tone channel. If the channel is busy, it waits a random time and tries again. If the channel is idle, it transmits the preamble on the data channel. If the receiver node successfully retrieves the preamble, it sends back a busy tone to acknowledge the reception. When the sending node receives the busy tone, it starts transmitting the data portion of the packet. While receiving data, the receiver node keeps sending busy tones. A Markov chain model was used in [52] to analyze the performance of RI-BTMA.

The digital-sense multiple access (DSMA) protocol is adopted in many full-duplex wireless data communication networks such as cellular digital packet data (CDPD) [53,54] and terrestrial trunked radio networks [55]. In such networks, uplink and downlink data are transmitted on separate frequency channels. The downlink transmission is based on a fixed allocated scheme (such as TDMA), and the uplink uses a contention-based DSMA protocol. In each downlink frame, the status of the uplink channel, indicated by a busy or idle flag, is piggybacked. A backlogged node senses the binary flag before transmission. If the channel is idle, it transmits the packet. If the channel is sensed busy, it waits a random time before sensing the channel again.

Protocol	Throughput
Pure ALOHA	$S = Ge^{-2G}$
Slotted ALOHA	$S = Ge^{-G}$
Slotted 1-persistent CSMA	$S = \frac{G(1+a=e^{-aG})e^{-G(1+a)}}{(1+a)(1-e^{-aG})+ae^{-G(1+a)}}$
Slotted nonpersistent CSMA	$S = \frac{aGe^{-aG}}{1-e^{-aG}+a}$
Slotted nonpersistent CSMA-CD	$S = \frac{GTe^{-G}}{TGe^{-G}+(1-e^{-G}-Ge^{-G})\gamma+2-e^{-G}}$

Table 2.1: Throughput expressions. Note a denotes the normalized propagation delay. In the throughput expression of the slotted nonpersistent CSMA-CD [5], T denotes the packet length (measured in slots) and γ is the time until all nodes stop transmission given a collision occurs.

More recently, Haas and Deng [56] introduced a dual busy tone multiple access (DBTMA) scheme and claimed to completely solve the hidden/exposed node problems. As the name suggests, DBTMA uses two out-of-band busy tone channels to protect RTS packets and data packets respectively. The transmit busy tone, which indicates whether RTS packets are being sent, provides protection for the transmission of RTS packets. The receive busy tone is used to acknowledge RTS packets and protect data transmission. Prior to the transmission of RTS packets, nodes are required to sense the busy tone channels. If either channel is busy, a node defers the transmission of the RTS packet. When a signal of receive busy tone is detected, even a node that has sent the RTS packet is required to abort the transmission. A further improvement of DBTMA is recently reported in [57] where collisions of data packets are claimed to be eliminated.

2.2.6 Performance Analysis of CSMA Protocols

The performance of a MAC protocol is strongly dependent on the network conditions such as traffic types and traffic loads. An appropriately developed model is able to give accurate and fast predictions of protocol performance under various network conditions. In contrast to simulation, analytical modeling provides more insights on the mechanism of a MAC protocol and thus may facilitate the enhancement of the protocol by optimizing system parameters.

To exactly analyze a protocol while considering all protocol details is usually very

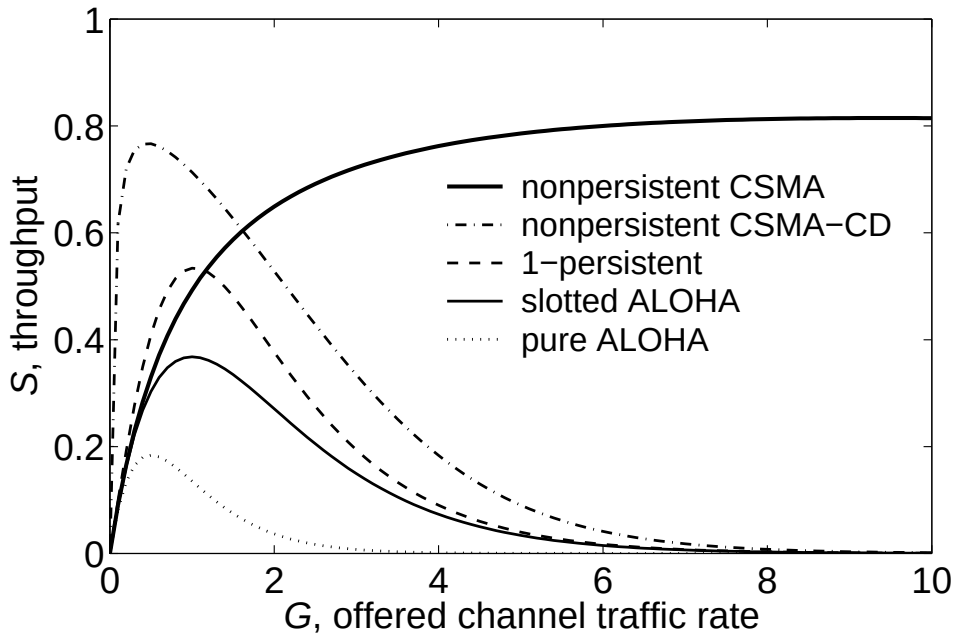

Figure 2.4: Throughput versus traffic load for the ALOHA and CSMA protocols. Note that the CSMA protocols are all slotted versions, and $a = 0.01$, $T = 20$ and $\gamma = 5$.

difficult and sometimes may not be necessary. Reasonable assumptions and approximations are often applied to simplify the analysis. A few analytical techniques have been developed to conduct performance analysis for CSMA protocols [58, Chapter 1, page 11].

The first technique, termed S-G analysis, was introduced by Abramson [13] to evaluate the performance of the ALOHA protocol by solving for the throughput (S) in terms of the offered channel traffic rate (G). This technique was then refined by Kleinrock and Tobagi [14] to analyze the persistent and nonpersistent CSMA protocols. A similar approach has been adopted to analyze the performance of nonpersistent CSMA-CD [5]. The S-G analysis typically rests on the assumptions of an infinite number of nodes, Poisson input, and statistical equilibrium [58, Chapter 1, page 15].

The throughput expressions of the ALOHA and CSMA protocols are summarized in Table 2.1, and Figure 2.4 shows plots of these expressions. Note that the throughput analysis of p-persistent CSMA is not presented here due to its tediousness. Interested readers are directed to [14] for details. It can be seen from Figure 2.4

that CSMA protocols generally achieve much higher throughput than ALOHA, and the slotted nonpersistent CSMA-CD can achieve relatively good performance compared to the slotted *1*-persistent CSMA. The nonpersistent CSMA enjoys a superior performance under high traffic load but exhibits moderate throughput for low traffic load.

Another approach that is commonly used for performance analysis of CSMA is Markov analysis. In this approach, Markovian models are formulated to capture the dynamic behaviors of the system, and the stationary state probability distribution is then calculated. Kleinrock and Lam [59] proposed a Markov analysis method to solve the stability problem in the slotted ALOHA system with a finite number of nodes. In [60], Markov chain models for the slotted nonpersistent CSMA and CSMA-CD with infinite population and unbuffered nodes were formulated. S. Tasaka [61] analyzed the dynamic behavior of the slotted nonpersistent CSMA-CD with finite population and buffered nodes by using a multidimensional Markov chain. An approximate analytical technique called equilibrium point analysis was then used to analyze the Markov chain model.

Bianchi [62] developed a two-dimensional Markov chain model to analyze the CSMA-CA scheme of the IEEE 802.11 DCF under saturation. This Markov chain model is used to capture the behavior of a single node and a throughput expression can then be derived. The accuracy of the model was extensively verified by comparisons with *ns*-2 [63] simulations. Based on the approach of Bianchi, similar Markov analysis methods have been used to analyze the IEEE 802.11 DCF under various network conditions (e.g., imperfect channel [64] and nonsaturation traffic [65]). It has also been extended to performance analysis of other wireless networks (e.g., IEEE 802.11e [66, 67] and IEEE 802.15.4 [44, 45]).

2.3 Energy Conserving CSMA-CA

The version of CSMA-CA proposed in the IEEE 802.15.4 MAC incorporates some new energy conserving features that make it distinct from others such as the IEEE 802.11 DCF. In the new energy conserving CSMA-CA, a node only performs channel

sensing at the end of its backoffs. Moreover, a contending node in the new mechanism does not freeze its backoff counter when other nodes are transmitting. In fact, the freezing of backoff counters is impossible if a contending node continuously decrements its backoff counter and only senses the channel at the end of its backoffs to avoid energy consumption on channel sensing. Note that in IEEE 802.11 DCF a node senses the channel status on every slot, and thus is able to freeze its backoff counter when other nodes are transmitting. In this chapter, we analyze the performance of the new CSMA-CA by capturing these prominent energy saving features. We now describe the mechanism in a generic fashion.

In a wireless network in which time is partitioned into equally-sized slots, a contending node that has buffered packets starts with a random backoff, the length of which (measured in slots) is randomly chosen in the range of $[0, W_0 - 1]$. The backoff counter is decremented by one at the beginning of every slot that follows. At the end of the backoff period, the node samples the channel to monitor the channel status. If the channel is busy, the node performs a second random backoff in the range of $[0, W_1 - 1]$. If the channel is idle, a second channel sampling is performed on the boundary of the next slot. The node commences its packet transmission on the next slot boundary if the channel is sensed idle at C consecutive slot boundaries, where C is a design parameter and its default value in IEEE 802.15.4 is two. Transmitted packets could collide if other nodes start transmitting at the same slot, and retransmission of collided packets can be coordinated by the functionalities in the MAC or higher layers. In our work, we do not consider retransmissions because we assume operation without acknowledgements, which is an energy-saving mode of IEEE 802.15.4 [1]. The process of determining the channel status is termed *channel sensing* in this chapter. A channel sensing may consist of one or more consecutive channel samplings.

Let $W_i, i = 0, 1, \cdots, M - 1$, be the backoff window for the ith backoff stage, where M denotes the maximum retry limit before the packet is discarded. It can be seen that when $M \to \infty$, a packet will not be discarded until transmitted. When exponential backoff is used, $W_i = \mu^i W_o$, where W_0 is the initial backoff window and μ is the backoff multiplier. When $\mu = 2$, the backoff protocol is known as (truncated)

BEB, which is adopted in many standards such as IEEE 802.3, IEEE 802.11 and IEEE 802.15.4.

We assume that the CSMA-CA operates in a single cell star wireless network of N nodes, and the message length is fixed to L time slots for all nodes.

2.4 Analysis under Saturation

In this section, we develop a new model for analyzing the energy conserving CSMA-CA under saturation conditions. By saturation we mean that each node in the network always has a buffered packet to transmit. We derive an explicit throughput expression, and then optimize the backoff parameters by maximizing the throughput. Finally, we present an asymptotic analysis and discuss the unfairness issues of the energy conserving CSMA-CA mechanism.

2.4.1 The Fixed Point Equation

Define ϕ as the channel sensing rate, i.e., the probability for a node to perform channel sensing in a given slot. We assume $C = 2$, which means that a packet will be transmitted after the channel is sensed idle at two consecutive slot boundaries. Let α and β be the probabilities of a busy channel for the first and the second channel sampling, respectively. According to Pollin *et al.* [45], α and β can be obtained as follows:

$$\alpha = L[1-(1-\phi)^{N-1}](1-\alpha)(1-\beta), \tag{2.1}$$

$$\beta = \frac{1-(1-\phi)^{N-1}}{2-(1-\phi)^{N-1}}. \tag{2.2}$$

Upon sensing a busy channel, a node performs another backoff. Let γ be the probability of performing another backoff. In the case of $C = 2$, a node backs off when the channel is sensed busy in either of the two channel samplings, and thus γ is given by

$$\gamma = \alpha + (1-\alpha)\beta. \tag{2.3}$$

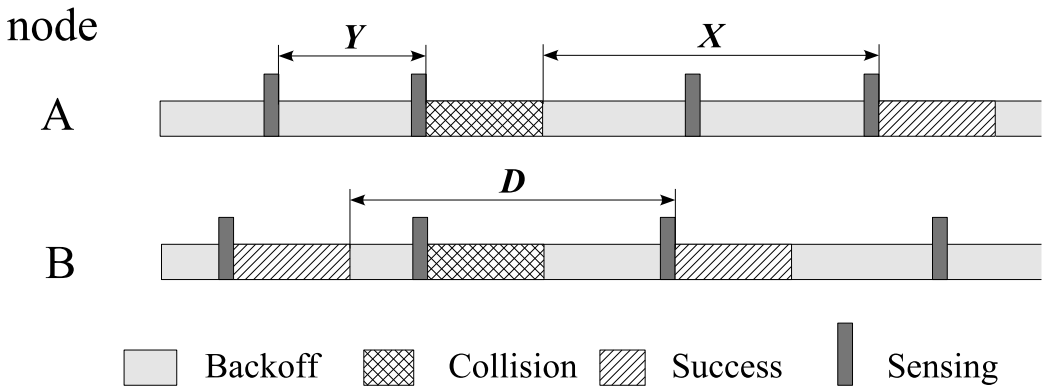

Figure 2.5: Example of node transmission in saturation traffic condition.

Combining (2.1), (2.2) and (2.3), γ can be expressed as a function of ϕ as follows:

$$\begin{aligned} \gamma &= F(\phi) \\ &= \frac{(1-(1-\phi)^{N-1})(L+1)}{(1-(1-\phi)^{N-1})(L+1)+1}. \end{aligned} \tag{2.4}$$

Our task is to find an expression for ϕ in terms of γ, and from this point, we diverge significantly from the approach of [45]. Let $B_i, i = 0, 1, \cdots, M-1$, be a random variable representing the length of the backoff period chosen by a node in its ith backoff stage, and $b_i = E[B_i] = \frac{W_i - 1}{2}$, where $E[.]$ denotes the expectation. We also denote by Δ the average duration spent in channel sensing that follows a backoff. If the channel is found busy in the first channel sampling, the node chooses another backoff at the boundary of the next slot, and thus one slot is spent in channel sensing. If the channel is idle in the first sampling, the node will continue to sense in the next slot. Thus, it is clear that $\Delta = 1 + 1 - \alpha = 2 - \alpha$, when $C = 2$. Combining (2.1) and (2.2), we get an expression of α as a function of ϕ,

$$\alpha = \frac{L(1-(1-\phi)^{N-1})}{1+(1-(1-\phi)^{N-1})(L+1)}. \tag{2.5}$$

Therefore, Δ can be rewritten as

$$\Delta = 1 + \frac{2-(1-\phi)^{N-1}}{1+(1-(1-\phi)^{N-1})(L+1)}. \tag{2.6}$$

Next, define Y as a random variable which describes the inter-sensing duration,

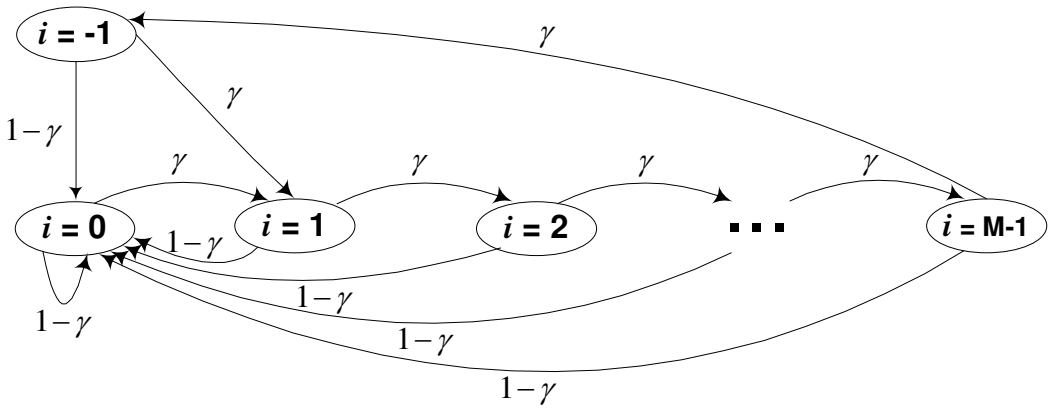

Figure 2.6: Markov chain for Ψ_n.

i.e., the time between two neighboring channel sensings (including Δ) of the tagged node (see Figure 2.5). There are $M+1$ distinct types of inter-sensing periods, where $M-1$ of these correspond to the $M-1$ different backoff periods $B_1, \ldots, B_{M-1}$ plus Δ. The additional two inter-sensing periods involve the B_0 backoff period for the current packet, and correspond to the two alternatives of a transmission of the preceding packet (with duration L) or a discard. Consequently, Y can be expressed as:

$$Y = \begin{cases} L + B_0 + \Delta, & \text{w.p.} \quad \pi_0 \\ B_1 + \Delta, & \text{w.p.} \quad \pi_1 \\ B_2 + \Delta, & \text{w.p.} \quad \pi_2 \\ \vdots & \\ B_{M-1} + \Delta, & \text{w.p.} \quad \pi_{M-1} \\ B_0 + \Delta, & \text{w.p.} \quad \pi_{-1} \end{cases} \tag{2.7}$$

where w.p. refers to "with probability". To find the probabilities π_i, $i = -1, 0, 1, \ldots, M-1$ we consider the stochastic process Ψ_n defining the evolution of the tagged node through the different types of inter-sensing periods. It can be shown that Ψ_n is described by the Markov chain in Figure 2.6 whose states map to the $M+1$ different inter-sensing periods. The Markov chain has the non-zero transition probabilities

$$\begin{aligned} Pr\{-1|M-1\} &= \gamma \\ Pr\{1|-1\} &= \gamma \end{aligned}$$

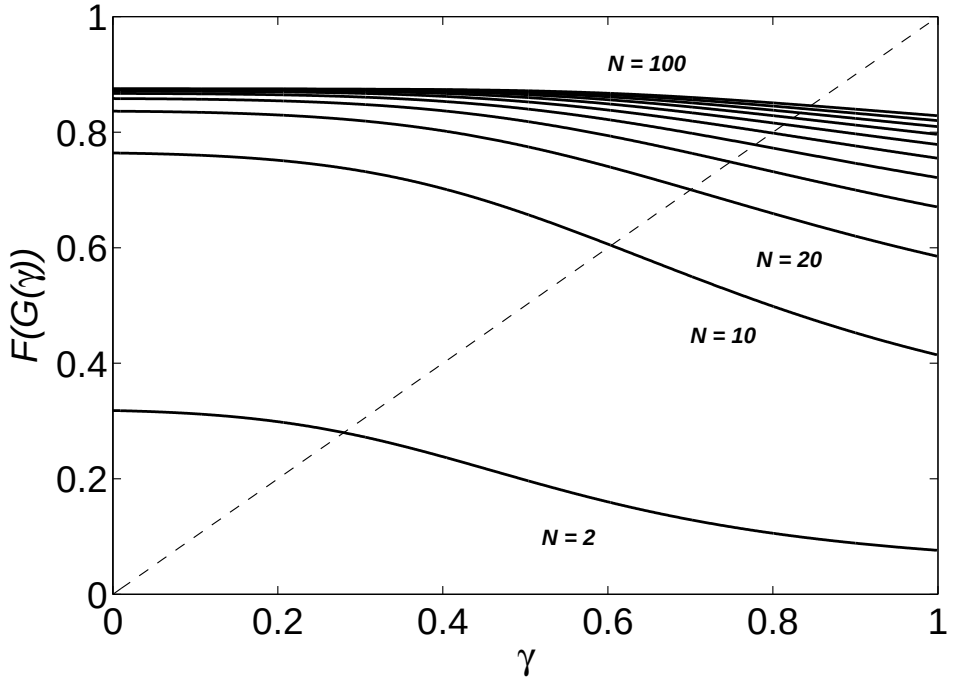

Figure 2.7: Plots of $F(G(\gamma))$ versus γ. $\mu = 2$, $W_0 = 16$, $L = 6$, $M = 6$.

$$\begin{aligned} Pr\{0|i\} &= 1-\gamma, \quad i = -1, 0, 1, \cdots, M-1 \\ Pr\{i+1|i\} &= \gamma, \quad i = 0, 1, \cdots, M-2 \end{aligned}$$

where the short notation $Pr\{j|i\} = Pr\{\Psi_{n+1} = j|\Psi_n = i\}$ is adopted.

The outcome probabilities of Y are given by the steady state probabilities of the Markov chain, namely $\pi_i = Pr\{\Psi_n = i\}$, $i = -1, 0, 1, \cdots, M-1$. It is straightforward to show that

$$\begin{aligned} \pi_{-1} &= \frac{(1-\gamma)\gamma^M}{1-\gamma^M}, \\ \pi_0 &= 1-\gamma, \\ \pi_i &= \frac{(1-\gamma)\gamma^i}{1-\gamma^M}, \quad i = 1, 2, \cdots, M-1. \end{aligned}$$

After some arrangements, the mean of the inter-sensing duration, $E[Y]$ can be written as

$$E[Y] = (1-\gamma)L + \frac{(1-\gamma)}{1-\gamma^{M+1}} \sum_{i=0}^{M-1} (\Delta + b_i)\gamma^i$$

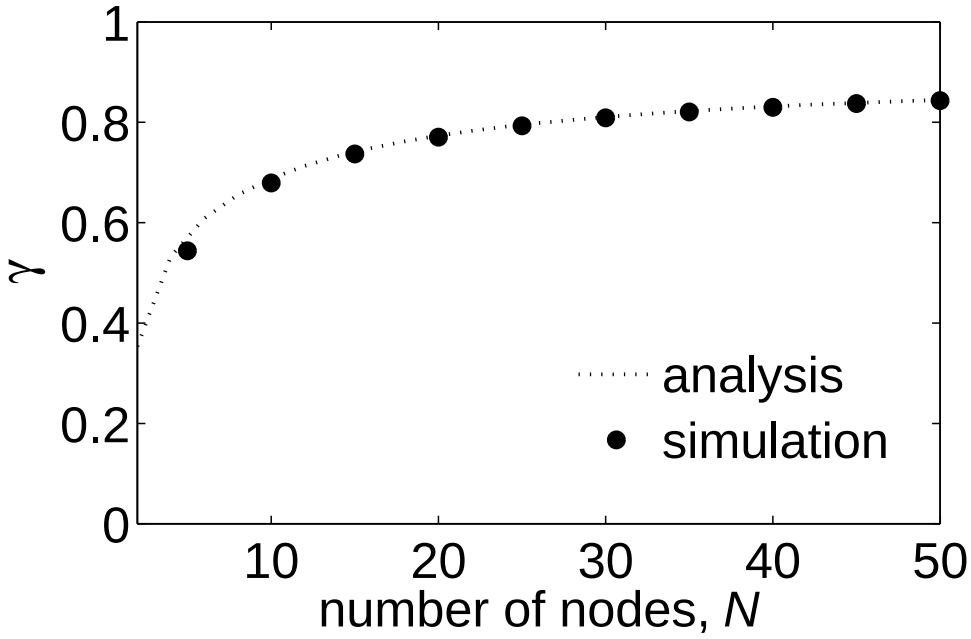

Figure 2.8: An example of comparison between analysis and simulation for γ. $\mu = 2$, $W_0 = 8$, $L = 6$, $M = 6$.

$$= (1-\gamma)L + \frac{1-\gamma}{1-\gamma^M}\sum_{i=0}^{M-1} b_i'\gamma^i \tag{2.8}$$

where $b_i' \equiv b_i + \Delta$. The channel sensing rate in the saturated traffic scenario can thus be expressed as a function of γ:

$$\begin{aligned} \phi &= G(\gamma) \\ &= \frac{1}{E[Y]} \\ &= \frac{1}{(1-\gamma)L + \frac{1-\gamma}{1-\gamma^M}\sum_{i=0}^{M-1} b_i'\gamma^i}. \end{aligned} \tag{2.9}$$

Now, we can obtain the solution of γ by solving the following fixed point equation:

$$\gamma = F(G(\gamma)). \tag{2.10}$$

Since $G(\gamma)$ is a continuous function for $\gamma \in [0,1]$ and $F(\phi)$ is continuous for $\phi \in$

$[0, 1]$, $F(G(\gamma))$ is thus a composition of continuous functions. Hence, we have a continuous mapping for $F(G(\gamma))$ from $[0, 1]$ to $[0, 1]$. According to Brouwer's fixed point theorem [68], there always exist a fixed point in $[0, 1]$. Note that the mapping is not surjective. This is because, in general, the range of $F(\gamma)$ is not equal to $[0, 1]$, and the range of $G(\gamma)$ is also not $[0, 1]$. The uniqueness of the fixed point of (2.10), however, is difficult to prove, because $G(\gamma)$ is not monotonic while $F(\phi)$ is a monotonic (non-decreasing) function. According to our extensive numerical experiments, unique fixed points of (2.10) can always be guaranteed. We leave the mathematical proof of the uniqueness of the fixed point for future investigations.

The solution of ϕ can then be found from (2.9). Figure 2.7 demonstrates the fixed points obtained from the intersections between the plots of (2.10) and the "y=x" line. The accuracy of γ obtained from the fixed point solution has been verified with simulation. Figure 2.8 shows an example where the agreement between analysis and simulation can be found.

2.4.2 Throughput Analysis

Let X be a random variable representing the inter-transmission duration, i.e., the length of the time between two neighboring packet transmissions of the tagged node. These transmissions include both successes and collisions. Note that since packets can be discarded without transmission, X can span multiple packet lifetimes. Let D be a random variable representing the inter-successful-transmission duration, i.e., the length of the time between two neighboring successful packet transmissions of the tagged node. Clearly, D can be equal to exactly one X, or consist of multiple X's and the durations of the intervening collided packets when collisions are involved (see Figure 2.5 for illustration).

The length of X depends on the number of backoff stages a node undergoes before a packet is transmitted. Figure 2.9 shows the evolution of backoff stages that may contribute to X. Labeling the backoff stages with the index j, $j = 0, 1, 2, \cdots$, we let p_j be the probability that a contending node enters backoff stage j in steady state. Since every X period must start with a random backoff, we have $p_0 = 1$. The node will enter the next backoff stage if the channel is sensed busy, so $p_j = \gamma p_{j-1}$,

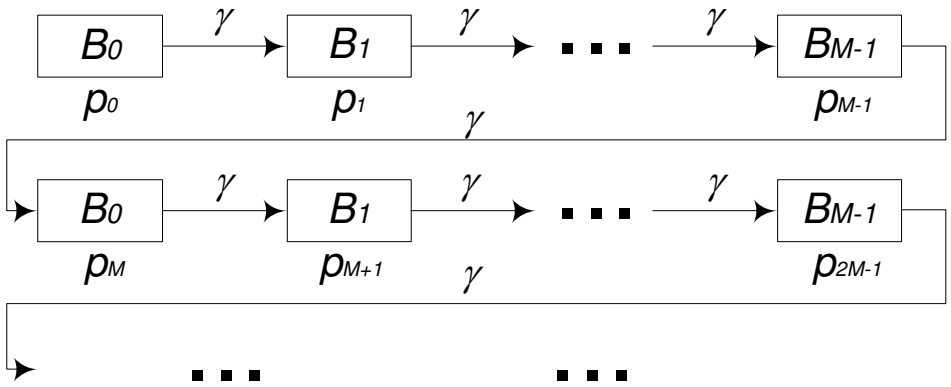

Figure 2.9: Evolution of backoff stages when involving packet discards.

and therefore $p_j = \gamma^j$ by mathematical induction. The probability that a node will transmit a packet at backoff stage j is $p_j - p_{j+1} = (1-\gamma)\gamma^j$. The above interpretation of X is similar to that of the expected medium access delay in [69].

We define $\Omega^{(i)} = \sum_{j=0}^{i} B_j$, $i = 0, 1, \cdots, M-1$. Because $B_j's$ are random variables, $\Omega^{(i)}$ is also a random variable which describes the sum of the first $i+1$ random backoffs. Clearly, we have $E[\Omega^{(i)}] = \sum_{j=0}^{i} b_j$. From the above development, we see that X can be written as

$$X = \sum_{j=1}^{q} \Omega_j^{(M-1)} + \Omega^{(i)} + \Delta_{i,q}, \quad \text{w.p.} \quad (1-\gamma)\gamma^{qM+i},$$
$$\text{for } i = 0, 1, \ldots, M-1, q = 0, 1, \ldots, \infty \quad (2.11)$$

where $\Omega_j^{(M-1)}$'s are i.i.d instances of $\Omega^{(M-1)}$, q denotes the number of packet discards that a node experiences before transmitting a packet, and $\Delta_{i,q} = (qM + i + 1)\,\Delta$. It is understood that $\sum_{j=1}^{0} \Omega_j^{(M-1)} = 0$. The expectation of X is

$$\begin{aligned} E[X] &= \sum_{i=0}^{M-1} \sum_{q=0}^{\infty} (qE[\Omega^{(M-1)}] + E[\Omega^{(i)}] + \Delta_{i,q}) \times (1-\gamma)\gamma^{qM+i} \\ &= \frac{\sum_{i=0}^{M-1} b_i' \gamma^i}{1-\gamma^M}. \end{aligned} \quad (2.12)$$

Let θ be the conditional probability that the tagged node's transmission suffers a collision. Clearly, given that the tagged node is transmitting, θ is the probability

that at least one of the other $N-1$ nodes attempt to transmit in the same slot,

$$\theta = 1 - (1-\phi)^{N-1}. \tag{2.13}$$

Let K be a random variable representing the number of collisions that occur in D, and X_k be an instance of X that denotes the inter-transmission duration for the kth collision in D, where k is an outcome of K. Now, K is geometrically distributed with parameter θ, and therefore, D is a geometric random sum:

$$D = \sum_{i=0}^{K} X_i + KL. \tag{2.14}$$

The expectation of D is

$$\begin{aligned} E[D] &= \sum_{k=0}^{\infty} [(k+1)E[X] + kL]\ (1-\theta)\theta^k \\ &= \frac{E[X] + L\theta}{1-\theta} \\ &= \frac{E[X] + L}{(1-\phi)^{N-1}} - L. \end{aligned} \tag{2.15}$$

On average, the time between successful packets (from any nodes) on the channel is $\frac{L+E[D]}{N}$. As a result, the normalized throughput in the saturated traffic scenario is

$$S = \frac{NL}{L + E[D]} \tag{2.16}$$

$$= \frac{NL(1-\phi)^{N-1}}{\sum_{i=0}^{M-1} b_i' \gamma^i + L}. \tag{2.17}$$

In Figures 2.10 and 2.11, we show the saturation throughput results for a wide range of system parameters. In our plots, the curves represent analytical results and the symbols drawn along the curves are simulation results. It can be seen that the analytical results closely match the simulation. A detailed description for the simulation is presented in Section 2.6.

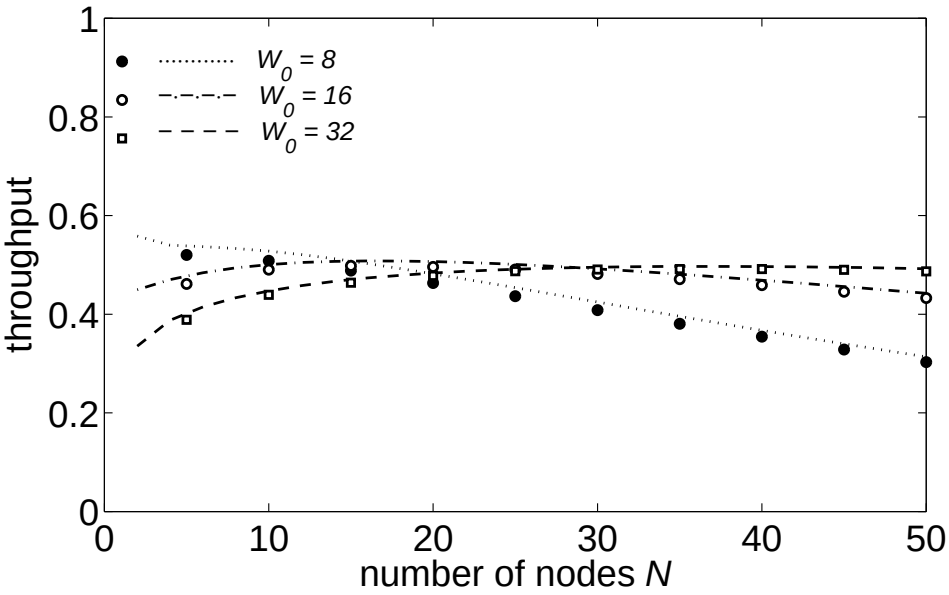

(a) μ=2.

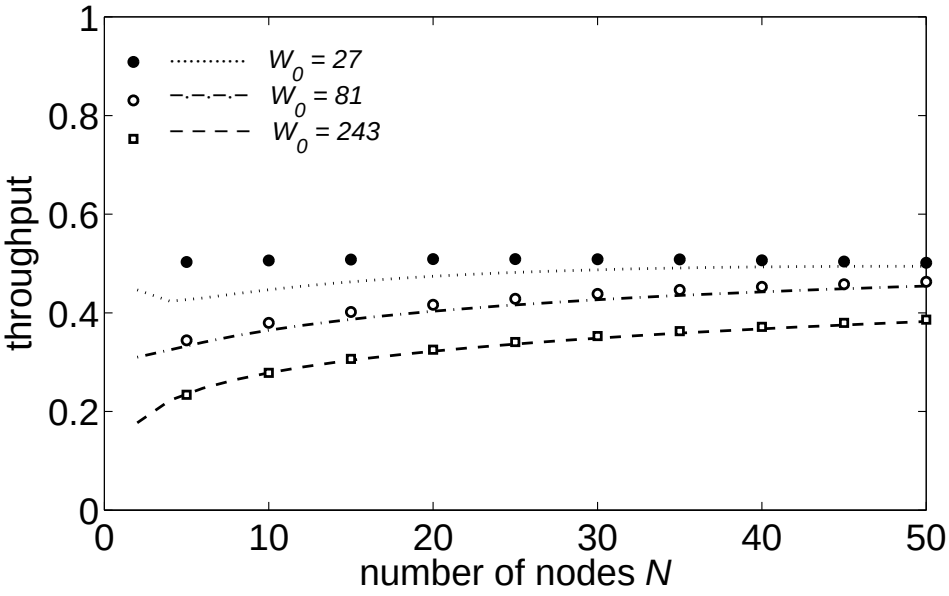

(b) μ=3.

Figure 2.10: Saturation throughput. $L = 6$, $M = 6$.

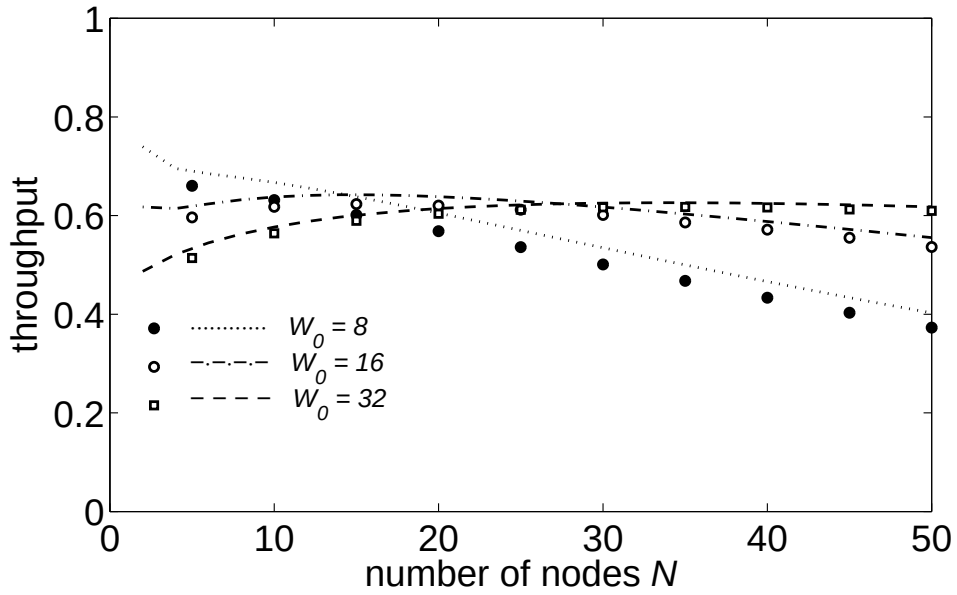

(a) μ=2.

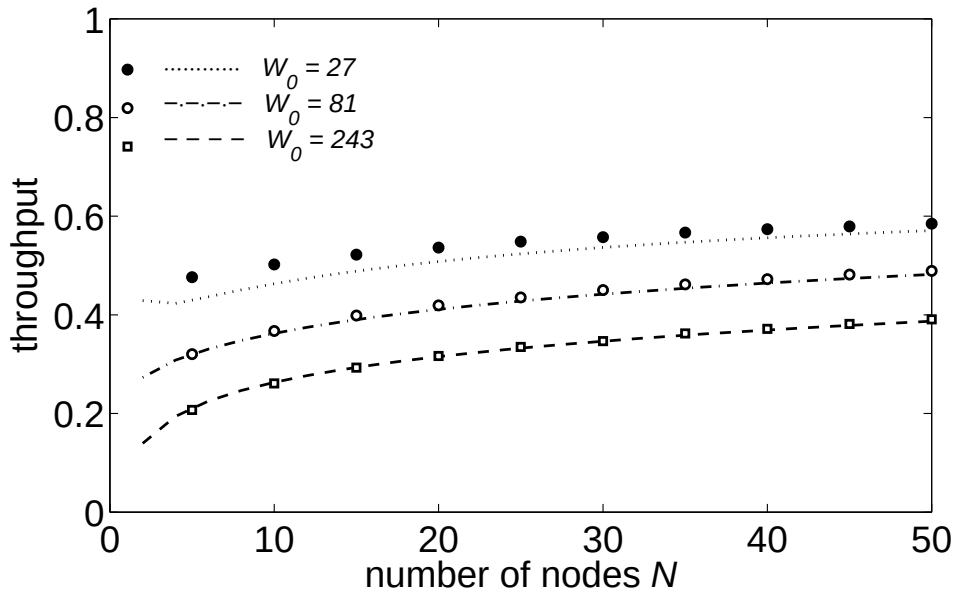

(b) μ=3.

Figure 2.11: Saturation throughput. $L = 12$, $M = 6$.

2.4.3 Optimizing Backoff Parameters

Backoff parameters can be optimized by maximizing the throughput. To maximize throughput, $E[D]$ needs to be minimized. Combining (2.9) and (2.12), $E[X]$ can be rewritten as

$$E[X] = \frac{1}{\phi(1-\gamma)} - L. \tag{2.18}$$

Combining (2.4), (2.15) and (2.18), $E[D]$ can be rewritten as

$$E[D] = \frac{(1-(1-\phi)^{N-1})(L+1)+1}{\phi(1-\phi)^{N-1}} - L. \tag{2.19}$$

We take the first-order derivative of $E[D]$ with respect to ϕ and equate it to zero. After some algebra, we have

$$(1-\phi)^N(L+1) = (1-N\phi)(L+2). \tag{2.20}$$

When $\phi << 1$,

$$(1-\phi)^N \approx 1 - N\phi + \frac{N(N-1)\phi^2}{2}. \tag{2.21}$$

Substituting (2.21) to (2.20),

$$N(N-1)(L+1)\phi^2 + 2N\phi - 2 = 0. \tag{2.22}$$

Therefore, we have

$$\phi_{opt} = \frac{-N + \sqrt{N^2 + 2N(N-1)(L+1)}}{N(N-1)(L+1)}. \tag{2.23}$$

The other root of (2.22) is negative, and therefore not a valid solution. Figure 2.12 shows values of ϕ_{opt} for various N's and L's. Substituting ϕ_{opt} into (2.4), the optimal

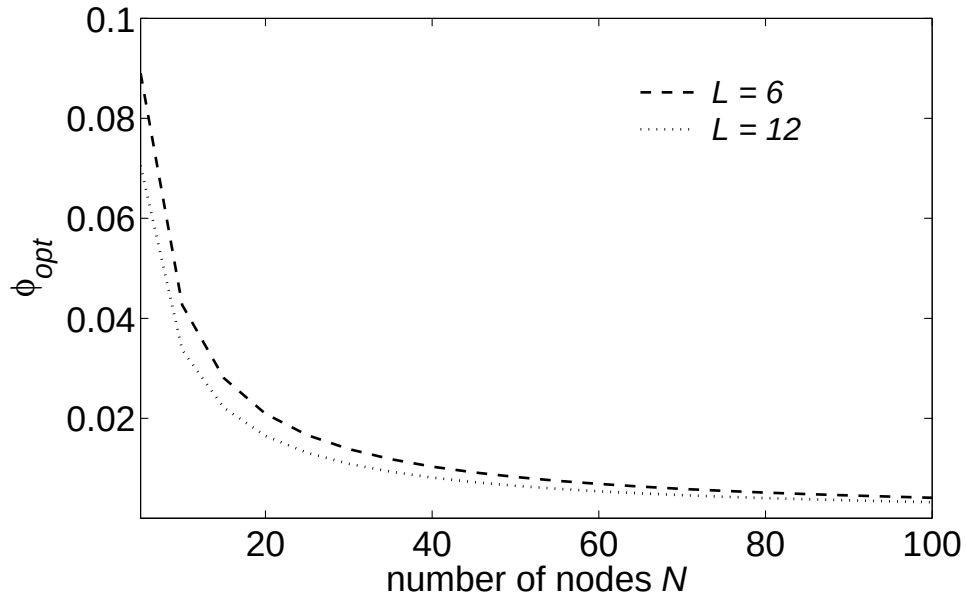

Figure 2.12: Plots of ϕ_{opt}.

value of γ_{opt} is given by

$$\gamma_{opt} = \frac{(1-(1-\phi_{opt})^{N-1})(L+1)}{(1-(1-\phi_{opt})^{N-1})(L+1)+1} \tag{2.24}$$

Substituting ϕ_{opt} into (2.5), we get

$$\alpha_{opt} = \frac{L(1-(1-\phi_{opt})^{N-1})}{1+(1-(1-\phi_{opt})^{N-1})(L+1)}. \tag{2.25}$$

Therefore,

$$\Delta_{opt} = \frac{(L+2)[1-(1-\phi_{opt})^{N-1}]+2}{(L+1)[1-(1-\phi_{opt})^{N-1}]+1}. \tag{2.26}$$

We then substitute (2.23), (2.24) and (2.26) into (2.9) to obtain

$$\sum_{i=0}^{M} b_i' \gamma_{opt}^i = (1-\gamma_{opt}^{M+1})(\frac{1}{\phi_{opt}(1-\gamma_{opt})} - L). \tag{2.27}$$

Since $b_i = \frac{W_i - 1}{2}$, and $W_i = \mu^i W_0$ for exponential backoffs, (2.27) becomes

$$\sum_{i=0}^{M} (\frac{\mu^i W_0 - 1}{2} + \Delta_{opt})\gamma_{opt}^i = (1-\gamma_{opt}^{M+1})(\frac{1}{\phi_{opt}(1-\gamma_{opt})} - L). \tag{2.28}$$

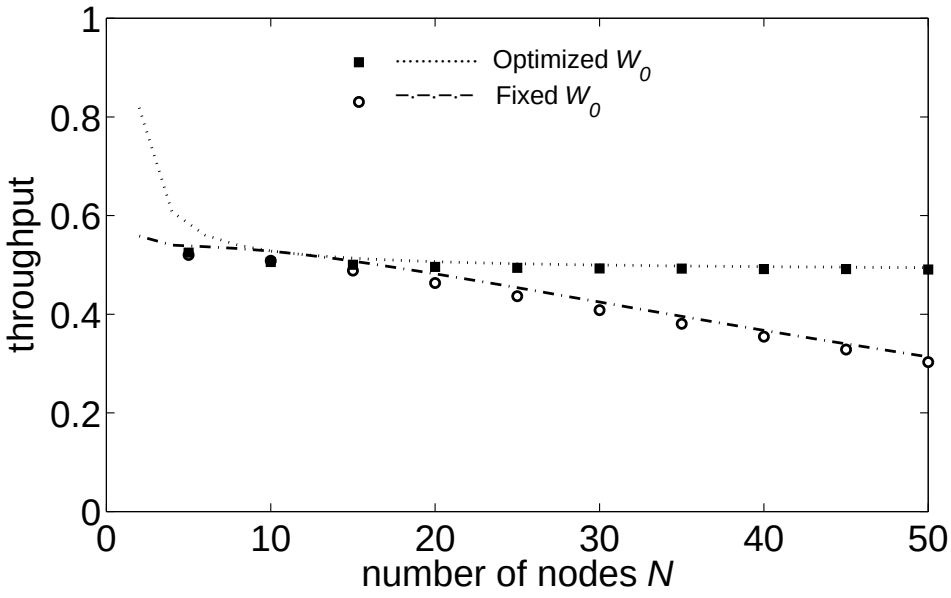

(a) $W_0 = 8$, $L = 6$.

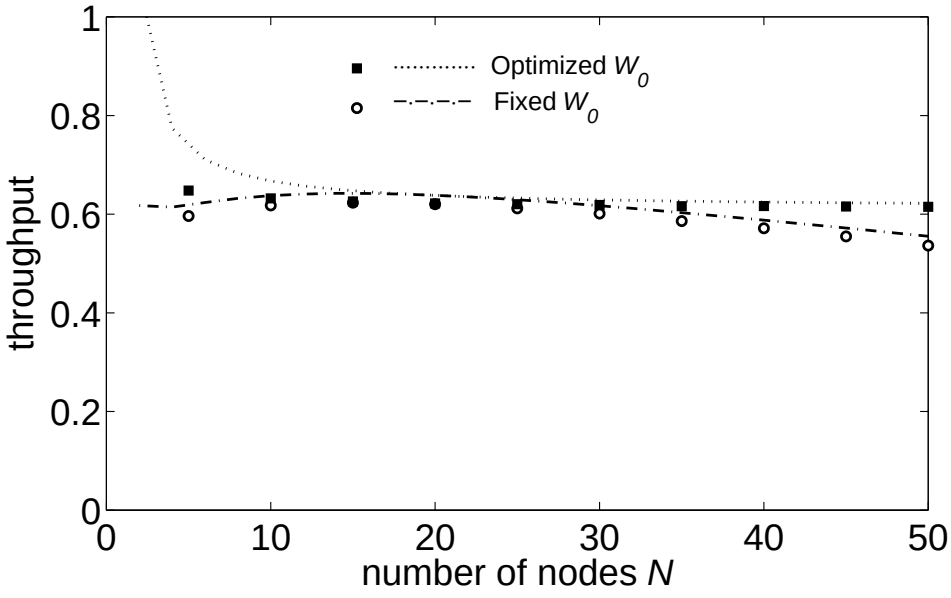

(b) $W_0 = 16$, $L = 12$.

Figure 2.13: Throughput with optimized backoff parameters, $\mu = 2$, $M = 6$.

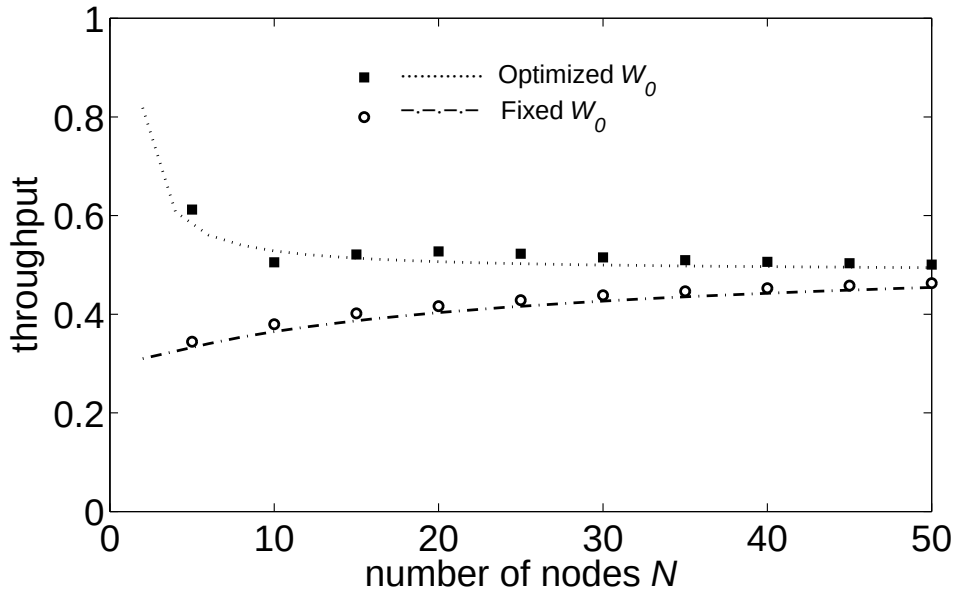

(a) $W_0 = 27$, $L = 6$.

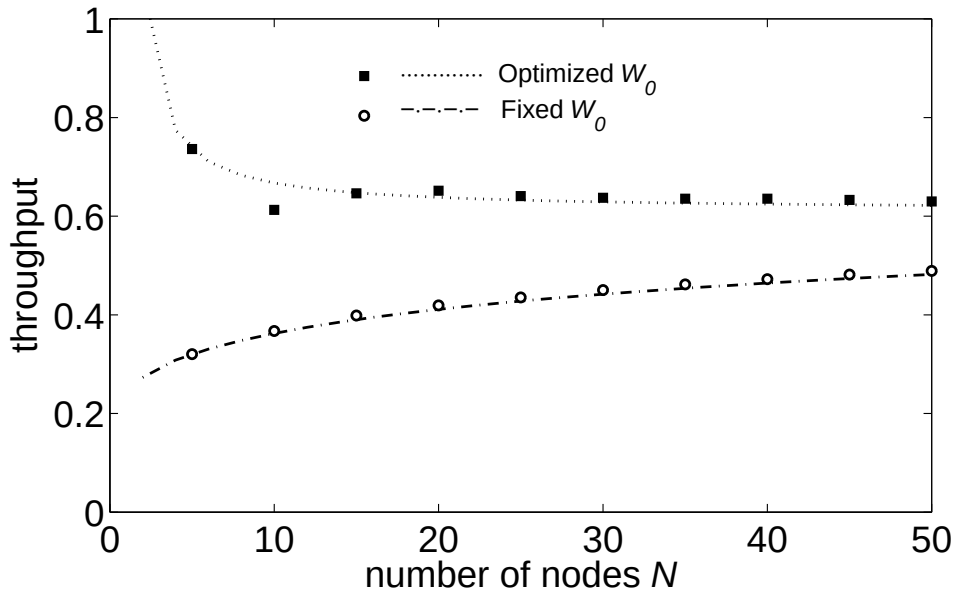

(b) $W_0 = 81$, $L = 12$.

Figure 2.14: Throughput with optimized backoff parameters, $\mu = 3$, $M = 6$.

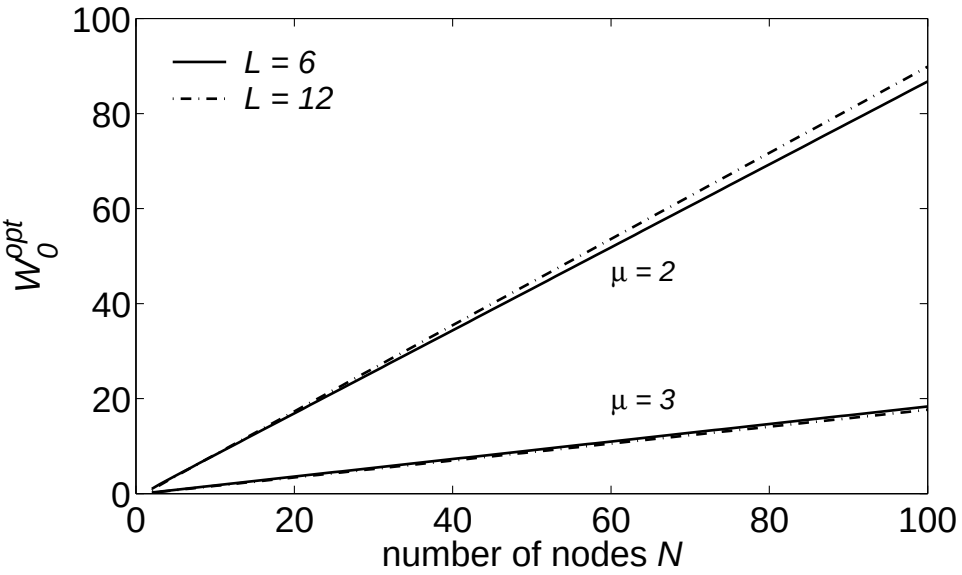

Figure 2.15: W_0^{opt} versus N, $M = 6$.

After some arrangements, the optimal initial backoff window W_0^{opt} can be obtained as follows:

$$W_0^{opt} = \frac{(1-\gamma_{opt}^M)(1-\mu\gamma_{opt})(\frac{\Delta_{opt}}{1-\gamma_{opt}} + \frac{2}{\phi_{opt}(1-\gamma_{opt})} - 2L)}{1-(\mu\gamma_{opt})^M}. \tag{2.29}$$

For the case when the number of reattempts is unlimited (i.e., $M \to \infty$), the optimal initial backoff window is simplified to

$$W_0^{opt} = (1-\mu\gamma_{opt})(\frac{\Delta_{opt}}{1-\gamma_{opt}} + \frac{2}{\phi_{opt}(1-\gamma_{opt})} - 2L) \tag{2.30}$$

where the condition $\gamma_{opt} < \frac{1}{\mu}$ must hold.

When N is large such that $N \approx N-1$, the optimal ϕ becomes

$$\widetilde{\phi}_{opt} = \frac{-1+\sqrt{2L+3}}{N(L+1)}. \tag{2.31}$$

The optimal initial window can then be approximated by a linear form as follows.

$$\widetilde{W_0}^{opt} = xN + y \tag{2.32}$$

where $x = \frac{2(L+1)[\mu-(\mu-1)\sqrt{2L+3}]}{-1+\sqrt{2L+3}}$ and $y = \frac{[\mu-(\mu-1)\sqrt{2L+3}][(L+2)(-1+\sqrt{2L+3})-2(L^2-1)]}{(L+1)\sqrt{2L+3}}$ are

constants.

As shown in Figures 2.13 and 2.14, the protocol with optimized initial backoff window sizes is able to achieve much better throughput than that with fixed initial backoff window sizes. Figure 2.15 shows that the optimal initial backoff window W_0^{opt} grows almost linearly when the number of nodes N increases, which agrees with the result in (2.32). The determination of the optimal backoff parameters is dependent on the knowledge of N. In practice, the network size N may not be known beforehand. Our optimization results, nevertheless, may still provide helpful insights toward the protocol and facilitate the selection of protocol parameters even when N is not known exactly.

2.4.4 Asymptotic Behavior

In this subsection, we investigate the asymptotic performance of our analytical model when the number of nodes goes to infinity. To simplify analysis, we examine the asymptotic performance when $M \to \infty$. From (2.4), we can express ϕ as a function of γ:

$$\phi = 1 - \left(1 - \frac{\gamma}{(1-\gamma)(L+1)}\right)^{\frac{1}{N-1}}. \tag{2.33}$$

Thus, we take the limit of ϕ,

$$\lim_{N\to\infty} \phi = \lim_{N\to\infty} \left(1 - \left(1 - \frac{\gamma}{(1-\gamma)(L+1)}\right)^{\frac{1}{N-1}}\right) = 0. \tag{2.34}$$

When $M \to \infty$, we have

$$\begin{aligned}
\sum_{i=0}^{\infty} b_i' \gamma^i &= \sum_{i=0}^{\infty} (b_i + \Delta)\gamma^i \\
&= \sum_{i=0}^{\infty} (\frac{\mu^i W_0 - 1}{2} + \Delta)\gamma^i \\
&= \frac{W_0}{2} \sum_{i=0}^{\infty} (\mu\gamma)^i + (\Delta - \frac{1}{2}) \sum_{i=0}^{\infty} \gamma^i
\end{aligned}$$

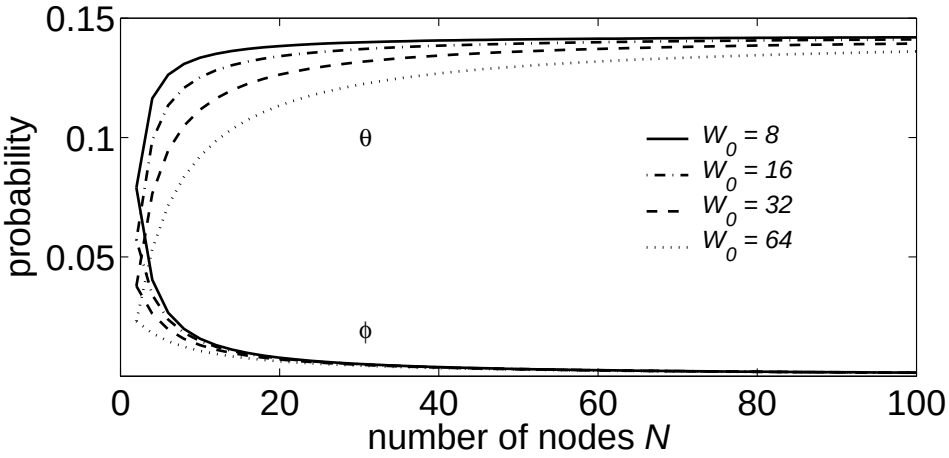

(a) $L = 6$.

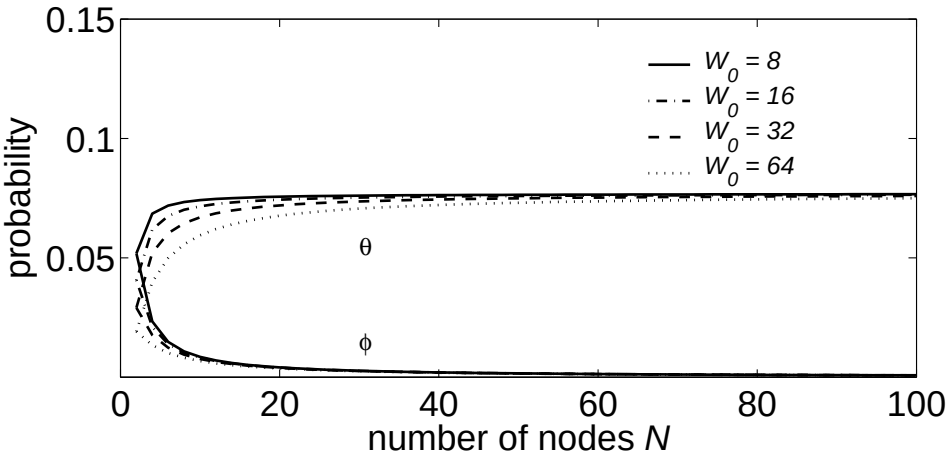

(b) $L = 12$.

Figure 2.16: Plots of ϕ and θ.

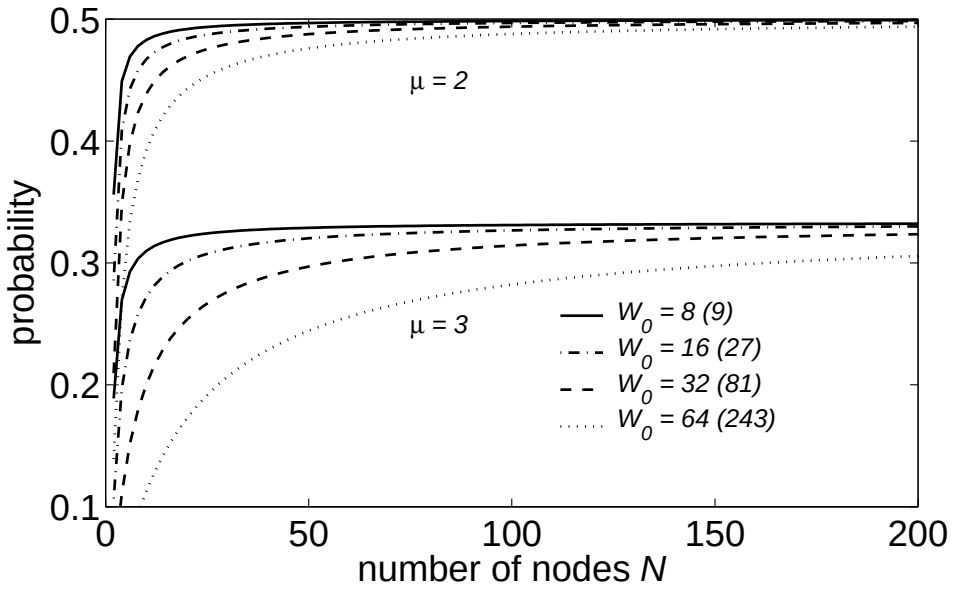

Figure 2.17: Plots of γ.

$$= \frac{W_0}{2(1-\mu\gamma)} - \frac{\Delta - \frac{1}{2}}{1-\gamma} \tag{2.35}$$

where the condition $\gamma < \frac{1}{\mu}$ must hold. Then, (2.9) becomes

$$\begin{aligned} \phi &= \frac{1}{(1-\gamma)(L + \frac{W_0}{2(1-\mu\gamma)} - \frac{\Delta-\frac{1}{2}}{1-\gamma})} \\ &= \frac{2(1-\mu\gamma)}{(1-\gamma)\left(2L(1-\mu\gamma) + W_0\right) + 2(\Delta - \frac{1}{2})(1-\mu\gamma)}. \end{aligned} \tag{2.36}$$

Since $\Delta = 2 - \alpha$ and $0 \leq \alpha \leq 1$, it is known that $1 \leq \Delta \leq 2$, and the value of the denominator of (2.36) is bounded. Since $\lim_{N\to\infty} \phi = 0$, we have

$$\lim_{N\to\infty} \frac{2(1-\mu\gamma)}{(1-\gamma)\left(2L(1-\mu\gamma) + W_0\right) + 2(\Delta - \frac{1}{2})(1-\mu\gamma)} = 0 \tag{2.37}$$

which implies that $\lim_{N\to\infty} 2(1-\mu\gamma) = 0$, and thus the limit of γ is given by

$$\lim_{N\to\infty} \gamma = \frac{1}{\mu}. \tag{2.38}$$

A. Limit of $N\phi$

Let $(1-(1-\phi)^{N-1})(L+1) = A$. According to (2.4), γ can be rewritten as

$$\gamma = \frac{A}{A+1}. \tag{2.39}$$

Substitute (2.39) into (2.36),

$$\phi = \frac{2(A(1-\mu)+1)(A+1)}{2(A(1-\mu)+1)(L+(\Delta-\frac{1}{2})(A+1))+W_0(A+1)}. \tag{2.40}$$

Since $\lim_{N\to\infty}\phi = 0$, we have

$$\lim_{N\to\infty}\frac{2(A(1-\mu)+1)(A+1)}{2(A(1-\mu)+1)(L+(\Delta-\frac{1}{2})(A+1))+W_0(A+1)} = 0.$$

It is obvious that $\lim_{N\to\infty} A \neq -1$, so $\lim_{N\to\infty} A(1-\mu) = -1$.

From the definition of A, we get

$$\begin{aligned}(1-\phi)^{N-1} &= 1-\frac{A}{L+1}\\ &= \frac{1}{\mu-1}\left(\frac{(\mu-1)(L+1)-A(\mu-1)}{L+1}\right).\end{aligned} \tag{2.41}$$

Multiplying both sides by $1-\phi$, and taking the limit as $N\to\infty$,

$$\begin{aligned}\lim_{N\to\infty}(1-\phi)^N &= \lim_{N\to\infty}\frac{1-\phi}{\mu-1}\left(\frac{(\mu-1)(L+1)-A(\mu-1)}{L+1}\right)\\ &= \frac{(L+1)(\mu-1)-1}{(L+1)(\mu-1)}\end{aligned} \tag{2.42}$$

because $\lim_{N\to\infty}\phi = 0$ and $\lim_{N\to\infty} A(1-\mu) = -1$.

Taking the natural logarithm of both sides of (2.42),

$$\lim_{N\to\infty}\frac{N\phi\ln(1-\phi)}{\phi} = \ln\left(\frac{(L+1)(\mu-1)-1}{(L+1)(\mu-1)}\right). \tag{2.43}$$

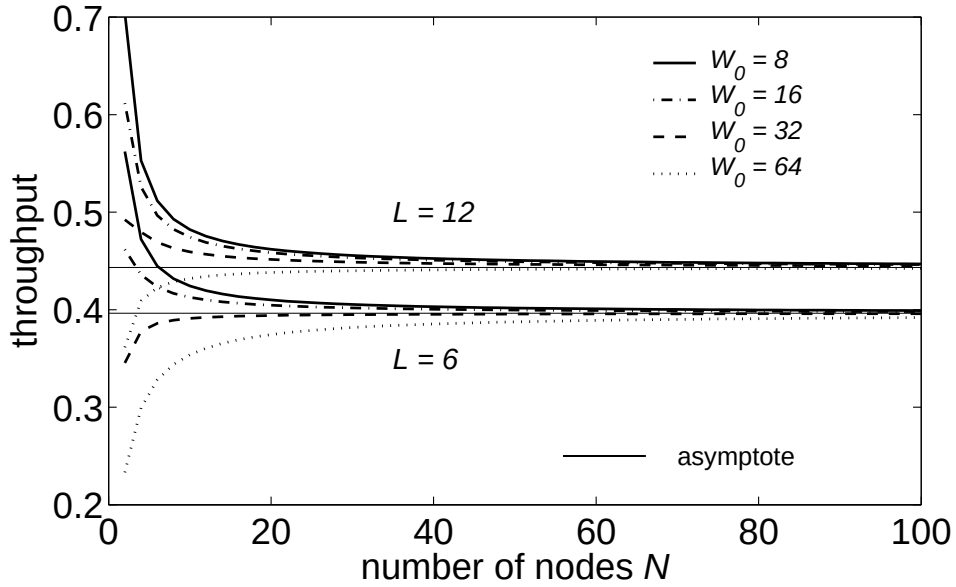

Figure 2.18: Asymptotic saturation throughput. $\mu = 2$.

Now, since $-\ln(1-\phi) = \phi + \frac{\phi^2}{2} + \frac{\phi^3}{3} + \cdots$, we conclude that

$$\lim_{N\to\infty} \frac{\ln(1-\phi)}{\phi} = -1. \tag{2.44}$$

Therefore,

$$\lim_{N\to\infty} N\phi = \ln\left(\frac{(L+1)(\mu-1)}{(L+1)(\mu-1)-1}\right). \tag{2.45}$$

B. Asymptotic Saturation Throughput

Combining (2.15), (2.17) and (2.18), we can express the throughput S as a function of ϕ and γ:

$$S = N\phi L(1-\phi)^{N-1}(1-\gamma). \tag{2.46}$$

With the knowledge of the limits of $N\phi$, γ and $(1-\phi)^N$, the asymptotic throughput is given by

$$S^* = \lim_{N\to\infty} \left(N\phi L(1-\phi)^{N-1}(1-\gamma)\right)$$

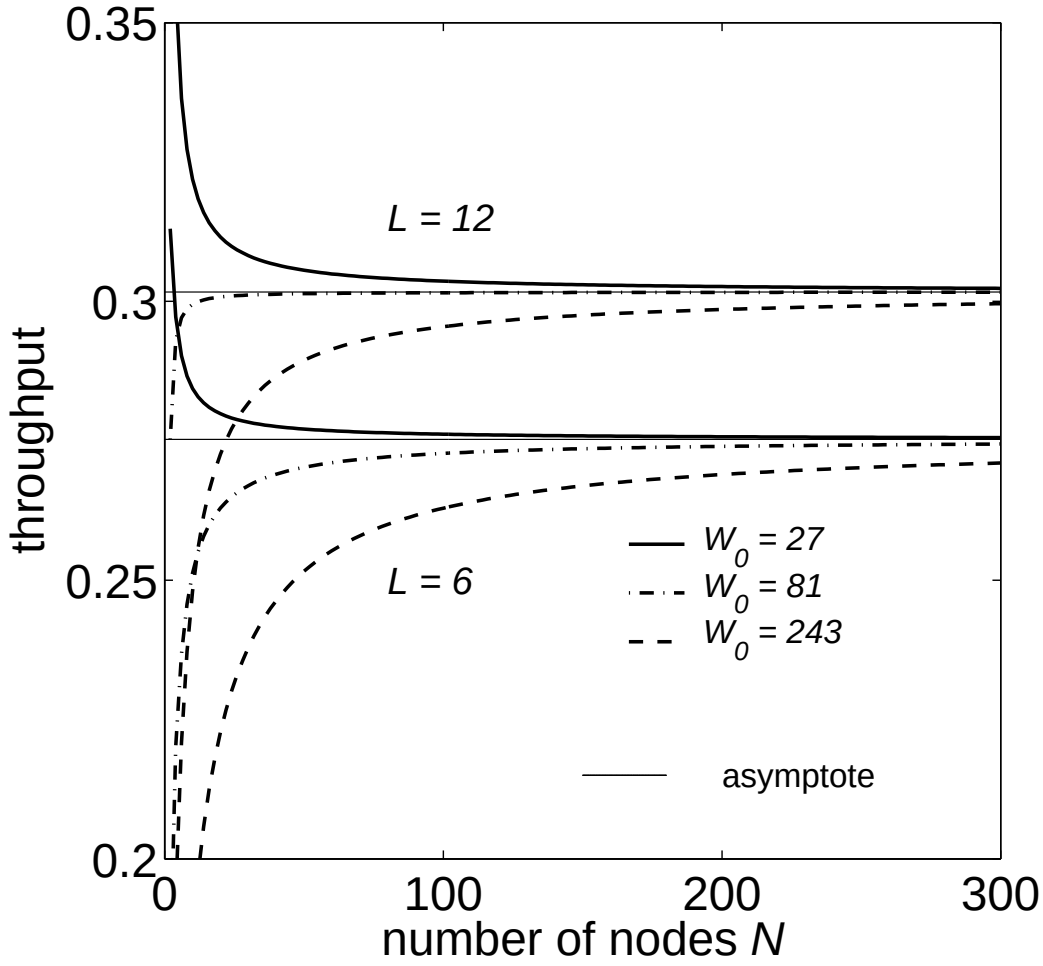

Figure 2.19: Asymptotic saturation throughput. $\mu = 3$.

$$
\begin{aligned}
&= L \lim_{N\to\infty} N\phi \lim_{N\to\infty} \frac{(1-\phi)^N}{(1-\phi)} \lim_{N\to\infty} (1-\gamma) \\
&= \frac{L\left((L+1)(\mu-1)-1\right)}{\mu(L+1)} \ln \frac{(L+1)(\mu-1)}{(L+1)(\mu-1)-1}. \qquad (2.47)
\end{aligned}
$$

2.4.5 Unfairness Issues

A fundamental assumption of our analysis for the saturation condition is that the system always operates in a steady state, where all nodes "see" the same channel conditions. However, when simulating the energy conserving CSMA-CA protocol under certain circumstances, we observed a phenomenon of multistability where the system constantly switches among multiple operation points. The existence of multistability in fact results in short term unfairness among nodes and subsequently the inaccuracy of our analytical model. Ramaiyan *et al.* [70] reported the same multistability problem for IEEE 802.11e networks. In [70], the authors counted the numbers of collisions and attempts experienced by a node in a series of fixed time periods, and defined the ratio between the two numbers as an indicator of the short term average collision probability (similar to γ in our work). This metric seems to be problematic when the number of attempts is too small and thus becomes statistically insignificant.

In this chapter, we illustrate the multistability by defining a metric which counts the number of times a busy channel is sensed by an arbitrary node and divides it by a predefined number of attempts (referred to as a "virtual frame") to guarantee its statistical significance. We simulated the energy conserving CSMA-CA protocol in a network where $N = 10$, $L = 6$, $\mu = 2$ and the length of a virtual frame is fixed to be 100. For each virtual frame (i.e., each 100 attempts), a point for the probability of busy channel is calculated. In Figure 2.20(a), we show a snap shot of the γ seen by an arbitrary node when the initial backoff window W_0 is 8, and M is unlimited. It can be observed that, for systems with small initial backoff windows, the short term average of γ seen by an arbitrary node exhibits a significant fluctuation around the long term average of γ. Using a smaller initial backoff window of 4 as in Figure 2.20(b), the channel is even monopolized by some nodes during certain periods of time since they always see a clear channel. This phenomenon was

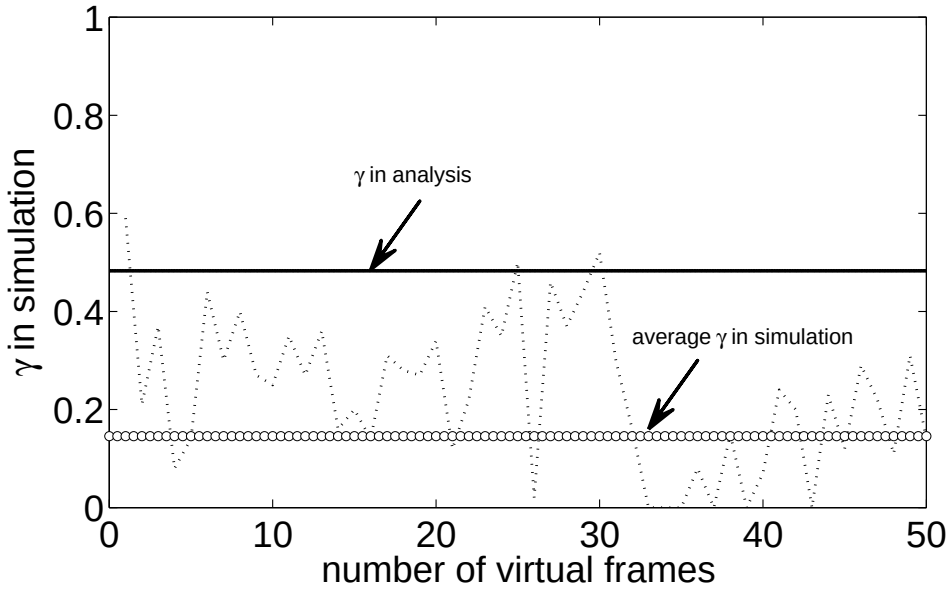

(a) $W_0 = 8$.

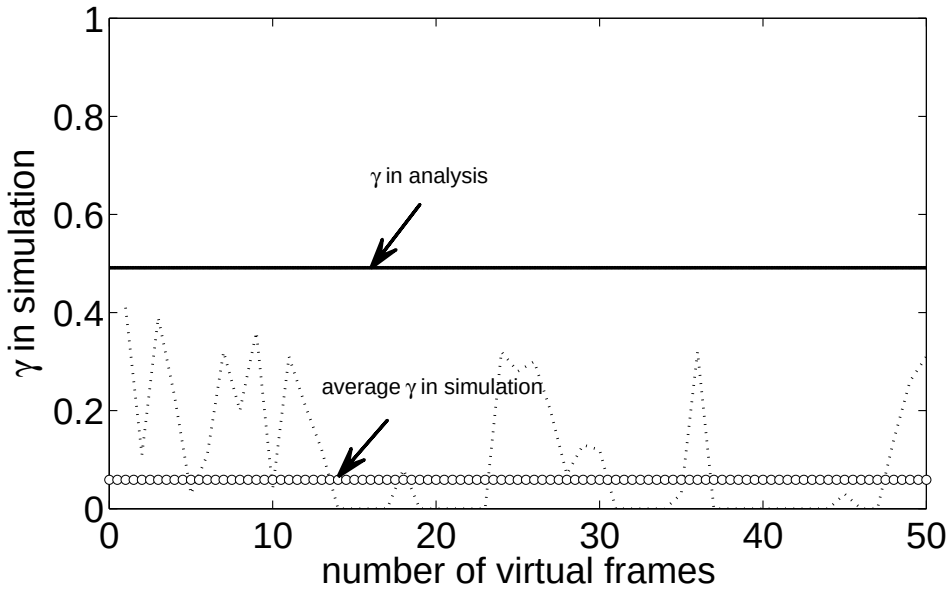

(b) $W_0 = 4$.

Figure 2.20: The γ seen by an arbitrary node in simulation. Also plotted are the average γ seen by all nodes in simulation and the γ obtained from the fixed point equation. $M \to \infty$.

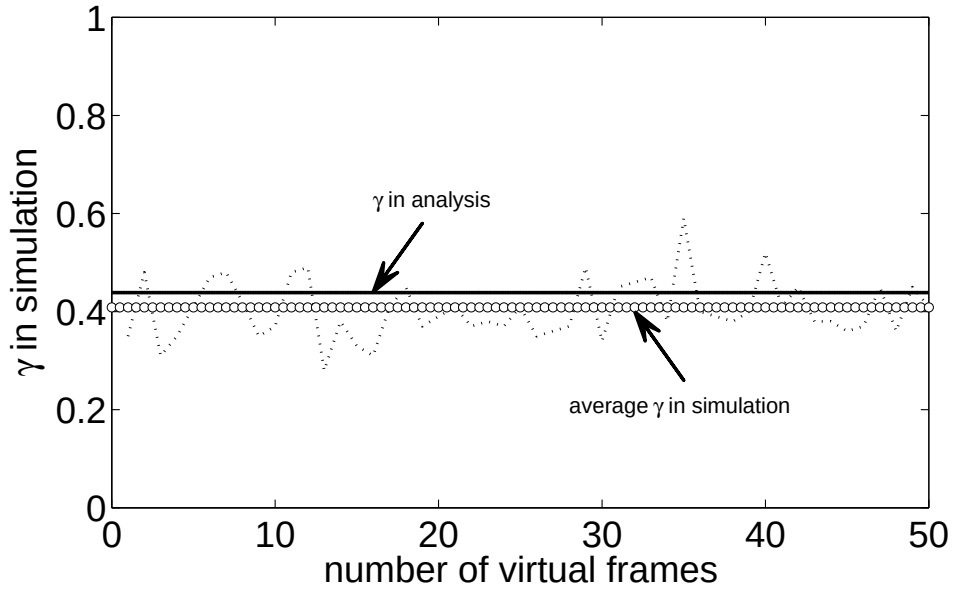

Figure 2.21: The γ seen by an arbitrary node in simulation. Also plotted are the average γ seen by all nodes in simulation and the γ obtained from the fixed point equation. $W_0 = 32$, $M \to \infty$.

also reported as "capture effect" in [69]. In contrast, when W_0 becomes big enough, the channel condition is more equally observed by different nodes and the unfairness problem is significantly mitigated. Figure 2.21 shows the plot for γ when W_0 grows to 32. Similar results were observed when M is small (e.g., $M = 6$), even for small initial backoff windows.

Figures 2.20 and 2.21 also show comparisons between the long term average γ obtained from simulations and the analytical γ attained from the fixed point equation. It is observed that there exist significant discrepancies between analysis and simulation when the system suffers from multistability (as seen in Figure 2.20), while our analysis can accurately predict the system's behavior when the problem of multistability is mitigated (as shown in Figure 2.21).

In addition, unfairness of the energy conversing CSMA-CA can be caused by a scenario where a node that has just completed a packet transmission chooses a backoff counter of zero prior to transmitting its next packet; in other words, it does not back off and immediately executes channel sampling in the next slot. In this case, it is clear that this node will always find a free channel and start transmitting after channel sensing. When the initial backoff window is smaller, the probability

of choosing a zero backoff is greater and thus the unfairness issue becomes more prominent. Our analytical model can be modified to incorporate this "zero backoff" effect by separating a zero backoff from a non-zero backoff. We do not show the details here. An easy way to eliminate this effect is to prohibit the nodes which have just finished transmission from choosing zero backoffs.

2.5 Extended Analysis to a Nonsaturation Condition

We have studied the performance of the energy conserving CSMA-CA mechanism under saturation. In real networks, however, the saturation condition is usually not valid [65]. In this section, we extend the analytical framework to a specific non-saturation traffic scenario, namely periodic traffic, which typically occurs in many monitoring sensor networks. In the traffic scenario we consider, packets arrive at each node with a fixed inter-arrival time η, and packets for different nodes arrive in an asynchronous manner.

Let H be a random variable representing the length of the idle period (in which the tagged node waits for the next packet arrival) that immediately follows the node's transmission (either success or collision) of its last packet (see Figure 2.22). The value of H depends on η and the packet access time. We introduce a positive integer number m to define the boundary between positive outcomes of H and zero-valued outcomes. H can then be expressed by

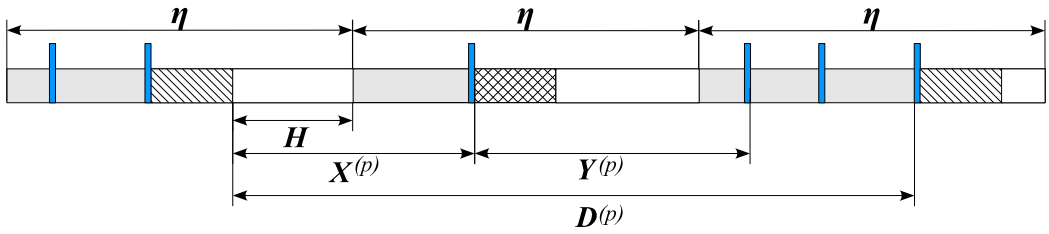

Figure 2.22: Node transmission under nonsaturation condition. Legend used here is the same as in Figure 2.5.

$$H = \begin{cases} \eta - \Omega_0 - \Delta_0 - L, & \text{w.p.} \quad (1-\gamma)\rho \\ \eta - \Omega_1 - \Delta_1 - L, & \text{w.p.} \quad (1-\gamma)\gamma\rho \\ \vdots & \\ \eta - \Omega_i - \Delta_i - L, & \text{w.p.} \quad (1-\gamma)\gamma^i\rho, \\ \vdots & \\ \eta - \Omega_m - \Delta_m - L, & \text{w.p.} \quad (1-\gamma)\gamma^m\rho, \\ 0, & \text{w.p.} \quad (1-\gamma)\gamma^{m+1}\rho, \\ \vdots & \\ 0, & \text{w.p.} \quad (1-\gamma)\gamma^{M-1}\rho \end{cases} \tag{2.48}$$

where the normalization factor $\rho = \frac{1}{1-\gamma^M}$, $\Delta_i = (i+1)\,\Delta$, and $m = \text{argmax}_i\, E[\eta - \Omega_i - \Delta_i - L] \geq 0, \quad 0 \leq i \leq M-1$. As seen from the definition, the value of m reveals the average time that the tagged node spends in waiting for the next packet arrival. When η is relatively large, $m = M-1$ and on average, the tagged node has to wait a non-zero period of time for the next packet. When η is small such that $m < M-1$, the tagged node on average, immediately has a new packet in buffer if it completes the transmission of the current packet after $m+1$ or more backoff stages. The expectation of H can be given by

$$E[H] = \begin{cases} \frac{(\eta-L)(1-\gamma^{m+1})}{1-\gamma^M} - \frac{\sum_{i=0}^{m} b_i'(\gamma^i - \gamma^{m+1})}{1-\gamma^M}, & \text{if } m < M-1 \\ \\ \eta - L - \frac{\sum_{i=0}^{M-1} b_i'(\gamma^i - \gamma^M)}{1-\gamma^M}, & \text{if } m = M-1 \end{cases} \tag{2.49}$$

Denote the inter-sensing duration of the tagged node in the periodic traffic sce-

nario by $Y^{(p)}$. Paralleling the development in Section III, we can write $Y^{(p)}$ as

$$Y^{(p)} = \begin{cases} L + H + B_0 + \Delta, & \text{w.p. } \omega_0 \\ B_1 + \Delta, & \text{w.p. } \omega_1 \\ \vdots & \\ B_i + \Delta, & \text{w.p. } \omega_i \\ \vdots & \\ B_{M-1} + \Delta, & \text{w.p. } \omega_{M-1} \\ \zeta & \text{w.p. } \omega_{-1} \end{cases} \tag{2.50}$$

where ζ is given by

$$\zeta = \begin{cases} B_0 + \Delta, & \text{if } m < M-1 \\ \eta - \Omega_{M-1} - \Delta_{M-1} + B_0 + \Delta, & \text{if } m = M-1 \end{cases} \tag{2.51}$$

and ω_i's are steady state probabilities of the associated Markov chain, which takes the same form as Figure 2.6. The steady state probabilities are

$$\begin{aligned} \omega_{-1} &= \frac{(1-\gamma)\gamma^M}{1-\gamma^M}, \\ \omega_0 &= 1-\gamma, \\ \omega_i &= \frac{(1-\gamma)\gamma^i}{1-\gamma^M}, \quad i = 1, 2, \cdots, M-1. \end{aligned}$$

The expectation of $Y^{(p)}$ is

$$E[Y^{(p)}] = \begin{cases} \frac{1-\gamma}{1-\gamma^M}\left[\eta(1-\gamma^{m+1}) + (\gamma^{m+1} - \gamma^M)L + \tau\right], & \text{if } m < M-1 \\ \frac{\eta(1-\gamma)}{1-\gamma^M}, & \text{if } m = M-1 \end{cases} \tag{2.52}$$

where $\tau = \sum_{i=m+1}^{M-1} b_i' \gamma^i + \sum_{i=0}^{m} b_i' \gamma^{m+1}$. Thus, the channel sensing rate in the non-

saturation condition is

$$\phi = \frac{1}{E[Y^{(p)}]} = \begin{cases} \frac{1-\gamma^M}{(1-\gamma)[\eta(1-\gamma^{m+1})+(\gamma^{m+1}-\gamma^M)L+\tau)]}, & \text{if } m < M-1 \\ \\ \frac{1-\gamma^M}{\eta(1-\gamma)}, & \text{if } m = M-1 \end{cases} \tag{2.53}$$

2.5.1 Throughput Analysis

Let $X^{(p)}$ and $D^{(p)}$ be random variables representing the inter-transmission and inter-successful-transmission durations in the periodic traffic scenario, respectively. Using a similar approach to the saturation scenario, $X^{(p)}$ can be expressed as

$$X^{(p)} = \begin{cases} H + q\Omega_{M+1} + \Omega_i + \Delta_{i,q}, \quad \text{w.p.} \quad (1-\gamma)\gamma^{qM+i}, & \text{if } m < M-1 \\ \\ H + q\eta + \Omega_i + \Delta_{i,q}, \quad \text{w.p.} \quad (1-\gamma)\gamma^{qM+i}, & \text{if } m = M-1 \end{cases}$$
$$\text{for } i = 0, 1, \ldots, M-1, q = 0, 1, \ldots, \infty \tag{2.54}$$

where q denotes the number of packet discards that a node experiences before transmitting its packet, and $\Delta_{i,q} = (qM + i + 1)\,\Delta$. The expectation of $X^{(p)}$ is

$$E[X^{(p)}] = \begin{cases} \frac{(\eta-L)(1-\gamma^{m+1})+\tau}{1-\gamma^M}, & \text{if } m < M-1 \\ \\ \frac{\eta+\gamma^M M\Delta}{1-\gamma^M} - \frac{\Delta\gamma}{1-\gamma} - L, & \text{if } m = M-1 \end{cases} \tag{2.55}$$

Clearly, the relationship between $X^{(p)}$ and $D^{(p)}$ holds as in (2.14) and (2.15) of the saturation analysis. The normalized throughput $S^{(p)}$ in the periodic traffic scenario is given by

$$S^{(p)} = \begin{cases} \frac{NL(1-\phi)^{N-1}(1-\gamma^M)}{\eta(1-\gamma^{m+1})+L(\gamma^{m+1}-\gamma^M)+\tau}, & \text{if } m < M-1 \\ \\ \frac{NL(1-\phi)^{N-1}(1-\gamma)(1-\gamma^M)}{(1-\gamma)(\eta+M\Delta\gamma^M)-(1-\gamma^M)\Delta\gamma}, & \text{if } m = M-1 \end{cases} \tag{2.56}$$

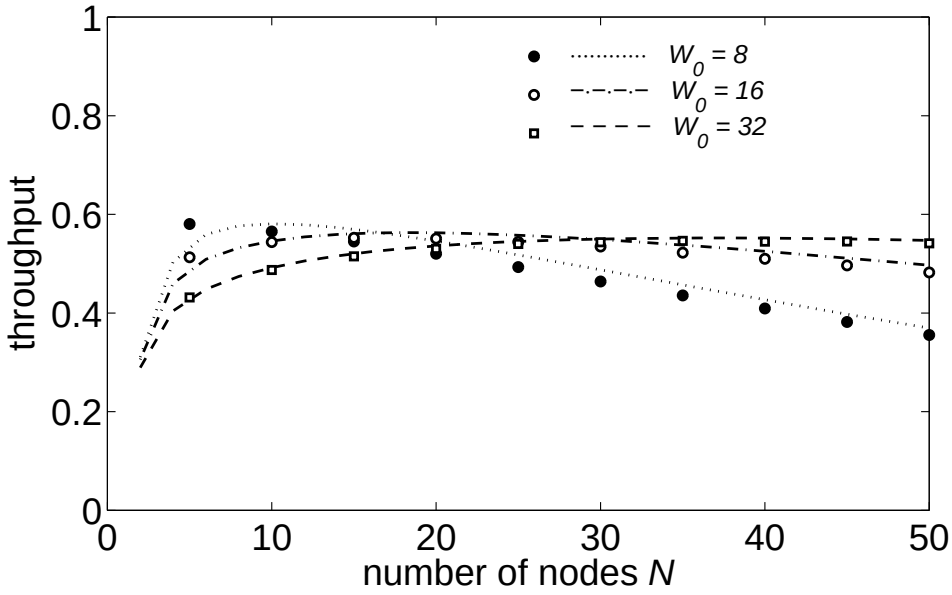

(a) $\eta = 30$.

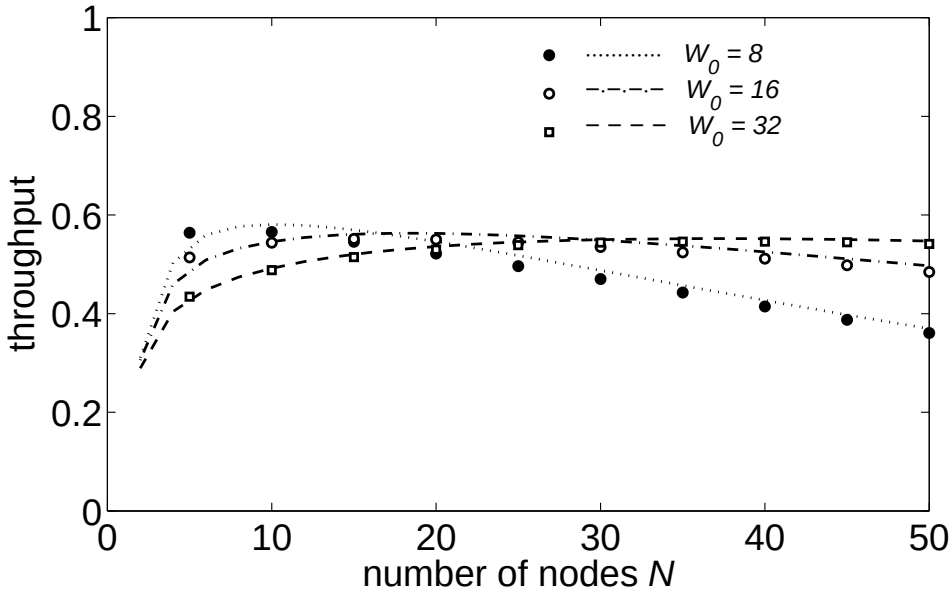

(b) $\eta = 50$.

Figure 2.23: Nonsaturation throughput when $m < M-1$: analysis versus simulation. $L = 8$, $\mu = 2$, $M = 6$.

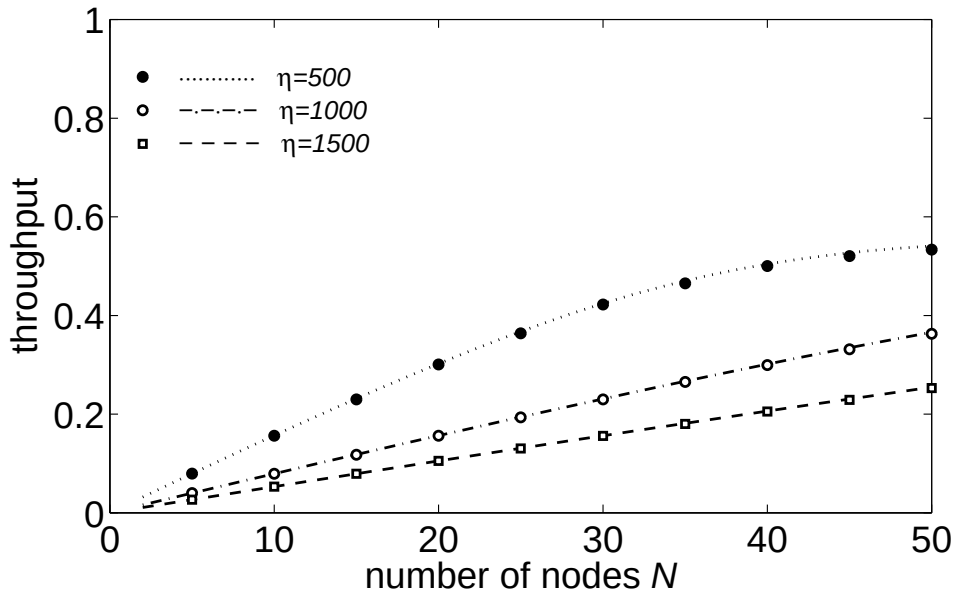

Figure 2.24: Nonsaturation throughput when $m = M-1$: analysis versus simulation. L=8, $M = 6$.

It is interesting to note that the throughput for $m = M-1$ is no longer a function of the average backoff windows b_i's and the message length L because the backoff periods are dominated by η. The throughput results of the nonsaturation condition are depicted in Figure 2.23 and 2.24.

2.6 Evaluation and Discussion

To verify the accuracy of the proposed analytical model, we compare the analysis with simulation. We implemented a simulator of the energy conserving CSMA-CA in the C++ programming language. The simulation results were obtained by running 500,000 time slots and each point was averaged over 10 independent simulation runs. Exponential backoff protocols with different backoff multipliers were used. In all of the cases considered, the maximum retry limit for each packet, M, was set equal to six, and the backoff windows keep increasing upon sensing a busy channel until the packet is transmitted or M is reached.

Figures 2.10 and 2.11 show the throughput validation in the saturation traffic scenario for different message lengths L, backoff multipliers μ and initial backoff windows W_0. It can be seen that our analytical results closely match the simulation

results. For the nonsaturation traffic scenario, the throughput was investigated when $m < M - 1$ and $m = M - 1$, which correspond to relatively small and big packet arrival intervals compared to the average packet access time, respectively. As depicted in Figures 2.23 and 2.24, our analytical results show excellent agreement with simulation. As discussed in Section 2.4.5, the multistability problem occurs when M goes to infinity and W_0 is small, and thus different results can be produced by analysis and simulation. The accuracy of our model still holds when W_0 is big enough (e.g., 32 or greater) for unlimited M. In a practical protocol for wireless networks, especially for wireless sensor networks, a small M is usually used to avoid intolerably long packet latency and more importantly, energy waste. Simulation results were omitted for the asymptotic analysis.

It is observed that the throughput of the energy conserving CSMA-CA can be low when backoff parameters (e.g., μ and W_0) are inappropriately chosen. Figures 2.13 and 2.14 show the agreement between simulation and analysis for saturation throughput when the initial backoff windows were optimized for μ=2 and $\mu = 3$, respectively.

2.7 Summary

In this chapter, we have reviewed the relevant literature on the development of CSMA protocols and their analysis techniques. We then proposed a new analytical approach to model an energy conserving CSMA-CA mechanism which uses limited channel sensing and no freezing of backoff counters. The performance of the energy conserving CSMA-CA has been investigated under both the saturation and nonsaturation traffic conditions. For the saturation condition, we also presented optimization results to maximize throughput, conducted asymptotic analysis and discussed unfairness issues of the protocol. Although similar unfairness problems for IEEE 802.11e have been reported in [70], we identified new unfairness issues including the "zero-backoff" effect. At the same time, we also defined a reasonable metric, which takes statistical significance into account, to measure short-term unfairness issues. Simulation results show that our analysis agrees well with simulation. Our model is

quite flexible and it could be put to other uses than those shown in this chapter, such as the study of packet delay statistics or the study of the performance of different backoff algorithms.

Chapter 3

Analysis of IEEE 802.15.4 Packet Delivery

3.1 Introduction

The IEEE 802.15.4 standard [1] has been recently ratified, and it defines MAC and physical (PHY) layer specifications for LR-WPANs. A comparison between LR-WPAN with other wireless technologies is shown in Table 3.1. The Zigbee Alliance [71] was established in 2002 as an association of companies to develop higher layer standards such as network, security and application protocols for LR-WPANs based on IEEE 802.15.4.

The IEEE 802.15.4 standard specifies a MAC protocol that includes a duty cycling operation where nodes are allowed to stay in sleep state for most of the time to save energy, and a CSMA-CA mechanism for contention-based channel access. The IEEE 802.15.4 MAC features a number of salient energy saving characteristics that distinguish it from MAC layers in traditional wireless networks. It is important to understand the performance of this new MAC protocol under various network scenarios.

In Chapter 2, we generalized the energy conserving CSMA-CA mechanism adopted in IEEE 802.15.4 and presented analytical models to analyze and optimize its performance under both saturated and periodic traffic conditions. In this chapter, we analyze the IEEE 802.15.4 MAC with all design features under a more realistic bursty traffic type that would appear in many IEEE 802.15.4 networks with spatially correlated nodes, and develop a new approach that is based on a non-stationary Markov chain to accurately predict the packet delivery statistics of the standard.

The remainder of this chapter is structured as follows. In Section 3.2, the IEEE

	WLAN	UMTS	LR-WPAN
Range	∼50 m	∼2000 m	∼10 m
Data rates	∼11 Mb/s (180 Mb/s)	< 2 Mb/s (42 Mb/s)	< 0.25 Mb/s
Power consumption	medium	low	ultra low
Node size	larger	smaller	smallest
Cost/complexity	high	high	ultra low

Table 3.1: A comparison of LR-WPAN with other wireless technologies. Partly taken from [6].

802.15.4 MAC is introduced. Related work on the performance evaluation of the standard is reviewed in Section 3.3. In Section 3.4, we describe our analytical model in detail. Finally, numerical results and discussion are presented in Section 3.5.

3.2 IEEE 802.15.4 Overview

An IEEE 802.15.4 LR-WPAN network typically consists of a large number nodes that operate in the range of 10 m or less and consume minimal energy. The standard can operate in multiple frequency bands: the 868 MHz band with data rates of 20 kb/s, the 915 MHz band with data rates of 40 kb/s, and the license-free industrial scientific medical (ISM) 2.4 GHz band with data rates of 250 kb/s. There are 27 channels that can be allocated in IEEE 802.15.4: one channel in the 868 MHz band, ten channels in the 915 MHz band and 16 channels in the 2.4 GHz band. The standard uses binary phase shift keying (BPSK) for chip modulation in the 868 MHz and 915 MHz bands, and offset quadrature phase shift keying (O-QPSK) in the 2.4 GHz band. The IEEE 802.15.4 physical parameters are summarized in Table 3.2.

Two different types of nodes are defined based on computation and processing capability. The first node type is called a full function device (FFD), which can act as a PAN coordinator, cluster head, or a normal node. The second type is a reduced function device (RFD), which is intended for extremely simple functions and can serve only as a normal node. An FFD can communicate with RFDs and other FFDs, and an RFD can talk only to its associated FFD.

In an IEEE 802.15.4 network, one node is appointed as the central controller,

Frequency band	Bit rate	Symbol rate	Channels	Modulation
868 MHz	20 kb/s	20 ks/s	1	BPSK
915 MHz	40 kb/s	40 ks/s	10	BPSK
2.4 GHz	250 kb/s	62.5 ks/s	16	O-QPSK

Table 3.2: IEEE 802.15.4 Physical Parameters.

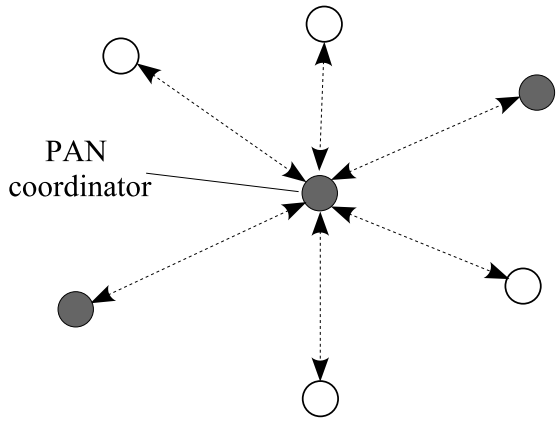

(a) Star topology.

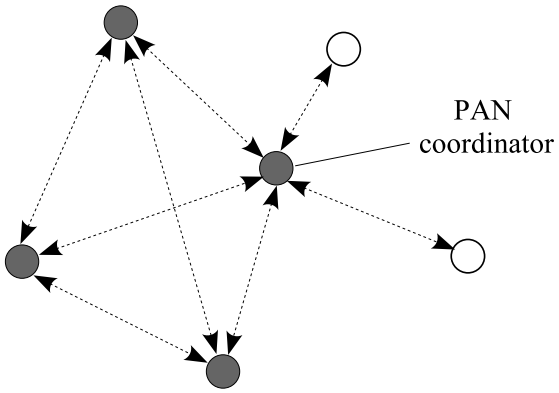

(b) Peer-to-peer topology.

Figure 3.1: Examples of star and peer-to-peer topologies. The gray colored nodes represent FFDs and the white colored nodes represent RFDs. Reproduced from [1].

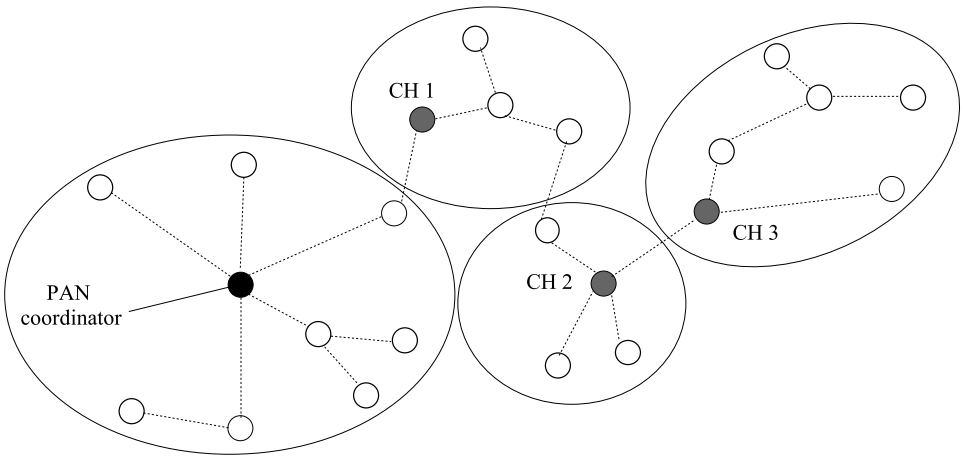

Figure 3.2: A cluster tree network. The gray colored nodes represent cluster heads. The white colored nodes represent the associated nodes.

i.e., the network coordinator. Depending on the requirements of the intended application, an IEEE 802.15.4 network can be organized in either star or peer-to-peer topology. Examples of star and peer-to-peer networks are shown in Figure 3.1. In a star network, the overall communication is centrally controlled by the network coordinator. In other words, a node can talk to other nodes only through the network coordinator. The star topology is typically adopted in applications such as personal computer peripherals, home automation and personal health care. In a peer-to-peer network, any node can directly communicate with another node as long as they are located in the radio range of each other. It may be preferred to use the peer-to-peer topology for applications such as industrial control and monitoring, inventory tracking and intelligent irrigation systems. Figure 3.2 shows a cluster tree network that is a typical use of the peer-to-peer topology. One of the advantages for the cluster tree structure is the increased coverage area. However, the network may suffer a substantial increase in packet delay, especially when low duty cycles are used.

The standard can operate in beacon-enabled or nonbeacon-enabled modes. In beacon-enabled mode, a beacon frame is broadcast by the network coordinator for maintaining network synchronization. In the nonbeacon-enabled mode, there is no beacon frame and operation is asynchronous. A slotted CSMA-CA is used in beacon-enabled networks, where beacon messages are periodically sent by the network coordinator to its associated nodes. In nonbeacon-enabled networks, a simpler unslotted

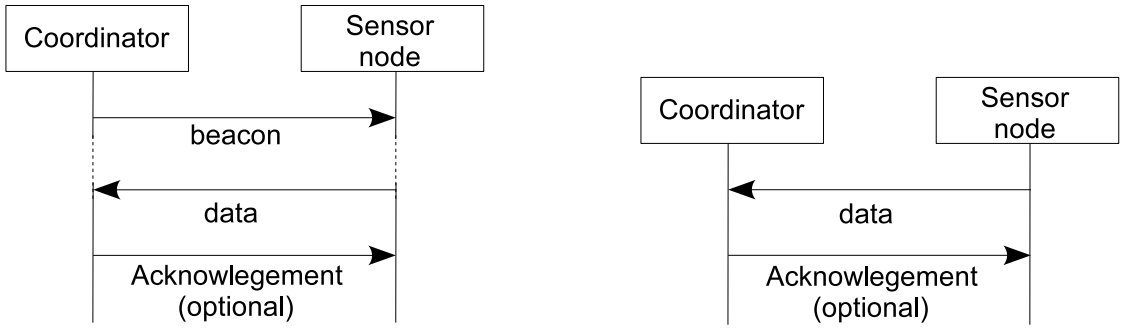

(a) Beacon-enabled mode.

(b) Nonbeacon-enabled mode.

Figure 3.3: Data communication to a coordinator. Reproduced from [1].

CSMA-CA mechanism is adopted. Figure 3.3 illustrates how a node transmits data to a coordinator in beacon-enabled and nonbeacon-enabled modes.

3.2.1 Superframe Structure

In this work, we focus on beacon-enabled networks laid out in a single-hop star topology. Such a network operates with a superframe structure, which may consist of active and inactive portions, as depicted in Figure 3.4. Let time be divided into consecutive time intervals called *beacon intervals* (BI). At the beginning of a BI, the nodes simultaneously wake up and the coordinator broadcasts a message called the *beacon frame* (BF) to the nodes. The BF includes, among other things, the next wake-up time, which is used to establish network synchronization. The BF is immediately followed by the contention access period (CAP), in which backlogged nodes can contend for the medium and transmit their packets.

The superframe duration (SD), which denotes the active portion of the superframe, may consist of a BF, a CAP and a contention free period (CFP). If a node is allowed to transmit in the CFP, it will be allocated guaranteed transmission slots and can transmit without contention. In this work, we set the length of CFP to 0; in other words, we assume that the nodes are only permitted to operate in contention-based access mode. The MAC attributes *macBeaconOrder* (BO) and *macSuperframeOrder* (SO) describes the BI and SD, respectively, where BO and SO are integers and $0 \leq SO \leq BO \leq 14$. More specifically, the lengths of BI and

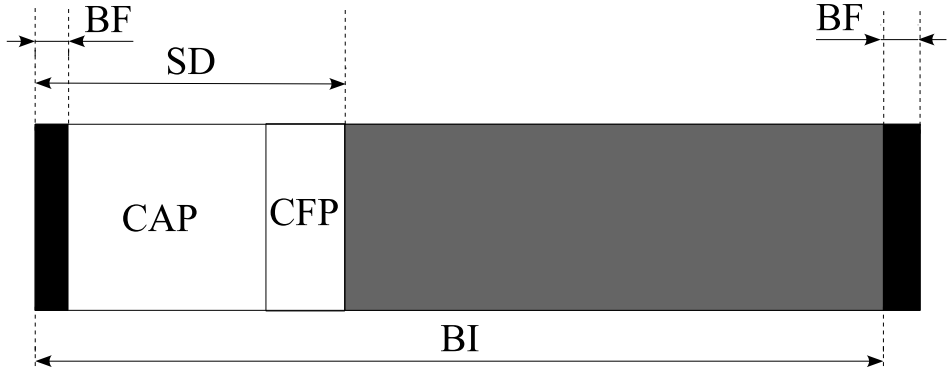

Figure 3.4: Superframe structure. The gray area represents inactive duration of time.

SD (measured in symbols) are given by

$$BI = aBaseSlotDuration \times aNumSuperframeSlots \times 2^{BO}$$
$$SD = aBaseSlotDuration \times aNumSuperframeSlots \times 2^{SO}$$

where *aBaseSlotDuration* is set equal to 60 symbols and *aNumSuperframeSlots* is equal to 16 in the standard. Note that in IEEE 802.15.4, all constants have a common prefix of "a" (e.g., aBaseSlotDuration), and all attributes have a prefix of "mac" (e.g., macBeaconOrder). Table 3.3 shows some example values of BO and SO in different frequency bands with the lengths of their corresponding BI and SD.

3.2.2 Slotted CSMA-CA

The IEEE 802.15.4 MAC uses the slotted CSMA-CA mechanism (see Figure 3.5 for a flow chart) for contention-based channel access in the beacon-enabled mode. The time during a CAP is slotted and each slot is named *aUnitBackoffPeriod*, which is set equal to 20 symbols. A backlogged node starts with a random backoff, the length of which (measured in slots) is uniformly chosen in the range of $[0, 2^{BE} - 1]$, where the integer-valued parameter BE represents the *backoff exponent* and takes an initial value given by *macMinBE*. At the end of the backoff period, the node performs a clear channel assessment (CCA) to monitor the channel status.

If the channel is idle, it performs another CCA on the boundary of the next

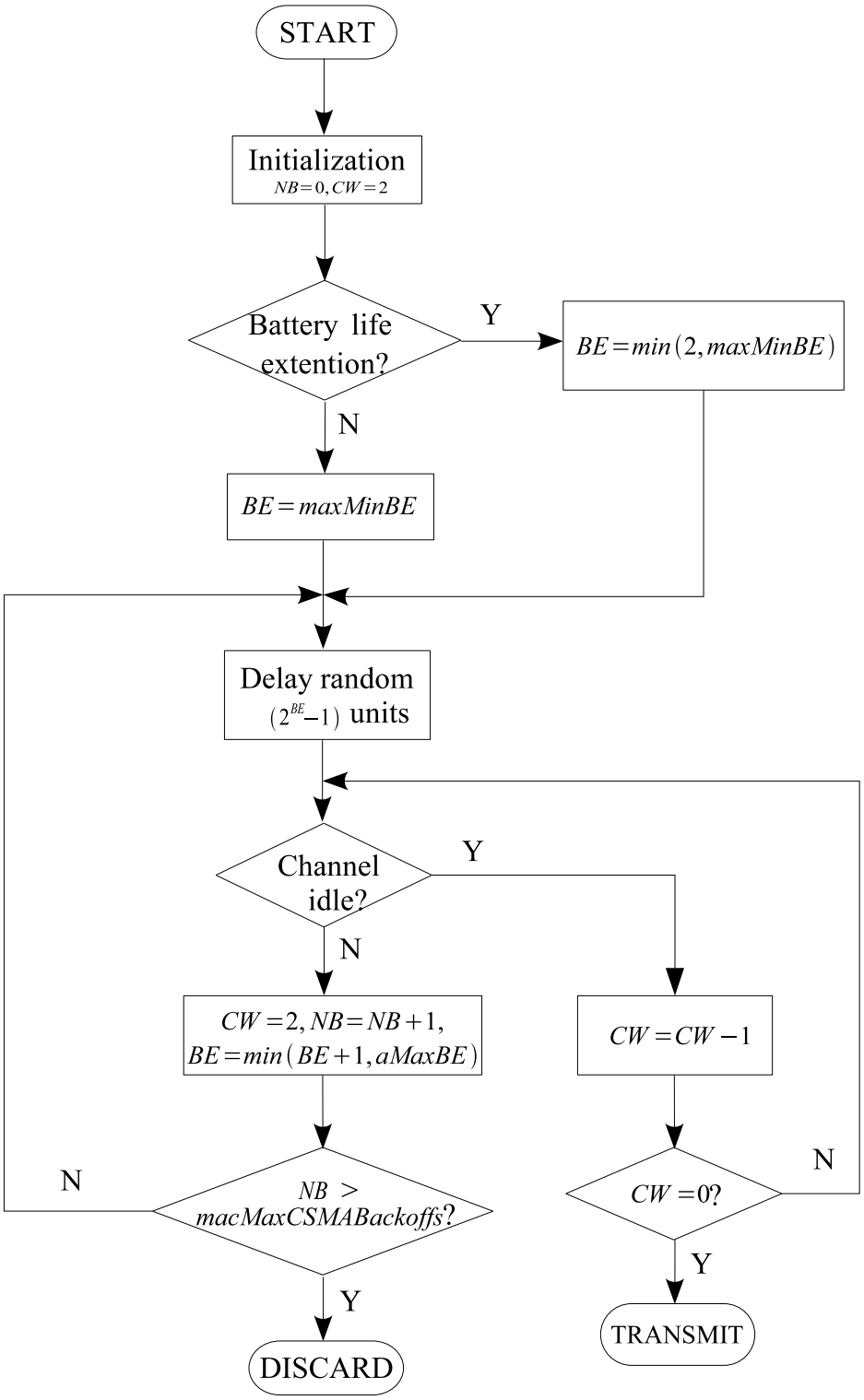

Figure 3.5: Flow chart of the slotted CSMA-CA in IEEE 802.15.4.

BO, SO	lengths of BI, SD (seconds)			length of SD (slots)
	868 MHz	915 MHz	2.4 GHz	
0	0.048	0.024	0.015	48
1	0.096	0.048	0.031	96
2	0.192	0.096	0.061	192
3	0.384	0.192	0.123	384
4	0.768	0.384	0.246	768
5	1.536	0.768	0.492	1536
6	3.072	1.536	0.983	3072
7	6.144	3.072	1.966	6144
8	12.288	6.144	3.932	12288
9	24.576	12.288	7.864	24576
⋮	⋮	⋮	⋮	

Table 3.3: BO and SO with lengths of their corresponding BI and SD in different frequency bands.

slot. The node commences transmission of its packet on the next slot boundary if the channel is sensed idle at CW consecutive slot boundaries and the packet can be completely transmitted in the current SD. The parameter CW stands for the *contention window* length, and is set equal to two in the slotted CSMA-CA and one in the unslotted CSMA-CA. After the transmission, the node will immediately go back to sleep to save energy. The standard includes a battery life extension mode, in which $BE = \min(2, macMinBE)$.

If the channel is detected to be busy, the node increases its BE by one and performs another random backoff. In response to repeated backoff periods ending in busy detections, the value of BE increases up to a maximum value *aMaxBE*, where it remains for the rest of the attempts. The packet is discarded after a maximum number of attempts, *macMaxCSMABackoffs*, is reached.

For an application that requires acknowledgement for a packet transmission, the node will wait for an acknowledgement frame from the coordinator. The time to wait for an acknowledgement frame is determined by the MAC attribute $macAckWaitDuration$, which is equal to 54 or 120 symbols, depending on the frequency band used. If an acknowlegement frame is not received within $macAckWaitDuration$, the node concludes that the transmitted packet is not prop-

erly received and retransmits the packet. The packet will be discarded after a maximum of $aMaxFrameRetries$ failed retransmissions. The acknowledgement mode is optional in the standard.

3.3 Related Work

Performance evaluations of the IEEE 802.15.4 MAC have so far mainly been simulation-based. Zheng and Lee [72, 73] developed an *ns*-2 based simulator (included in *ns*-2.26 [63] and later versions) for the standard that covers all the PHY and MAC primitives, and carried out a comprehensive performance study including evaluations of both the beacon-enabled and nonbeacon-enabled modes, and slotted and unslotted CSMA-CAs. Results of comparisons between IEEE 802.15.4 and IEEE 802.11 in terms of packet delivery ratio, signaling overhead and hop delay have been reported in [73]. Lu *et al.* [74] also simulated a beacon-enabled IEEE 802.15.4 network in an *ns*-2 environment and discussed the trade-offs between throughput, energy consumption and delay. Their results revealed that the use of a low duty cycle enables a significant energy saving at the cost of increased packet delay and degraded data throughput.

Golmie *et al.* [75] studied the suitability of IEEE 802.15.4 for medical environments using the OPNET simulation tool. They evaluated the performance improvements due to packet segmentation and backoff parameter tuning in terms of packet loss, throughput and packet delay. In [76], Timmons and Scanlon simulated a star-topology body area network consisting of up to ten body implanted nodes and an external node acting as a coordinator. Their results were focused on the long-term power consumption of the nodes. In [77], the standard was assessed for ultra low power radios operating in dense networks, and the authors found that the average power per node can be reduced to as low as 211 μW.

In addition, a few analytical studies of the IEEE 802.15.4 MAC have appeared recently. Park *et al.* [44] proposed a per-user Markov chain model of IEEE 802.15.4 and analyzed the throughput and energy consumption under saturation conditions. Their approach closely follows the method of Bianchi [62] for modeling the IEEE

802.11 distributed coordination function (DCF). In [45], Pollin *et al.* extended the approach of [44] by proposing an improved Markov chain model and a more accurate method to compute the probabilities of performing the two CCAs in the slotted CSMA-CA. However, the extension of their model to periodic traffic was ambiguously explained.

Misic *et al.* [78,79] proposed a similar Markov chain model to that of Bianchi [62], and provided a detailed queuing analysis of star-topology IEEE 802.15.4 networks in the beacon-enabled mode. The impact of different MAC parameters (e.g., packet arrival rate, network size and message length etc.) was investigated in [80]. However, their approach seems to be overly complicated and the accuracy of their analysis is unconfirmed.

Ramachandran *et al.* [81] performed an analysis of throughput and energy consumption by modeling the IEEE 802.15.4 CSMA-CA as non-persistent CSMA with random backoff under Poisson packet arrivals. Their results showed that shutting down the radios between packet transmissions significantly saves substantial energy without compromising throughput. They also identified certain delay-sensitive scenarios where setting the inactive period in a superframe may not be appropriate and proposed a modification of setting CW equal to one instead of two (as a default value in the standard) in the beacon-enabled mode when acknowledgements are not used.

Singh and Kumar [82] carried out a saturation throughput analysis for IEEE 802.15.4 CSMA-CA using an embedded Markov renewal process that yields a fixed point equation, and then they extended the analysis to model the finite arrival rate case. The authors validated their analysis against the simulation results obtained from the IEEE 802.15.4 *ns*-2 module developed by [73] after a few bugs in the module were rectified.

The systems analyzed in the aforementioned studies mostly operate under steady state conditions. Leibnitz *et al.* [83] identified a scenario where each node in a network only has one packet to send and all of the nodes initiate their transmission attempts in a synchronized manner. They then presented a non-stationary analysis for the IEEE 802.15.4 CSMA-CA using a two-dimensional Markov model, and

derived expressions for throughput and energy consumption. However, the state transitions of the proposed non-stationary Markov chain does not appear to be consistent with their stated assumption of the non-acknowledgement mode, and a two-dimensional chain seems to be insufficient to distinguish successful and aborted attempts in order to derive the probability of success.

In [84], Yedavalli and Krishanmachari considered the same traffic scenario as [83] and termed it "one-shot data" (OSD). The authors modeled the IEEE 802.15.4 CSMA-CA as p-persistent CSMA and analyzed the throughput and packet delay under saturation conditions. They then extended their analysis to the OSD traffic condition using a quasi-stationary approach, i.e., the system enters a new stationary stage upon every successful packet transmission. One of the main simplifying assumptions in their work is that a packet will be retransmitted an unlimited number of times until it is successful, which may lead to intolerable packet delays in practice. Finally, the authors proposed an enhancement to the standard by adjusting the backoff windows after every successful transmission.

In this chapter, we formulate a new three-dimensional non-stationary Markov chain model to evaluate the performance of the IEEE 802.15.4 MAC. Our model captures the qualitative behavior of the non-stationary system operating in the OSD traffic condition and accurately approximates the packet delivery statistics.

3.4 Non-stationary Markov Chain Modeling

3.4.1 Model Assumptions

Wireless sensor networks are an important class of LR-WPANs. In this work, we assume an IEEE 802.15.4 wireless network consisting of C sensor nodes located within radio range of the network coordinator. The network is organized in a star topology and operates using the IEEE 802.15.4 beacon-enabled mode in the 2.4 GHz frequency band. Therefore, the nodes in the network are synchronized and they attempt to transmit using the slotted CSMA-CA mechanism. The MAC parameters are set according to the default values specified in the standard and the packet length

is fixed to L time slots for all nodes.

In many sensor networks that serve to monitor the environment, information is gathered by sensor nodes and forwarded to the network coordinator. As such, communication is primarily on the uplink (from nodes to coordinator), to which we restrict our attention in this work. Schemes of acknowledgement and retransmission are usually used for reliable data transmissions in traditional packet switched communication networks [11]. As one of the main energy saving characteristics of IEEE 802.15.4, it is nevertheless optional for a receiver to transmit an acknowledgement after it receives a packet. We refer to the scenario when acknowledgements are turned off as the non-acknowlegement (NACK) mode. In wireless sensor networks, the NACK mode may be suitable for many scenarios where sensors are redundantly deployed or where only a fraction of reports need to be collected [85,86]. We assume the NACK mode in this work.

It is assumed that all nodes are located within each others' carrier sensing range and thus a node is able to determine the real channel activity (whether other nodes are transmitting or not) through channel sensing. In other words, the hidden/exposed terminal problems [87] of wireless networks are not considered here.

In addition, we concentrate our analysis on the MAC layer and assume ideal operations in other layers. We also set $CW = 1$ to simplify the analysis. Note that in [81], it is shown that setting $CW = 1$ improves both throughput and energy efficiency in the NACK mode.

3.4.2 One-shot Data Collection

A scenario of *batched arrivals* [88] where many nodes attempt to transmit packets at the same time is problematic for CSMA [89], since the collision rate will be high. However, this is precisely the type of workload anticipated for many sensor network applications [86,90,91]. Such a traffic scenario is called one-shot data (OSD) in [84]. In the following, we identify a few typical examples where the OSD traffic pattern might take place.

- Real-time pressure monitoring: A star-topology sensor network is deployed to

monitor the pressure change in different parts of a workshop, and it operates using the IEEE 802.15.4 beacon-enabled mode. Each node is required to send a pressure report every five minutes to the network coordinator when a network active period starts, and it is allowed to sleep immediately after the message transmission.

- Bush fire detection system: A large-scale cluster tree (see Figure 3.2) sensor network is deployed in a rural area and operates using the IEEE 802.15.4 nonbeacon-enabled mode. A local bush fire triggers a number of sensor nodes on the spot to be activated and immediately start sending reports to their cluster heads.

In both of the two scenarios, each node only has one packet to transmit every time and the nodes simultaneously start their transmission attempts. While most performance analyses of wireless networks address the traffic conditions of saturation and stochastic packet arrivals (e.g., Poisson packet arrivals), it is important to understand the performance of the IEEE 802.15.4 MAC under the OSD traffic condition.

3.4.3 Attempt Probability

Here, we present an expression for the attempt probability P_n, which we define as the probability that the concerned node senses the channel in a particular slot n. We use an approach that has been successfully used to analyze the truncated binary exponential backoff algorithm in Ethernet [92]. The same technique was extended to the IEEE 802.11 distributed coordination function in [89].

The probability P_n can be approximated by:

$$P_n = \sum_{m=0}^{M} P_n(m),\ n = 0, 1, 2, \ldots \tag{3.1}$$

where $P_n(m)$ denotes the component probability that a node chooses slot n for its mth attempt, and M equals *macMaxCSMABackoffs*. $P_n(m)$ is determined using the

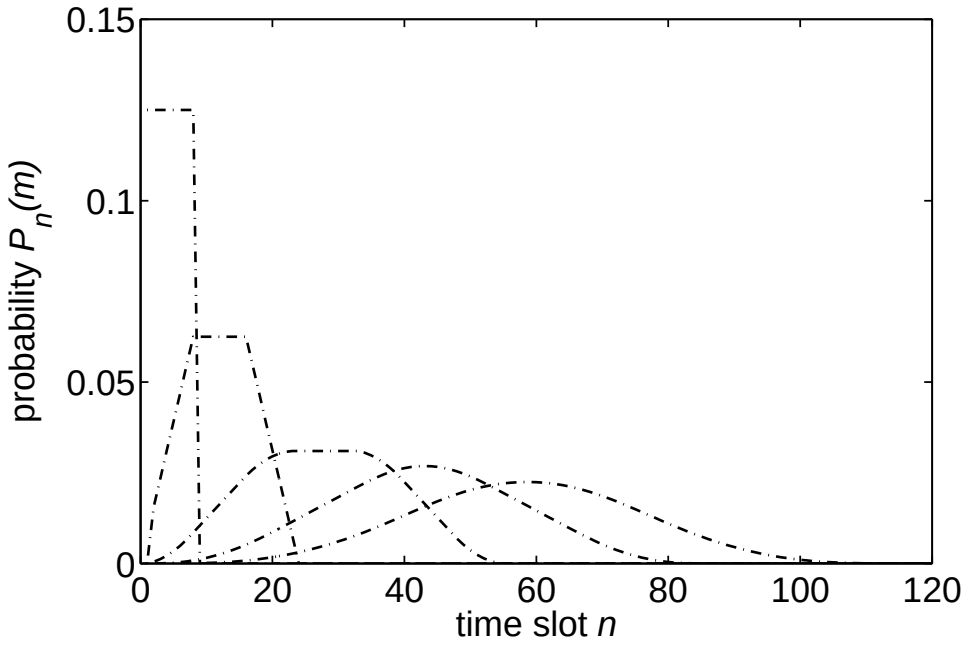

Figure 3.6: Attempt probability components. $macMinBE = 3$, $M = 4$, $aMaxBE = 5$. The lines represent the component probabilities $P_n(0)$, $P_n(1)$, $\cdots$, $P_n(4)$ from left to right.

following recursive equations:

$$\begin{aligned} P_n(0) &= \begin{cases} \frac{1}{W_0}, & 0 \le n < W_0 \\ 0, & \text{otherwise} \end{cases} \\ P_n(m) &= \frac{1}{W_m} \sum_{k=\max(0,n-W_m+1)}^{n} P_k(m-1), \quad m > 0 \end{aligned} \tag{3.2}$$

where W_0 denotes the initial backoff window and is equal to $2^{macMinBE}$, and W_m denotes the backoff window for the mth attempt and is given by $min(2^m W_0, 2^{aMaxBE})$, $m = 0, 1, \cdots, M$. The same result can be obtained using a convolution method [83], as we now show. Let B_m be a uniform random variable representing the length of the backoff period that the concerned node chooses in its mth backoff stage, and its probability mass function (pmf) is given by

$$p_m(b_m) = Pr\{B_m = b_m\} = \frac{1}{W_m} \tag{3.3}$$

where b_m denotes an outcome of B_m, and $b_m = 0, 1, \cdots, W_m - 1$. Define $D_m =$

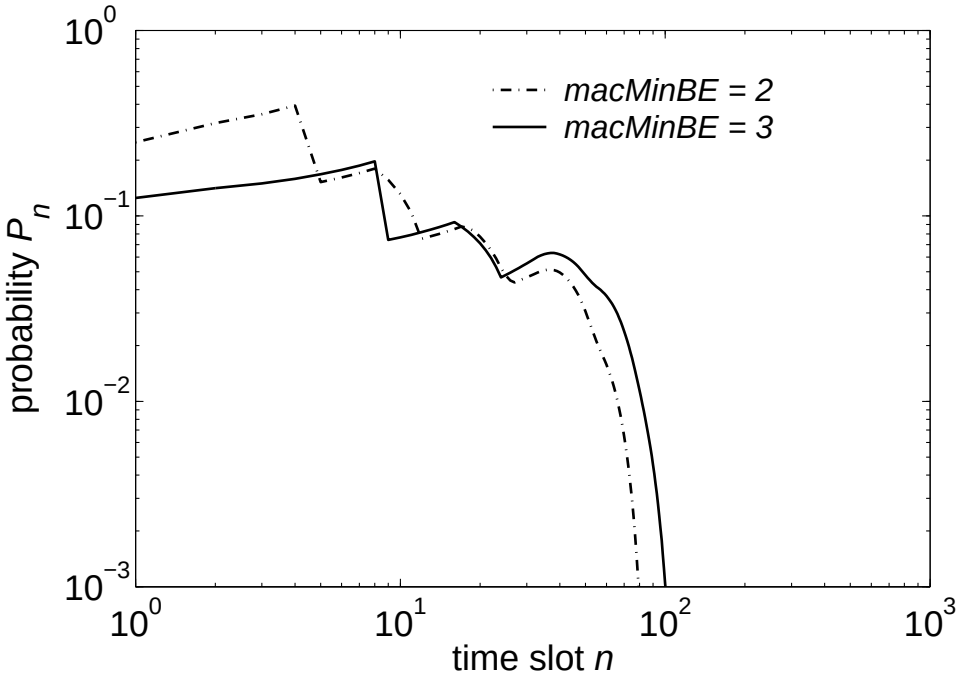

Figure 3.7: Attempt probability. $M = 4$, $aMaxBE = 5$.

$\sum_{i=0}^{m} B_i$, and thus D_m is a sum of random variables, so it is also a random variable that represents the total backoff duration until the mth backoff stage. The pmf of D_m is

$$\begin{aligned} p(d_m) &= Pr\{D_m = d_m\} \\ &= Pr\{B_0 + B_1 + \cdots + B_m = d_m\} \\ &= p_0 * p_1 * \cdots * p_m(d_m) \end{aligned} \tag{3.4}$$

where d_m denotes an outcome of D_m and the symbol $*$ represents the discrete convolution operator. The distribution function $p(d_m)$ represents the probability for the concerned node to choose a certain slot for its mth backoff, and is equivalent to $P_n(m)$ (see Figure 3.6 for an illustration). Figure 3.7 shows the attempt probability P_n for $aMaxBE = 5$, and, alternately, $macMinBE = 2$ and $macMinBE = 3$, and the distinctive saw tooth pattern is consistent with the results in [89, 92].

3.4.4 Non-stationary Markov Chain

In this section, we present our non-stationary Markov chain model. We first classify the nodes in the network as active nodes or inactive nodes. The former includes:

1. *backoff nodes* which are nodes in the backoff state, and
2. *transmitting nodes* which are nodes that are currently transmitting their packets.

The latter includes:

1. *successful nodes*, which have successfully completed their transmissions without collision;
2. *collided nodes*, which simultaneously detected an idle channel and started transmitting in the same slot (as a result their packets collided);
3. *aborted nodes*, which have discarded their packets after exceeding the *macMaxCSMABackoffs* attempts or could not finish transmission in the current CAP.

Consider the following non-stationary three-dimensional Markov chain denoted by
$\psi_n(c, r, u)$, where c is the number of backoff nodes, r describes the number of slots that have been used for the ongoing transmission or transmissions if multiple nodes start transmitting in the same slot (i.e., in the case of collision), and u, the number of nodes that have successfully accessed the channel (with no collision). The quantity u includes the successful nodes as defined above, and is one more than the number of successful nodes if the ongoing transmission involves only one node.

Assuming perfect CCA operations, let us divide the state space into:

1. *contention states*, in which the channel is clear (i.e., $r = 0$) and so if backoff nodes attempt, they detect the clear channel and start transmitting in the next slot since $CW = 1$. Note that contention states with $c = 0$ are absorbing states.

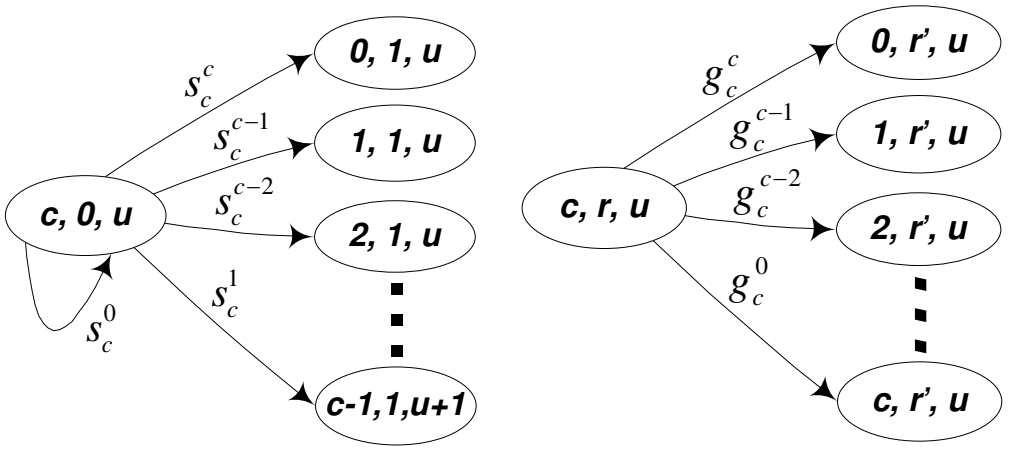

(a) Contention state transitions. (b) Transmission state transitions.

Figure 3.8: State transitions.

2. *transmission states*, in which some node(s) are transmitting (i.e., $r \neq 0$), and if backoff nodes attempt, they find the channel busy and then perform another random backoff until *macMaxCSMABackoffs* is reached.

The transition probabilities for contention states and transmission states are illustrated in Figure 3.8. For contention states, the time-varying transition probabilities are given by the following binomial form:

$$s_c^j(n) = \binom{c}{j} P_n^j (1 - P_n)^{c-j}, \qquad j = 0, 1, ..., c, \tag{3.5}$$

where j denotes the number of nodes attempting in slot n and we define $s_0^0 = 1$. When $j = 1$, one node attempts and starts transmission in the next slot, and the next state at slot $n + 1$ becomes $\psi_{n+1}(c - 1, 1, u + 1)$. When $2 \leq j \leq c$, multiple nodes attempt in the same slot and simultaneously find the channel clear. They start transmitting in the next slot and hence collide, and the next state is $\psi_{n+1}(c-j, 1, u)$. When $j = 0$, no node attempts and the next state variables remain unchanged. Similarly, for transmission states, the time-varying transition probabilities are given by

$$g_c^k(n) = \binom{c}{k} P_n(M)^k (1 - P_n(M))^{c-k}, \qquad k = 0, 1, ..., c, \tag{3.6}$$

where k denotes the number of nodes that perform their last attempt in slot n and $P_n(M)$ is defined in (3.2) with $m = M$, and we define $g_0^0 = 1$. If a node performs its last (i.e., Mth) attempt in a transmission state, it detects the channel busy and then it aborts. Therefore, if $1 \leq k \leq c$, these k nodes abort and the next state becomes $\psi_{n+1}(c-k, r', u)$, where $r' = \mod(r+1, L+1)$, meaning that r increases by one and returns to 0 after it reaches L (i.e., the packet(s) have finished transmission). When $k = 0$, no node performs its last attempt, and the next state is $\psi_{n+1}(c, r', u)$.

The state space with transitions is shown in Figure 3.9. Let us define the state vector at time slot n as

$$\begin{aligned}\Psi_n = \{&\psi_n(C,0,0), \psi_n(0,1,0), \ldots, \psi_n(0,0,0), \psi_n(1,1,0),\\ &\ldots, \psi_n(C-1,1,1), \psi_n(C-2,2,1), \ldots, \psi_n(0,0,C)\}.\end{aligned} \tag{3.7}$$

The initial Ψ_0 is given by $\{1, 0, 0, \ldots, 0\}$, since all C nodes commence at the beginning of a CAP period. Thus, the time-varying transition matrix T_n can be obtained using (3.5) and (3.6). The following simple power method is then applied,

$$\Psi_{n+1} = \Psi_n T_n. \tag{3.8}$$

3.4.5 Packet Delivery Analysis

Let X_n be a random variable representing the number of successfully transmitted nodes at time slot n. The mean of the number of successful nodes η_n is given by

$$\eta_n = \sum_{x=0}^{C} x\ p(X_n = x) \tag{3.9}$$

where $p(.)$ denotes the pmf of X_n, which is given by

$$p(X_n = x) = \sum_{c=0}^{C} \psi_n(c, 0, x) + \sum_{c=0}^{C} \sum_{r=1}^{L} \psi_n(c, r, x+1) \tag{3.10}$$

where the second term represents the case that the last node successfully obtains the channel but is still in transmission.

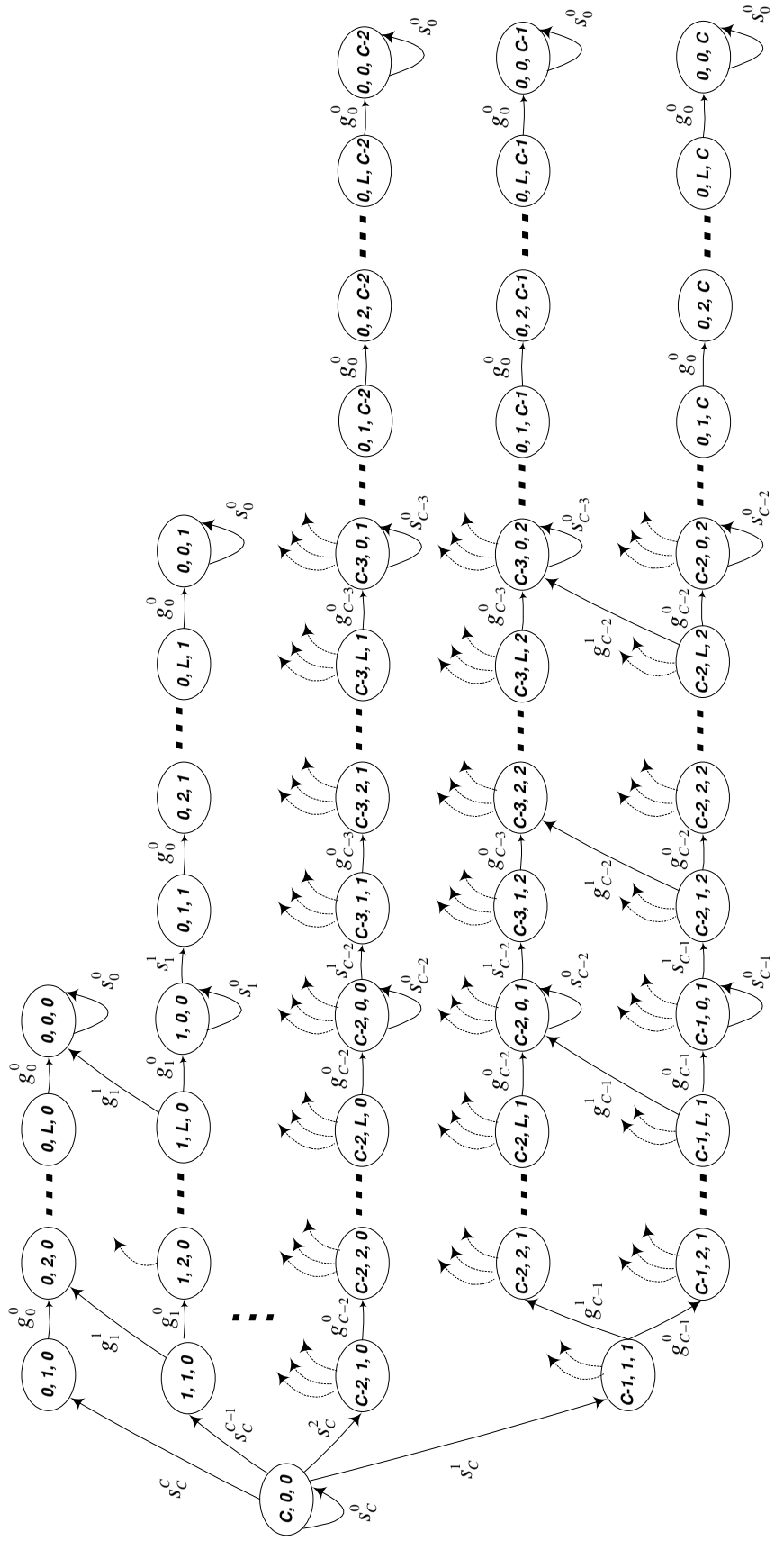

Figure 3.9: Markov chain model. Note that s_c^j and g_c^k represent $s_c^j(n)$ and $g_c^k(n)$, respectively.

Parameter	Value
$macMinBE$	3
$aMaxBE$	5
$macMaxCSMABackoffs$	4
contention window (CW)	1
Message length (PHY) (slots)	variable
Beacon frame length (slots)	3

Table 3.4: System parameters.

Packet losses can be caused by either collisions or discards[1]. Our Markov chain model gives an estimate of the pmf of the number of successful nodes, from which the average packet loss θ_n can be calculated as follows:

$$\theta_n = \sum_{x=0}^{C} (C - x)\ p(X_n = x) \tag{3.11}$$

and the average packet loss percentage ρ_n is given by

$$\rho_n = \frac{\theta_n}{C} \times 100. \tag{3.12}$$

3.5 Numerical Evaluation and Discussion

To verify the accuracy of the proposed model, we compared the analytical results with simulation. The simulation results were obtained using the IEEE 802.15.4 MAC implementation in the *ns*-2 simulator [63] (v2.28), together with the patches developed especially for the NACK mode by the authors of [81]. Each point of the simulation results was averaged over 1000 independent simulation runs. The default values of the IEEE 802.15.4 MAC parameters were used for evaluation, except that for CW we used one instead of two. We assessed the standard that operates in the 2.4 GHz frequency band. Because one *aUnitBackoffPeriod* is equal to 20 symbols,

[1] As stated in Section 3.4.1, we concentrate our study on the MAC layer performance and assume ideal operations in other layers. In practice, packet loss can occur for many other reasons such as link failure or congestion, etc.

it can be easily shown that its length is equal to 10 bytes according to Table 3.2. The length of beacon frames is set equal to three time slots. The system parameters that we used in this work are summarized in Table 3.4.

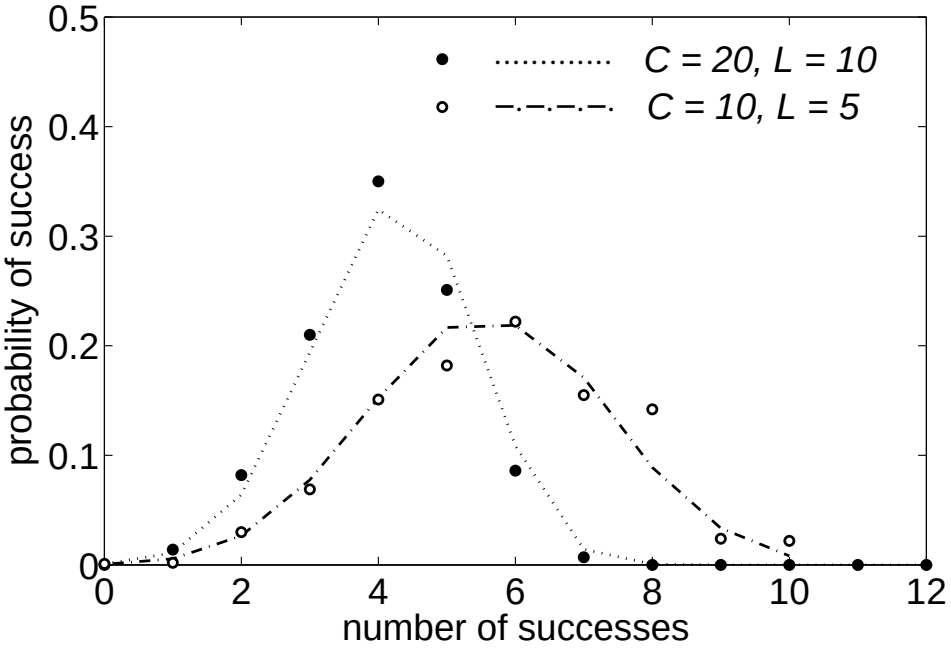

Figure 3.10: Probability mass function of number of successful nodes. Lines represents analytical results.

In Figure 3.10, we show examples of the probability mass function of the number of successful nodes. Lines represent analytical results in our plots. It can be observed that, in general, our analysis matches the simulation.

When we consider an IEEE 802.15.4 network that operates under the NACK mode and uses the default MAC parameters, it can be easily seen that nodes must finish their access (their packets are either transmitted or discarded) within 120 time slots. Thus, we evaluate the performance of the standard by setting $SO = 0, 1, 2$. As seen from Table 3.3, when $SO = 2$, the length of SD is equal to 192 slots, which is longer than the maximum packet access time. Figures 3.11-3.13 illustrate the average packet loss results under various scenarios. Figure 3.14 shows that the average packet loss in the battery extension mode is slightly more than the regular mode. This is because more nodes suffer collisions when the initial backoff window is smaller.

These results show that our analytical model is able to closely predict the packet

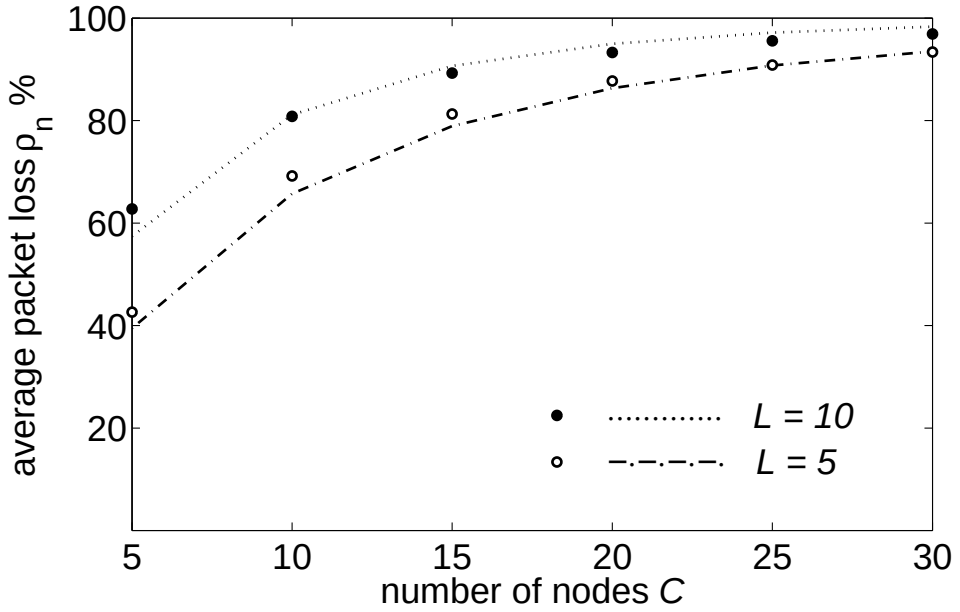

Figure 3.11: Average packet loss. $SO = 0$. The average packet loss ρ_n is indexed on the last time slot of the active period. This also applies to other figures plotting average packet loss in this chapter.

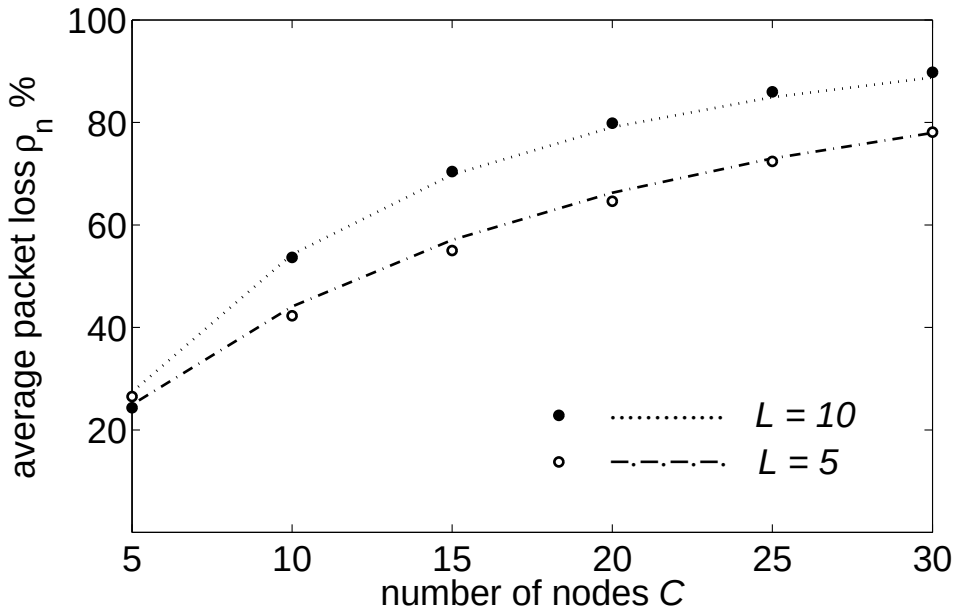

Figure 3.12: Average packet loss. $SO = 1$.

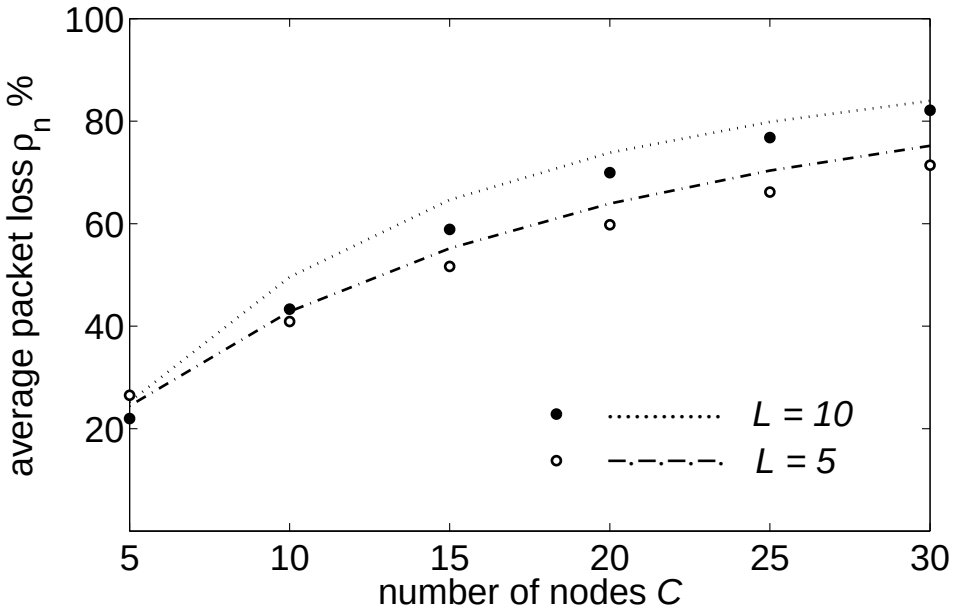

Figure 3.13: Average packet loss. $SO = 2$.

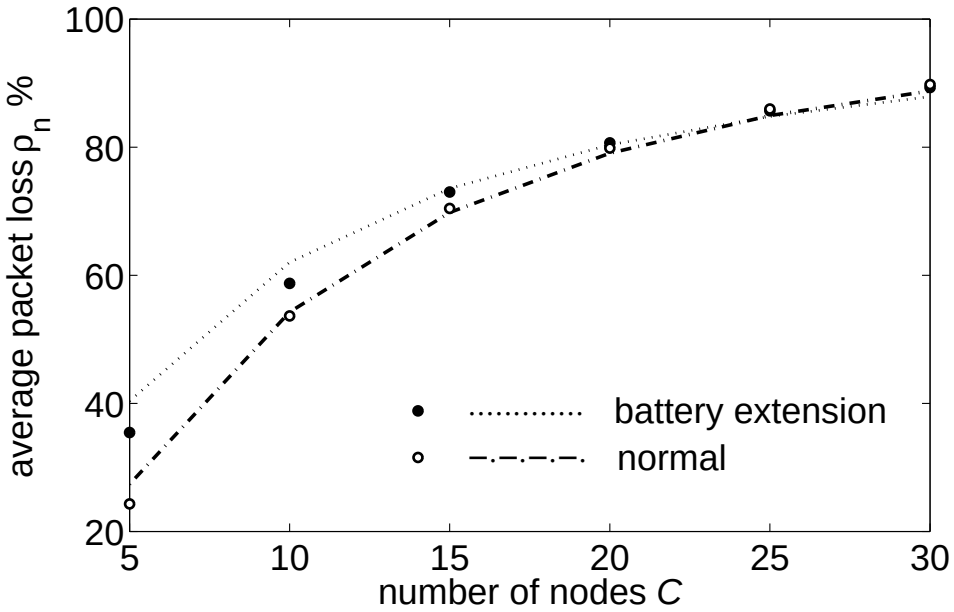

Figure 3.14: Average packet loss. Comparison with battery extension mode. SO=1. L=10.

delivery statistics. It can be seen that the discrepancy between analysis and simulation is slightly greater for $SO = 2$ than for $SO = 0$ and $SO = 1$. This is in fact caused by one of the limitations of our model, which we will discuss in Section 3.5.2.

According to our results, the average number of successful nodes can be very low and the average packet loss rate is considerable under the NACK mode. It is straightforward to see that more nodes will successfully deliver their packets (and thus the packet loss rate becomes lower) when a longer active time is used. It is also demonstrated that the cluster size and message length have a significant influence on the performance of packet delivery. In general, a network with more nodes and longer message length suffers more packet losses. The parameter values of the cluster size and message length need to be properly chosen for satisfactory packet delivery performance.

3.5.1 Alternative Backoff Strategy

As seen from the above results, when a relatively small initial backoff window is used (as the default backoff parameters of the standard), the packet loss rates are significant. This is because most channel activity is focused on the starting period, and thus it leads to a much increased level of contention, especially in case of a large number of nodes. Figure 3.15 shows the probability distribution of channel activity measured by simulation using the default backoff parameters of the standard when $C = 10$ and $L = 5$. It can be measured that 46.5% of the channel activity takes place in the first 24 time slots.

In [82], Singh and Kumar reported that the packet discard probability can be substantially decreased when large initial backoff windows are used in an IEEE 802.15.4 network. Nevertheless, it was found that unnecessary backoff time periods are wasted when using a large initial backoff window and letting the backoff windows grow exponentially as usual. In fact, the number of active nodes are gradually decreasing as time evolves in the OSD traffic scenario. It is unwise that a node backs off in larger and larger steps while the number of its competitors actually becomes less and less.

In this section, we consider a new backoff strategy and empirically choose a set

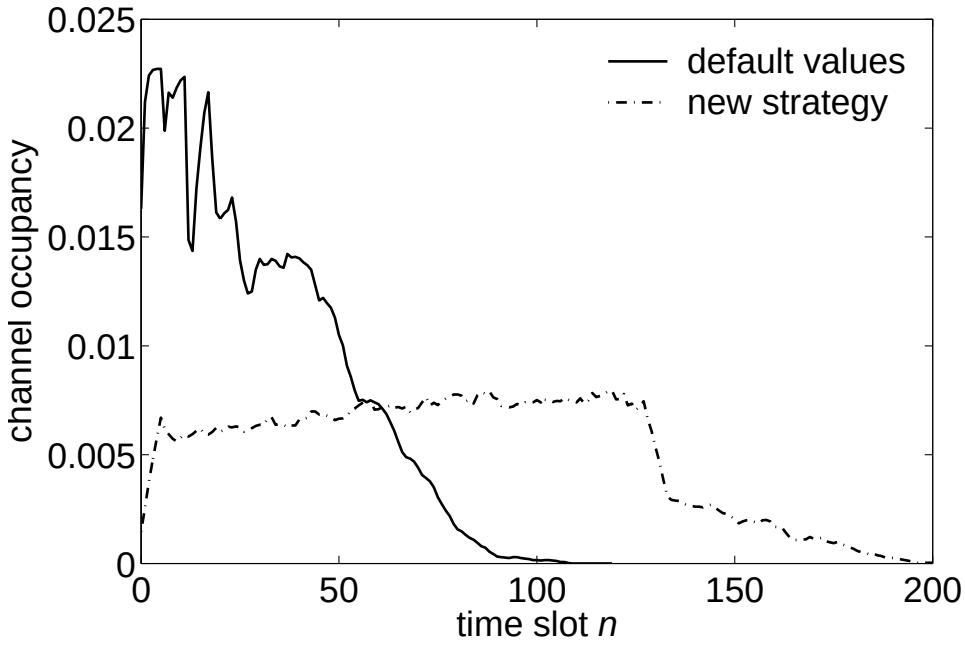

Figure 3.15: Average channel occupancy probabilities. Default values in IEEE 802.15.4 versus our new strategy. $C = 10$, $L = 5$.

of backoff parameters for the IEEE 802.15.4 MAC to reduce the contention level in the starting period and at the same time keep the worst case of packet delay in a reasonable range. In the new strategy, we use a large initial backoff window and a decreasing backoff protocol for subsequent backoffs. To demonstrate the effectiveness, we conducted the experiments by using an initial backoff of 128 slots, a backoff multiplier of 2^{-1}, a minimum backoff window of eight slots and setting $M = 4$. As shown in Figure 3.15, the channel activity is more evenly distributed under the new strategy when $C = 10$ and $L = 5$, compared to that of the default parameter values. The analytical results in Figure 3.16 show that packet loss percentage is substantially reduced. A possible direction for future investigation is to optimize the initial window size and the backoff multiplier depending on the number of nodes to achieve a satisfactory trade-off between packet delivery and packet delay.

3.5.2 Model Limitations

To model the qualitative behavior of the non-stationary system under the OSD traffic condition, we have employed an attempt probability approach, which is based on

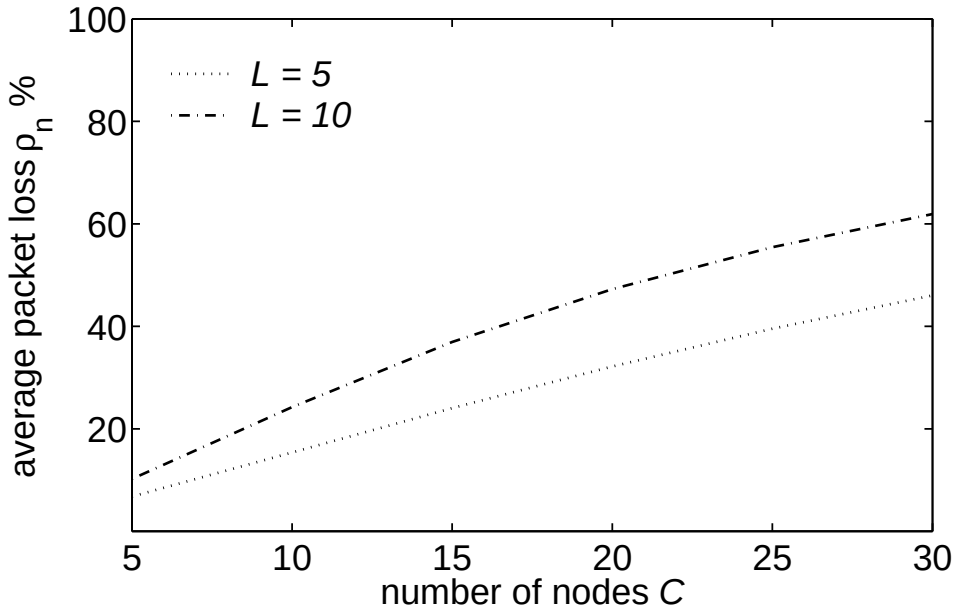

Figure 3.16: Average packet loss when alternative backoff parameters are used. $SO = 2$.

the assumption that the tagged node always reattempts up to the maximum number of attempts. As seen from Figure 3.7, the attempt probability is maintained at a certain level (depending on the chosen backoff parameters) and gradually decreases to some extremely small value.

In our analytical model, we used a non-stationary Markov chain to investigate the network dynamics from a perspective of the system level, and thus the behaviors of a particular node are not captured. Therefore, it is possible that some nodes may still be left unfinished in our analysis at the end of the maximum packet access period, which contradicts the situation in reality where every node must finish its access within the maximum packet access period. Moreover, we used the attempt probability approach which rests on the assumption that a given node will always reattempt until it reaches the maximum retry limit M. Therefore, the attempt probabilities used in our analysis are approximated based on a worst-case scenario, and may not exactly model the behaviors of the nodes in a real system. These approximations used in our model could lead to slightly inaccurate predictions in some cases (e.g., when $SO = 2$ in Figure 3.13).

It is straightforward that the packet delivery ratio would be significantly im-

proved when using larger backoff windows and a bigger M. At the same time, this would lead to longer packet delays and thus more energy wastage. There is an inherent trade-off between packet delivery and packet delay. It seems nevertheless difficult for our current model to accommodate the packet delay analysis.

3.6 Summary

In this chapter, we have given an overview of the recently ratified IEEE 802.15.4 standard for low-rate low-power WPANs, and then reviewed the related body on performance evaluation of the standard. We have developed a new three-dimensional Markov chain model for the IEEE 802.15.4 MAC that yields accurate packet delivery statistics in a star-topology beacon-enabled IEEE 802.15.4 network under the OSD traffic type when acknowlegements are not used. The accuracy of the model has been verified by *ns*-2 simulations. We discovered that the performance of the packet delivery in such networks can be very low. Our results suggest that the cluster size and message length need to be carefully chosen for satisfactory performance. We have also considered a new backoff strategy with a large initial backoff window and decreasing backoff windows for subsequent backoffs to improve the performance of the standard. Finally, limitations of our analytical model have also been discussed.

Chapter 4

Energy Optimization for Wireless Sensor Networks

4.1 Introduction

A sensor network is a collection of nodes with sensing, computing and communication capabilities that continuously observe and collect information on the entities or phenomena of interest in the physical world [93]. Initial research on sensor networks was driven by defense applications and can be dated back to the 1970s [94]. In these early sensor networks (e.g., a radar network used for air traffic control), the sensor nodes are usually large, expensive, and have unconstrained power supply.

Recent advances in MEMS technology, wireless networking and low-power processors have enabled the development of wireless sensor networks (WSNs) which typically consist of a large number of diminutive, cheap, and usually battery-powered microsensors. These sensor nodes can be scattered on the ground, in the air, under water, on human bodies, and in vehicles or buildings. Applications envisioned for WSNs include military sensing, surveillance systems, healthcare systems, industrial and manufacturing automation, distributed robotics, and environment monitoring [32, 33, 94].

Networked microsensor technology has been predicted to be one of the most important technologies for the 21st century, and it could revolutionize spatial information collection and drastically enhance our understanding of the physical environment [95]. On the other hand, it also poses new technical challenges in data processing, energy efficiency, network control and routing, collaborative information processing, sensor management, network security, and other fields [96]. In response to the opportunities and challenges, there has recently been a surge in research in-

terest in sensor networks. The IEEE 802.15.4 standard [1] has been defined and the Zigbee Alliance has been set up to promote low-power low-rate wireless personal area networks. Many WSN research groups (e.g., Smart Dust [97], PicoRadio [98], and WiseNet [99]) have been established. Hardware and software products for WSNs manufactured by companies like Chipcon, Crossbow and Ember are now commercially available.

One of the main challenges for a WSN is its need for an unprecedented system lifetime. In many application scenarios, a deployed WSN is targeted to operate autonomously for several years [99]. A typical sensor node is comprised of a few components such as one or more sensing units for measurement, a microprocessor and a small amount of memory for computing and data storage, and a short range radio for wireless communication [32]. Each of these components consumes energy when a sensor node works. Unlike the traditional wireless devices that are typically mains-powered or powered by rechargeable batteries, low-cost and disposable WSN sensor nodes are constrained by limited on-board batteries that usually cannot be replaced or recharged. As a result, it is necessary to minimize energy consumption at all levels of a WSN system.

In recent years, tremendous research efforts have been devoted to the area of low-power design for WSNs. In [100], Heinzelman *et al.* introduced a clustering protocol architecture called low-energy adaptive clustering hierarchy (LEACH). It randomly rotates the cluster head positions among all the nodes in the network to evenly distribute the energy load of cluster head operation and, as a result, maximizes the network lifetime. Estrin *et al.* [101, 102] proposed a data-centric routing protocol called directed diffusion, where a sensing task is disseminated throughout the network as a task of interest and the data of the events that match the interest are transmitted along multiple gradient paths. A survey of routing protocols for WSNs can be found in [103]. Ye *et al.* [104] identified the major sources of energy waste and proposed a MAC protocol for sensor networks where a low duty cycle is used to allow nodes to spend most of their time asleep. Data aggregation techniques were introduced to perform in-network filtering to combine the redundant messages from highly correlated sources that detect the common phenomena [105, 106]. In

the physical layer, energy-harvesting technologies that exploit solar, vibration, wind or other sources of energy were proposed to supplement power supply for sensor nodes [107].

It is recognized that MAC protocols play a crucial role in meeting the stringent requirement of energy consumption in sensor networks [99]. In this chapter, we restrict our attention to performance improvements for energy efficiency in the MAC layer. Given the low energy consumption requirement of sensor networks, simplicity has been an important feature in the design of MAC protocols including the IEEE 802.15.4 MAC. A question that may be posed is whether further simplification can be made to the MAC protocol. We consider here a simpler protocol, "select-and-transmit" (S&T), which resembles the first step of the slotted ALOHA protocol [42]; in this scheme, a sensor node chooses a transmission slot uniformly in an equally slotted period without using carrier sensing. We compare the S&T MAC protocol with the IEEE 802.15.4 MAC in terms of energy consumption over a wide range of scenarios. In this way, we challenge the IEEE 802.15.4 MAC and perhaps identify scenarios and applications where the standard may not be the best option.

Furthermore, we propose a new framework to minimize energy consumption for WSNs that operate using low duty cycles and are laid out in a single-hop star topology. Given the user-specific QoS requirements (e.g., packet delivery ratio and maximum delay constraints), we optimize the active and inactive time periods of sensor nodes such that the energy consumption per unit time in the entire network is minimized. The S&T MAC protocol and the IEEE 802.15.4 MAC are examined under this energy optimization framework.

The remainder of this chapter is organized as follows. In Section 4.2, we briefly review the energy saving techniques proposed in the MAC layer for WSNs. The S&T MAC scheme and its analysis are presented in Section 4.3. In Section 4.4, we describe the energy models and the energy optimization framework for both the S&T MAC and the IEEE 802.15.4 MAC. Numerical results and discussion are presented in Section 4.5.

4.2 MAC Layer Energy Saving Techniques

The primary design goal of WSN MAC protocols is to meet the stringent requirement of energy efficiency. Traditional performance metrics (e.g., throughput, delay and fairness) for data networks become secondary in WSNs and are usually traded for energy cost [108].

The major sources of energy waste in WSNs have been identified as idle listening, collisions, overhearing, protocol overhead and overemitting [104, 109]. Idle listening refers to the listening performed by nodes for receiving possible traffic that is in fact not sent, and it would occur in many sensor network applications where traffic load is low. Packet collisions also deteriorate the energy efficiency of a WSN. When a transmitted packet is involved in a collision, it would be discarded and possibly retransmitted. Another source of energy waste is overhearing, which means that a node receives packets that are actually not destined for itself. Moreover, protocol overhead consumes energy when control packets are exchanged in the network. The last primary reason for energy waste is overemitting, which occurs when a node sends a message but its intended receiving node is not ready. In the following, we briefly review the existing WSN protocols that use various strategies to eliminate or mitigate the aforementioned causes of energy waste.

4.2.1 Fixed Allocation Protocols

Collisions, idle listening and overhearing can be avoided by using fixed allocation schemes. In [110], Sohrabi *et al.* introduced a distributed protocol called self-organization medium access control for sensor networks (SMACS). This protocol enables nodes to discover their neighbors and build communication schedules without centralized control. Nodes transmit packets using TDMA schedules and randomly choose frequencies (or frequency hopping sequences) to allow concurrent transmissions.

Pei and Chien [111] proposed a power aware clustered TDMA (PACT) MAC protocol which uses passive clustering to rotate the duties of being the communication backbone nodes based on battery energy levels. In PACT, each frame consists

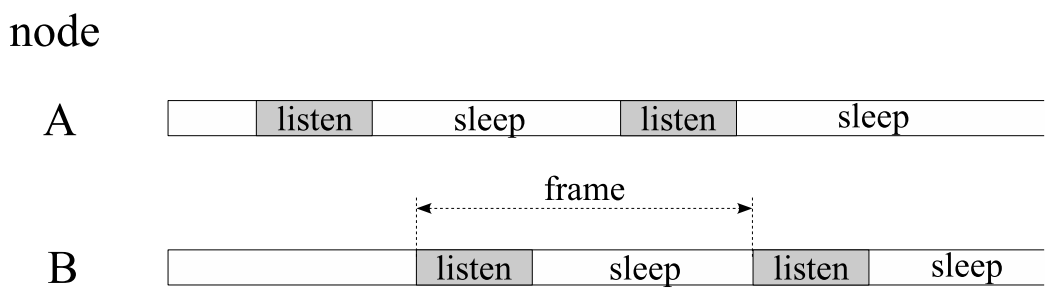

Figure 4.1: S-MAC duty cycle.

of control mini-slots and data slots. In the beginning of a frame, every node turns on its radio to confirm the allocation of the TDMA data slots by exchanging control packets in the control mini-slots. It then shuts down the radio during the slots where it does not transmit or receive packets.

Some other TDMA-based MAC protocols for WSNs can be found in [112–114]. These protocols are inherently free of collision and idle-listening, but they suffer from increased protocol overhead, packet delay and system complexity. In addition, it is inefficient to use static slot assignments in dynamic network environments where the number of active nodes are constantly varying.

4.2.2 Random Access Protocols

In a random access MAC protocol, backlogged nodes contend for the medium to transmit packets, and thus it is more flexible and requires less central control compared to a fixed allocation scheme. Ye *et al.* [104] proposed Sensor MAC (S-MAC), which uses CSMA-CA for channel access. As depicted in Figure 4.1, S-MAC operates using low duty cycles, and each node chooses a sleep schedule and shares it with its neighbors before a listen-sleep cycle starts. Nodes that have common sleep schedules form virtual clusters to reduce control overhead. In S-MAC, nodes only stay awake if involved in communication tasks. To reduce delay, S-MAC uses a technique called adaptive listening, in which a node who overhears its neighbor's transmission will wake up for a short period at the end of the transmission in case it is the next hop for the packet. S-MAC also introduces a message-passing technique, in which long messages are fragmented into many small fragments and transmitted

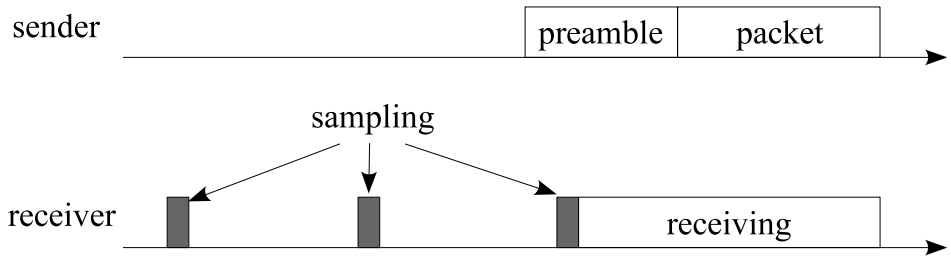

Figure 4.2: Preamble sampling technique.

in a burst, and only RTS/CTS exchange is used. The length of time period to transmit all the fragments and their ACK packets is included in the duration field of RTS/CTS packets. Nodes that hear these RTS/CTS packets will go to sleep until the transmission is finished.

One of the challenges of using S-MAC in a real sensor network is to appropriately determine a sleep schedule, especially under varying traffic loads. The timeout MAC (T-MAC) was introduced by van Dam and Langendoen [115] to adaptively choose a duty cycle. In T-MAC, if a node does not detect any activation event for an empirically determined time threshold *TA*, it assumes that no neighboring nodes want to communicate with it, and goes to sleep. When a node overhears an RTS/CTS message indicating that other nodes will commence transmitting, it temporarily turns off its radio. The node wakes up again at the end of the transmission and starts a new time-out. The advantage of T-MAC is that it dynamically adjusts itself to network traffic fluctuations. However, the aggressive turn-to-sleep policy may cause an early sleep phenomenon where a node goes to sleep when a neighbor node still has messages for it.

Lin *et al.* [116] proposed a dynamic sensor-MAC (DSMAC) by adjusting duty cycles with varying traffic conditions to achieve a good trade-off between energy consumption and packet delay. In DSMAC, all nodes use a common basic service duty cycle at the beginning. When a node sends a packet, the one-hop delay of the packet (the time difference between the arrival of a packet and its departure) is piggybacked. If the receiver node notices that the packet delay is intolerable, it makes a decision to double the duty cycle by reducing the length of sleep period. In the synchronization period of the next cycle, the new duty cycle is announced, and

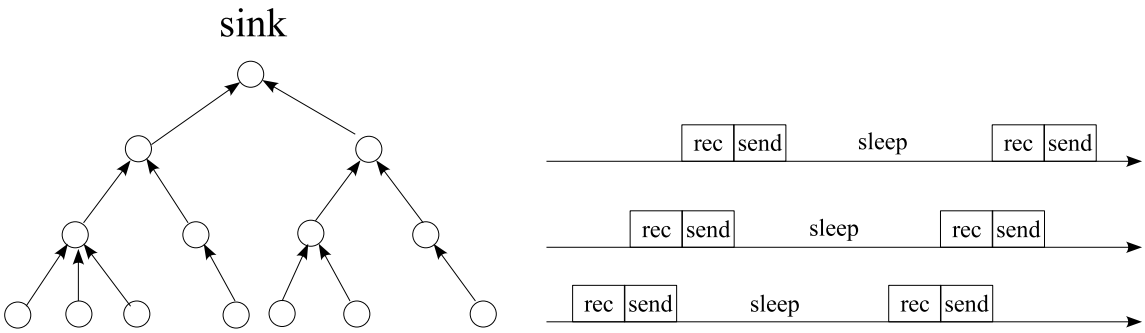

Figure 4.3: DMAC in data gathering tree (adapted form [2]).

a node will adopt it only if its queue is non-empty and the battery level is above a certain threshold.

In [117], Polastre *et al.* introduced a CSMA-based protocol called Berkeley MAC (B-MAC) which provides configurable interfaces of system services for performance optimization. In B-MAC, clear channel assessment is performed by using a weighted moving average of samples for effective collision avoidance. Instead of using exponential backoffs, B-MAC includes a configurable linear backoff mechanism to minimize packet delay. Furthermore, an adaptive low power listening technique is employed to reduce duty cycles and minimize idle listening.

El-Hoiydi *et al.* [118] developed the wireless sensor MAC (WiseMAC) protocol that uses a preamble sampling technique. Preamble sampling is based on a carrier sense technique that effectively shifts the energy cost from the receiver to the senders. As illustrated in Figure 4.2, a sender node transmits a wake-up preamble followed by the backlogged message. In WiseMAC, all nodes in the network perform channel sampling periodically with independent sampling offsets. If the channel is detected busy, it continues to listen and receives data. To reduce the energy caused by unnecessarily long preambles, the authors introduced a scheme where sampling schedules are shared among direct neighbors by piggybacking schedules into acknowledgement frames. Consequently, a sender node can transmit a minimized wake-up preamble just before the sampling moment of the intended receiver to minimize energy consumption.

Lu *et al.* [2] designed the data gathering MAC (DMAC) protocol to achieve very low packet delay without compromising energy efficiency. As shown in Figure 4.3,

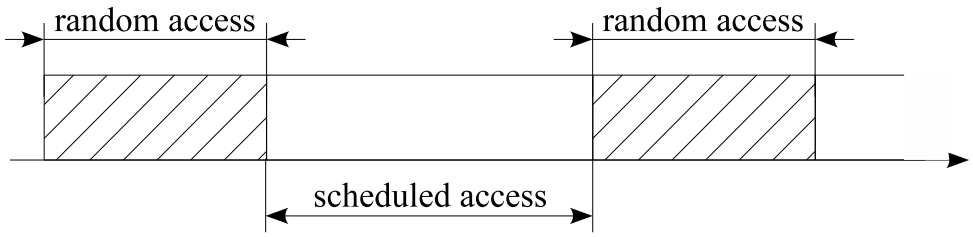

Figure 4.4: Slot organization in TRAMA.

a hierarchical node-to-sink data gathering tree is formed in DMAC. The protocol operates using a low duty cycle, and each cycle is divided into receiving, sending and sleep periods. The main design feature of DMAC is that it uses a staggered wake-up schedule such that packets can be transmitted continuously from nodes to sink along a multihop path (see Figure 4.3). In a receiving state, a node receives packets from its leaf nodes which contend for the medium based on a CSMA protocol.

Despite the flexibility and low protocol overhead, random access MAC protocols may suffer from collisions, idle listening, and long packet delay under high contention levels.

4.2.3 Hybrid TDMA/CSMA Protocols

A few hybrid MAC protocols that combine the strengths of TDMA and random access have been proposed. Rajendran [119] developed the traffic-adaptive MAC (TRAMA) protocol for energy-efficient and collision-free channel access in WSNs. In TRAMA, time is divided into random access and scheduled access periods, as depicted in Figure 4.4. In the random access period, nodes transmit signaling packets, establish two-hop topology information among neighboring nodes, and exchange transmission schedules. As a result, backlogged nodes are allocated dedicated slots in the scheduled access periods for data transmission.

In [120], Rhee *et al.* introduced a hybrid MAC protocol, called zebra MAC (Z-MAC), which operates adaptively to the contention level of the network. In Z-MAC, a time slot is assigned to an owner node of the slot, and the other nodes that can also use the slot are called non-owners of the slot. Unlike fixed slot assignment in TDMA, CSMA-based random access is used for data transmission in Z-MAC. The

owner node of a slot has the priority to access the slot by using a smaller initial contention window than those of the non-owner nodes. When the contention level is high, the owner nodes have prioritized channel access to their slots to avoid collisions so that Z-MAC behaves like TDMA. Under low contention, however, the protocol operates like CSMA because the owner node of a slot may not have data to transmit and the non-owner nodes can contend for the use of the slot. In this way, the Z-MAC protocol is able to dynamically switch between TDMA and CSMA depending on the traffic load.

4.2.4 Other Protocols

Some other WSN MAC protocols that use distinct energy saving techniques from the aforementioned protocols were also proposed. In [121], Schurgers *et al.* developed the sparse topology and energy management (STEM) protocol, in which a low-power secondary paging channel is used for transmitting wake-up signals. Upon receiving a wake-up signal, a node turns on its primary radio for data transmission. The authors show that the protocol is especially suitable for networks having sporadic traffic.

Tay *et al.* [86] proposed a CSMA/p^* protocol that uses optimal channel access probabilities for CSMA to minimize the probability of collision. The same authors empirically chose a non-uniform probability distribution for channel access and developed the Sift protocol that is a suboptimal version of CSMA/p^* in the case of unknown network size [122].

4.3 S&T MAC Scheme

In this section, we describe the S&T MAC scheme. We also derive the probability that at least k out of n nodes successfully transmit their packets under the S&T MAC. This is a new solution to a problem that bears some similarity to certain occupancy problems [123].

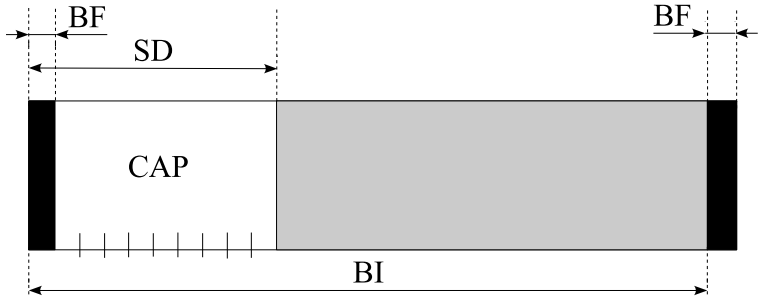

(a) Network coordinator superframe.

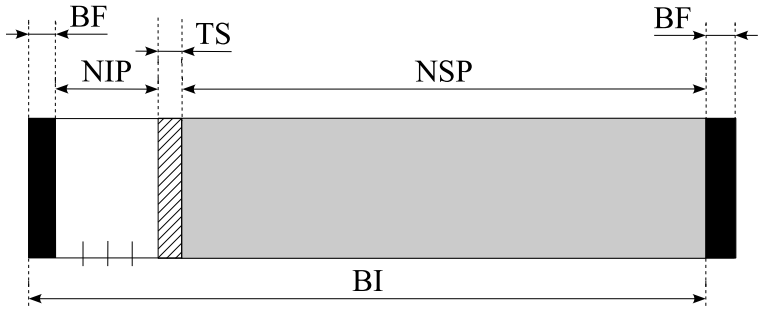

(b) Sensor node superframe.

Figure 4.5: S&T MAC superframe structures.

4.3.1 Protocol Description

The network scenario we consider, similar to that defined in IEEE 802.15.4, is a beacon-enabled star-topology network where one node is designated as the network coordinator. As shown in Figure 4.5(a), in the S&T superframe structure, we divide the superframe duration (SD) into coarse slots such that each slot is sufficient to transmit one packet. The slot size can be slightly increased if acknowledgment frames are required after the successful reception of the data by the coordinator.

In the S&T MAC, a backlogged node wakes up at the beginning of a beacon interval (BI), listens to the beacon frame (BF), and then chooses a slot for transmission in the contention access period (CAP) according to a uniform distribution, i.e., if TS denotes the index of the chosen slot, then $TS = i$, $i = 1, 2, ..., T$, with probability $1/T$. (Note that we call $i = 1$ the slot immediately after the BF.) Let T_{bn}, T and T_{bi} denote the lengths (all measured in number of slots) of BF, CAP and

BI, respectively.

After waiting for a node idle period (NIP), T_{nip}, which equals $TS - 1$ slots, the node transmits its packet and then goes back to sleep for a node sleep period (NSP), T_{nsp}, until the end of the current BI. If two or more nodes select the same slot, a collision results. The superframe structure for the nodes is illustrated in Figure 4.5(b).

4.3.2 Protocol Analysis

Because a node chooses a transmission slot uniformly in T, the mean of T_{nip} in the S&T MAC is given by

$$E[T_{nip}] = \frac{T-1}{2}. \tag{4.1}$$

We can also compute the mean of the node sleep period T_{nsp} as follows:

$$\begin{aligned} E[T_{nsp}] &= T_{bi} - T_{bn} - E[T_{nip}] - 1 \\ &= T_{bi} - T_{bn} - \frac{T+1}{2}. \end{aligned} \tag{4.2}$$

The probability of at least one collision in S&T MAC, p_c, is given by

$$\begin{aligned} p_c &= 1 - P(\text{no collision}) \\ &= 1 - \binom{T}{n} \Big/ T^n \end{aligned} \tag{4.3}$$

where n denotes the number of contending nodes. As depicted in Figure 4.6, the probability of at least one collision is almost unavoidable in S&T MAC, even when n is small and T is big. This is obviously undesirable for most of the traditional data networks, in which QoS requirements such as low loss rate and high throughput need to be met.

However, as discussed in Chapter 3, a considerable packet loss may still be tolerable in the context of sensor networks. This is because multiple nodes may be deployed in the same geographic area for fault-tolerance and reliability, and so it is highly possible that many nodes will sense the same events. In order to deliver

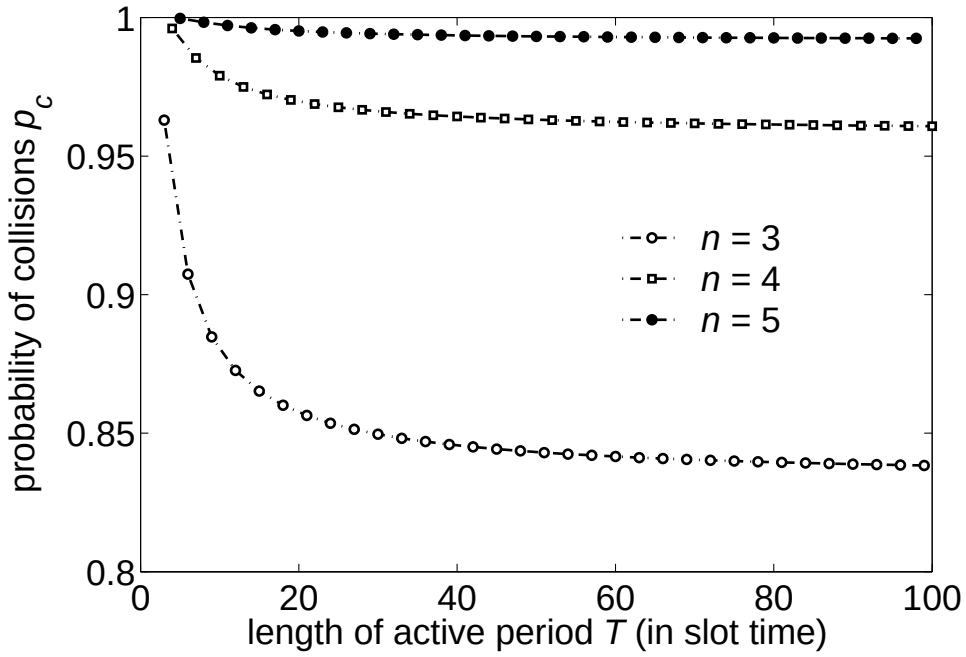

Figure 4.6: Probability of collision.

the information of an event to the coordinator, only one (or a few more for reliability) out of the nodes that observe the event is required to successfully report the event [86].

At this point, we digress slightly to mention an interesting fact concerning the throughput of the protocol. According to the results in Exercise 3.4 in [124], the expected number of slots with exactly one packet is given by

$$n_s = n\left(1-\frac{1}{T}\right)^{n-1}. \tag{4.4}$$

Let S be the normalized throughput which is defined as follows:

$$S = \frac{n_s}{T}. \tag{4.5}$$

Figure 4.7 shows the throughput for different scenarios. It can be observed that when the number of slots is equal to the number of nodes, i.e., $n = T$, the throughput is maximized.

We now derive the probability that at least k out of n nodes successfully transmit their packets (i.e., without collisions) in a given T using the S&T MAC scheme. This

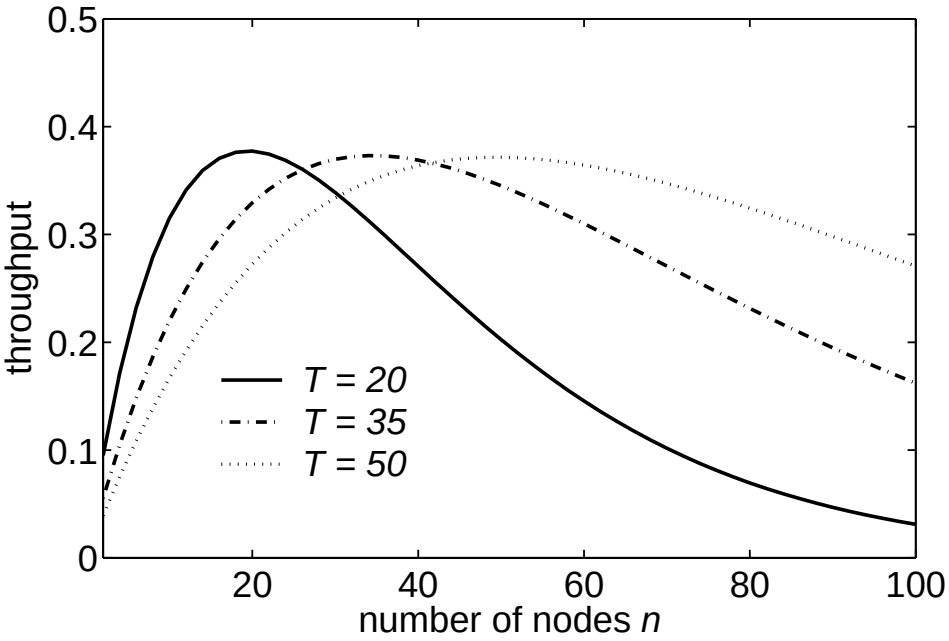

Figure 4.7: Throughput.

is in fact equivalent to a generalized birthday problem pertaining to the probability that at least k out of n people have different birthdays. Let P_k denote the probability that *exactly* k out of n nodes are successful. The following result holds.

Lemma 1. (a) If $n \leq T$,

$$P_n = \frac{T!}{T^n(T-n)!} \tag{4.6}$$

(b) If $0 \leq k \leq n-2$ and $k < T$,

$$P_k = \frac{1}{T^n} \times \sum_{w=k}^{\min(n,T)} \binom{n}{w}\binom{T}{w}\binom{w}{k} w!\,(-1)^{w-k}(T-w)^{n-w}. \tag{4.7}$$

Proof. See Appendix A. □

We define Q_k to be the probability that *at least* k out of n nodes are successful. It follows from Lemma 1 that for $1 \leq k \leq n-2$ and $k < T$

$$Q_k = 1 - \sum_{j=0}^{k-1} P_j \tag{4.8}$$

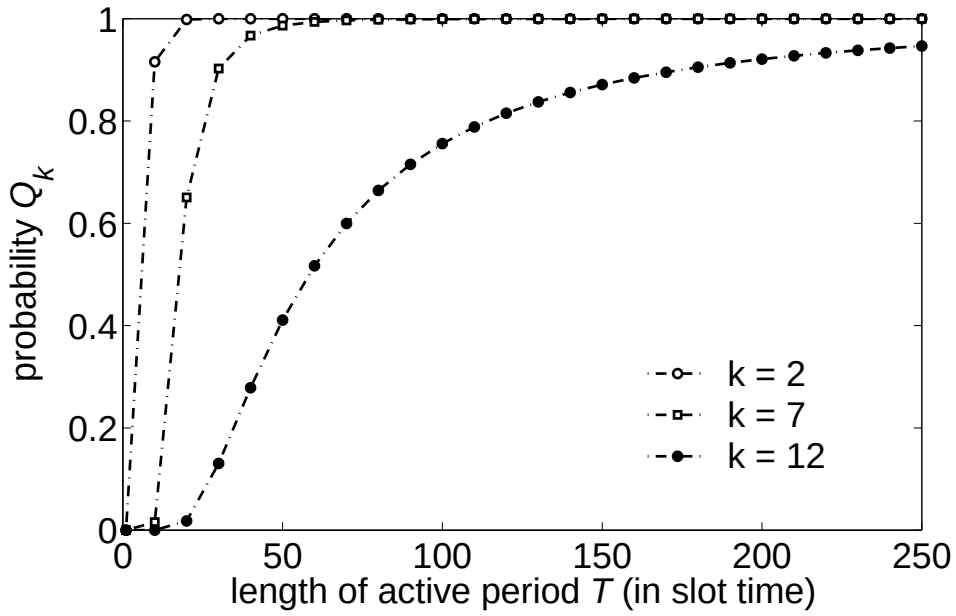

Figure 4.8: Probability Q_k versus length of active period T. $n = 15$.

where P_j is given by (4.7). Note that when $k = n - 1$, P_k is equal to P_n, i.e., the probability of $n-1$ successes out of n nodes is the same as the probability that all of the n nodes are successful. This is because the last node cannot collide with itself.

Figure 4.8 demonstrates that when k is relatively small compared to n, the probability Q_k can be made to quickly converge to 1 through a modest increase in T, while a much larger T is required for the same effect if k is large. A large active period T is undesirable since it corresponds to high energy consumption. These results suggest that the S&T MAC is most likely to be a competitive MAC solution for scenarios where only a small proportion of the packets are needed to report some event (e.g., event-driven workload [86]). It should be noted that the S&T MAC has the advantage of simplicity; it entails only a small number of operations which may facilitate the reduction of energy consumption for computation and possibly lead to simplification of hardware design.

4.4 Energy Optimization Framework

In this section, we first describe the energy models and then formulate optimization problems which minimize the energy consumption per unit time of the whole net-

work. We then apply the energy optimization framework to the S&T MAC and the IEEE 802.15.4 MAC.

Consider N to be a random variable representing the number of backlogged nodes at the beginning of a BI, and let n denote an outcome of N. We also allow the requirement for the number of successful packets k to vary as a function of n, and we capture this dependence through the notation $k(n)$. In addition, we introduce the following notation.

- N_{all} : number of nodes (excluding the coordinator) in the network.
- p_N : probability mass function of N.
- D_{max} : maximum delay constraint, [s].
- $W_{k(n)}$: probability of at least k successes out of n nodes for the IEEE 802.15.4 MAC.
- $Q_{k(n)}$: probability of at least k successes out of n nodes for the S&T MAC.
- $\eta_{k(n)}$: a user-specific QoS requirement for $W_{k(n)}$ and $Q_{k(n)}$.
- S_{bn} : slot duration for the BF, for the IEEE 802.15.4 MAC, [s].
- S_{sd} : length of SD in the IEEE 802.15.4 MAC, [s].
- S_{bi} : length of BI in the IEEE 802.15.4 MAC, [s].
- S_{nip} : average node idle time spent in backoff state, for the IEEE 802.15.4 MAC, [s].
- S_{nsp} : average node sleep time, for the IEEE 802.15.4 MAC, [s].
- m_{cca} : average number of CCA operations performed in one BI, for the IEEE 802.15.4 MAC.
- m_{tx} : average number of packet transmissions in one BI, for the IEEE 802.15.4 MAC.
- t_{slot} : slot size, for the S&T MAC, [s].

Parameter	Value
Voltage (V)	3
Transmit current (mA)	20
Receive current (mA)	15
Idle current (mA)	10
Average current for active coordinator (mA)	16
Sleep current (mA)	0.03
Initialize radio and time(mA, s)	6, 3.5×10^{-4}
Turn on radio and time (mA, s)	1, 1.3×10^{-3}
Sleep to RX and time (mA, s)	15, 2.5×10^{-4}

Table 4.1: Electrical specifications.

- P_{active} : average coordinator power consumption during SD, [mW].
- P_{idle} : node power consumption in idle period, [mW].
- P_{sleep} : node power consumption in sleep period, [mW].
- E_{sum}^{std} : overall energy consumption in one BI, for the IEEE 802.15.4 MAC, [mJ].
- $E_{sum}^{s\&t}$: overall energy consumption in one BI, for the S&T MAC, [mJ].
- E_0 : node energy consumption to wake up and listen to the BF, [mJ].
- E_t : node energy consumption to transmit a packet, [mJ].
- E_{cca} : energy consumption to perform a CCA operation, [mJ].

4.4.1 Energy Models

A typical sensor node consumes energy when it carries out different operations such as computation, data storage, radio communication, *etc.* In our energy models, we only investigate the energy consumption of the radio unit, which is highly relevant to the design of MAC protocols. A sensor node usually supports four modes of operation (e.g., the Chipcon CC1000 transceiver [125]):

- sleep, in which a node operates under a very low power consumption and its radio is completely turned off;
- idle, in which a node temporarily turns off some circuitries, and its radio unit operates in a low power mode and can be immediately turned on by receiving a corresponding command;
- transmit, in which a node transmits data;
- receive, in which a node receives data;

In addition, we also consider the energy consumption when a node turns on its radio, switches between transmitting and receiving states, and samples the channel to determine the channel status. In our energy models, we use the same electrical specifications as in [117], and they are summarized in Table 4.1.

In the following, we apply the energy models to the S&T MAC scheme and the IEEE 802.15.4 MAC. For simplicity, we do not use acknowledgments for both of the two MAC schemes and assume an ideal channel such that every transmitted packet that does not suffer a collision is successfully received.

S&T MAC

In the S&T MAC, the overall energy consumption in a network during one BI consists of a few components. Firstly, the network coordinator is active for $T_{bn} + T$ slots and inactive for $T_{bi} - T_{bn} - T$ slots. Secondly, every node spends energy E_0 in waking up and listening to the BF. When a node wakes up, it switches from sleep mode to receive mode and turns on its radio. Thirdly, the backlogged nodes transmit their packets by randomly selecting slots in T. Therefore, a backlogged node on average spends T_{nip} in the backoff state and goes back to sleep for T_{nsp}, i.e., the rest of the current BI. Finally, non-backlogged nodes immediately go to sleep after the BF and expend $P_{sleep}(T_{bi} - T_{bn})$ amount of energy.

Therefore, given that there are N_{all} nodes in a network and n of them are backlogged, the overall energy consumption in one BI for the S&T MAC, $E_{sum}^{s\&t}$, can be

given by

$$E_{sum}^{s\&t}(n) = \underbrace{\left(P_{active}(T_{bn}+T) + P_{sleep}(T_{bi}-T_{bn}-T)\right)t_{slot}}_{for\ coordinator} + \underbrace{N_{all}E_0}_{for\ all\ nodes}$$
$$+ \underbrace{n(P_{idle}E[T_{nip}]t_{slot} + E_t + P_{sleep}E[T_{nsp}]t_{slot})}_{for\ backlogged\ nodes} + \underbrace{(N_{all}-n)P_{sleep}(T_{bi}-T_{bn})t_{slot}}_{for\ non-backlogged\ nodes}. \tag{4.9}$$

IEEE 802.15.4 MAC

Similarly, the following four components contribute to the overall energy consumption of an IEEE 802.15.4 network in one BI. The first part is from the fact that the network coordinator is active for S_{sd} and inactive for $(S_{bi}-S_{sd})$. Secondly, each node in the network consumes E_0 in waking up and listening to the BF. Moreover, the backlogged nodes perform, on average, m_{cca} CCA operations in one BI and m_{tx} of the nodes eventually transmit their packets using the slotted CSMA-CA mechanism. The CCA mode we choose for our energy model is "carrier sense only", in which a busy medium is reported only when a signal with the modulation and spreading characteristics of 802.15.4 is detected [1]. A backlogged node on average spends S_{nip} in the backoff state and goes back to sleep for S_{nsp}, i.e., the rest of the current BI. Finally, non-backlogged nodes consume $P_{sleep}(S_{bi}-S_{bn})$ amount of energy in one BI.

In summary, the overall energy consumption in a BI for the IEEE 802.15.4 MAC, E_{sum}^{std}, is given by:

$$E_{sum}^{std}(n) = \underbrace{P_{active}S_{sd} + P_{sleep}(S_{bi}-S_{sd})}_{for\ coordinator} + \underbrace{N_{all}E_0}_{for\ all\ nodes}$$
$$+ \underbrace{m_{cca}E_{cca} + m_{tx}E_t + n(P_{idle}S_{nip} + P_{sleep}S_{nsp})}_{for\ backlogged\ nodes} + \underbrace{(N_{all}-n)P_{sleep}(S_{bi}-S_{bn})}_{for\ non-backlogged\ nodes}. \tag{4.10}$$

Note that there are two major differences between the energy consumption models of the two MAC schemes. Firstly, a S&T node does not perform carrier sensing before transmission. Secondly, in the standard, a backlogged node may not have

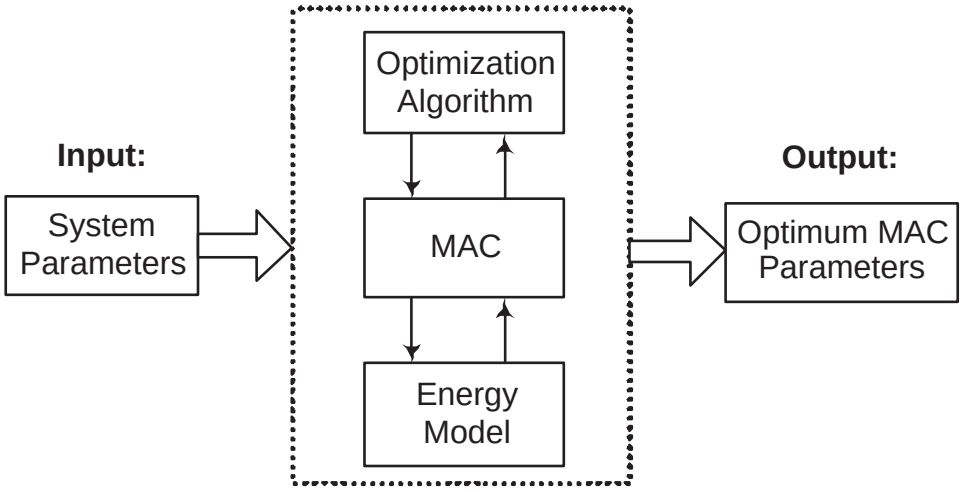

Figure 4.9: Energy minimization framework.

a chance to transmit its packet before the end of the current CAP, while in S&T MAC, every backlogged node transmits its packet.

4.4.2 Energy Consumption Optimization

In sensor networks, there is an inherent trade-off between energy efficiency and other performance metrics such as average packet delay and packet delivery ratio. To minimize energy consumption, sensor networks usually operate with extremely low duty cycles (e.g., 1% or 0.1%) such that sensor nodes are allowed to spend most of their time in sleeping. In the existing MAC protocols for WSNs, duty cycles are either empirically decided (e.g., as in S-MAC [104]) or adaptive only to traffic loads (e.g., as in T-MAC [115] and DSMAC [116]). The solution to the problem of optimal duty cycles while satisfying a range of user-specific QoS constraints still remains unaddressed.

In this work, we present an energy optimization framework which minimizes energy consumption in sensor networks and attains the flexibility to incorporate various QoS requirements. Figure 4.9 shows a general structure of the proposed framework. Given the system parameters such as the traffic models and the user-specific QoS parameters, we design duty cycle optimization algorithms that interact with the underlying MAC protocol and energy models. Our aim is to minimize the expectation of the overall energy consumption per unit time. To this end, we

describe the generic optimization problem as follows:

Objective function: *minimize: expected unit time energy consumption*

Decision variables: *sensor active and inactive time periods in one cycle*

Constraints: *packet delivery ratio and maximum packet delay .*

Taking the expectation of the overall energy consumption per unit time in one BI, we now formulate the energy optimization problem for the S&T MAC as follows:

$$\begin{aligned} \min : & \frac{1}{T_{bi}\ t_{slot}} \sum_{n=0}^{N_{all}} p_N(n)\ E_{sum}^{s\&t}(n) \\ s.t. \quad & Q_{k(n)} \geq \eta_{k(n)} \\ & (T_{bi} + T) t_{slot} \leq D_{max} \\ & T \geq k(n) \\ & T_{bi} \geq T + T_{bn} \end{aligned} \tag{4.11}$$

where $n = 0, 1, ..., N_{all}$. Here the decision variables are T and T_{bi}. The first constraint is to satisfy that at least k out of n nodes are successful with probability no less than $\eta_{k(n)}$, and the second constraint is to meet the maximum delay requirement. The third constraint is to set a lower bound for T, which must be greater than or equal to the number of the required successful nodes $k(n)$. The fourth constraint shows that the length of a SD is no longer than that of a BI.

Similarly, the optimization problem for the IEEE 802.15.4 MAC is formulated as follows:

$$\begin{aligned} \min : & \frac{1}{S_{bi}} \sum_{n=0}^{N_{all}} p_N(n)\ E_{sum}^{std}(n) \\ s.t. \quad & W_{k(n)} \geq \eta_{k(n)} \\ & S_{bi} + S_{sd} - S_{bn} \leq D_{max} \\ & 0 \leq SO \leq BO \leq 14 \end{aligned} \tag{4.12}$$

where $n = 0, 1, ..., N_{all}$. The decision variables are SO and BO. Note that S_{sd} and S_{bi}

are one-to-one functions of SO and BO, respectively. Again, the first and the second constraints are packet delivery ratio and maximum packet delay, respectively. The worst case packet delay we consider is equal to $S_{bi}+S_{sd}-S_{bn}$, which will be explained in the traffic model in the next section. The third constraint $0 \leq SO \leq BO \leq 14$ is defined in the standard.

4.5 Numerical Evaluation

In this section, we first describe the traffic model we used and define three different scenarios to evaluate the performance of the proposed energy optimization framework. We then solve the energy optimization problems for the S&T MAC and IEEE 802.15.4 MAC and present the numerical results.

4.5.1 Traffic Model

In the scenario we consider, a node becomes backlogged if during the previous BI (including the sleep time) one or more packets have been generated for transmission. The random variable N representing the number of backlogged nodes at the beginning of a BI is generally distributed and this distribution is denoted as $p_N(n)$, where n denotes an outcome of N.

We make the observation that if more than one packet is in the transmission buffer, it is possible for users to make choices regarding the order of transmission and whether redundant packets can be dropped. In particular, if packets awaiting transmission contain information on the same event, only the latest is relevant, and it is sensible to discard the old ones. In our setup, we assume that when a node generates a new packet, it will be accommodated into the transmission buffer if the buffer is empty. When there is already a packet in the node's buffer, the action taken depends on the status of the node. If the node is active, it means the buffered packet is attempting to transmit, so the new packet will wait to transmit in the next BI. If the node is sleeping, the new packet will replace the old one, which will be discarded.

Furthermore, since duty cycles of sensor networks are usually very low, we assume

Scenario	α_1	α_2
A	0.2	0.1
B	0.5	0.4
C	0.8	0.7

Table 4.2: Scenarios for evaluation.

that a packet which is generated in the previous BI will be discarded if it fails to be transmitted in the current SD. This explains the worst case delay constraints we used for the optimization problems for both MAC schemes.

4.5.2 Scenario Definition

As mentioned in Section 4.4, k is defined as a function of n. To evaluate the performance of energy consumption for the two MAC protocols, we define a generic function $k(n) = \min(\alpha_1 n, \alpha_2 N_{all})$, where $\alpha_1, \alpha_2 \in (0, 1)$ and $\alpha_1 \geq \alpha_2$. This function typically allows k to increase proportionally with n until it hits the upper bound $\alpha_2 N_{all}$ when n is close to N_{all}.

Three scenarios with different values of α_1 and α_2 are defined for evaluation, as shown in Table 4.2. In Scenario A, we are interested in the successful transmission of a very small proportion of the packets. Applications consistent with these scenarios could be event-driven sensor networks (refer to [86] for detailed examples). Conversely, in Scenario C most of the packets need to be transmitted successfully. Scenario B corresponds to an intermediate case.

4.5.3 Results and Discussion

We adopted the electrical specifications used in [117] (reproduced in Table 4.1), which are based on the CC1000 transceiver [125]. We assume that the transmit and receive power levels are constant and the same for all nodes. Some other system parameters are shown in Table 4.3. We also used the specifications of the various frequency bands (i.e., the frequency bands of 868 MHz, 915 MHz and 2.4 GHz) defined in IEEE 802.15.4 [1]. Note that the slot sizes we used in S&T MAC are

Parameter	Value
Data packet size (PHY) (bytes)	25
Beacon frame size (bytes)	25
Maximum packet delay (s)	5
Average packet arrival rate (packets/s)	0.5
QoS requirement $\eta_k(n)$	0.90
Number of slots for BF in S&T MAC, T_{bn}	1
Slot duration for S&T MAC	variable

Table 4.3: Other system parameters.

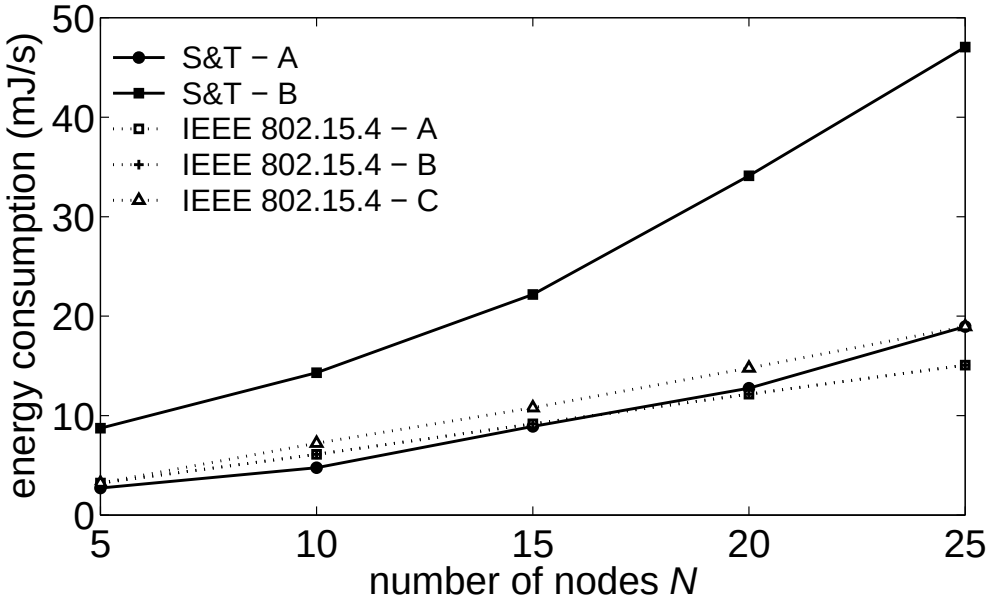

Figure 4.10: Minimal energy comparison between S&T MAC and IEEE 802.15.4 MAC in the 868 MHz frequency band.

0.01 s, 0.005 s, and 0.001 s corresponding to the frequency bands 868 MHz, 915 MHz and 2.4 GHz, respectively.

We chose Poisson processes for packet generation of the nodes, which means that for each node, the probability to become backlogged at the beginning of a BI is given by

$$p_{nd} = 1 - e^{-\lambda t} \tag{4.13}$$

where λ is the average packet arrival rate and and $t = T_{bi}\ t_{slot}$ for the S&T MAC and $t = S_{bi}$ for IEEE 802.15.4 MAC. Given a network with N_{all} sensor nodes, the

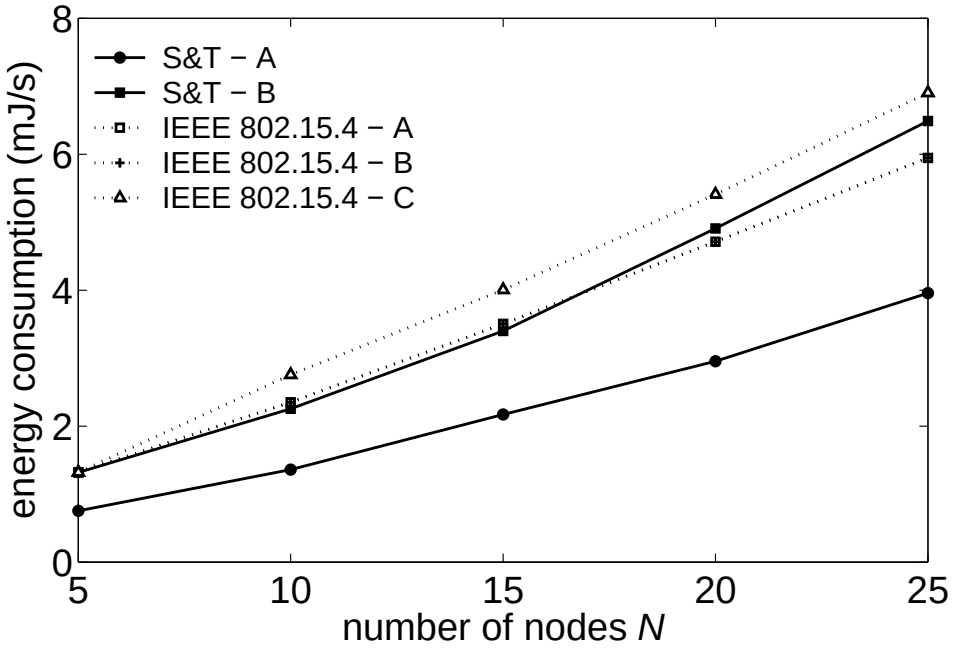

Figure 4.11: Minimal energy comparison between S&T MAC and IEEE 802.15.4 MAC in the 2.4 GHz frequency band.

probability mass function of N is given by

$$p_N(n) = \binom{N_{all}}{n} p_{nd}^n (1 - p_{nd})^{N_{all}-n}. \tag{4.14}$$

We implemented a simulator for the IEEE 802.15.4 MAC in the C++ programming language. For each set of parameters (i.e., SO, BO, n and N_{all}), we ran a simulation to obtain the packet delivery ratio $W_{k(n)}$ and all the parameters required to compute the energy consumption based on (4.10). We have repeated the process a sufficient number of times such that the radius of the 95% confidence interval based on student-t distribution is within 5% of the energy consumption value. For the S&T MAC, given a set of values of T, T_{bi}, n and N_{all}, we have the analytical results (4.1) and (4.2) for the two parameters required for the energy consumption computation, and therefore no simulations were required.

Since T, T_{bi}, SO and BO are all integer-valued and their ranges are limited by D_{max}, we were able to use exhaustive search to solve the optimization problems. For the case of the S&T MAC, we used the analytical result for $Q_{k(n)}$ (4.8) to exclude cases that violate the constraint $Q_{k(n)} \geq \eta_{k(n)}$. We used the GNU Multiple Precision

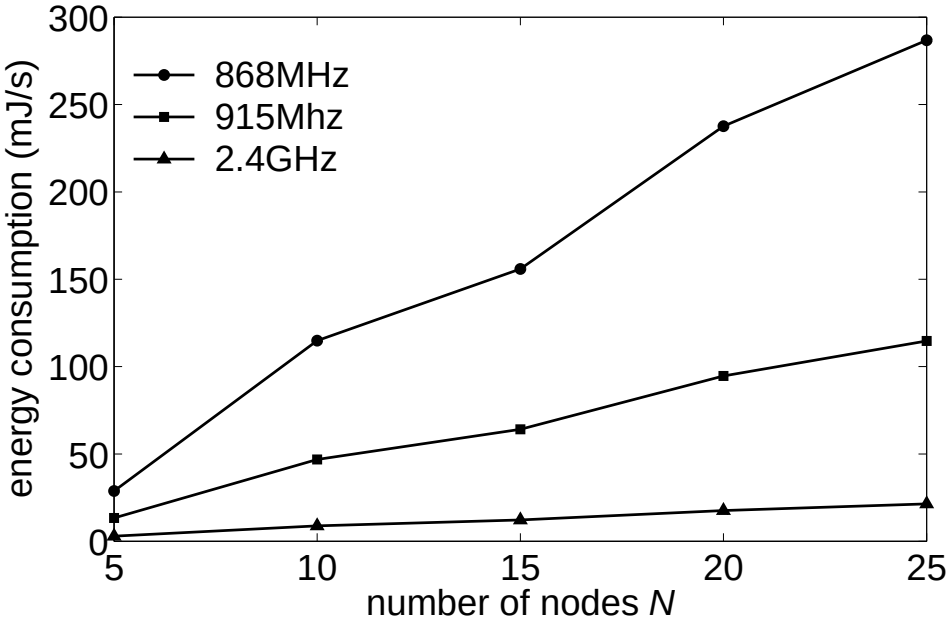

Figure 4.12: Minimal energy consumption of the S&T MAC in Scenario C.

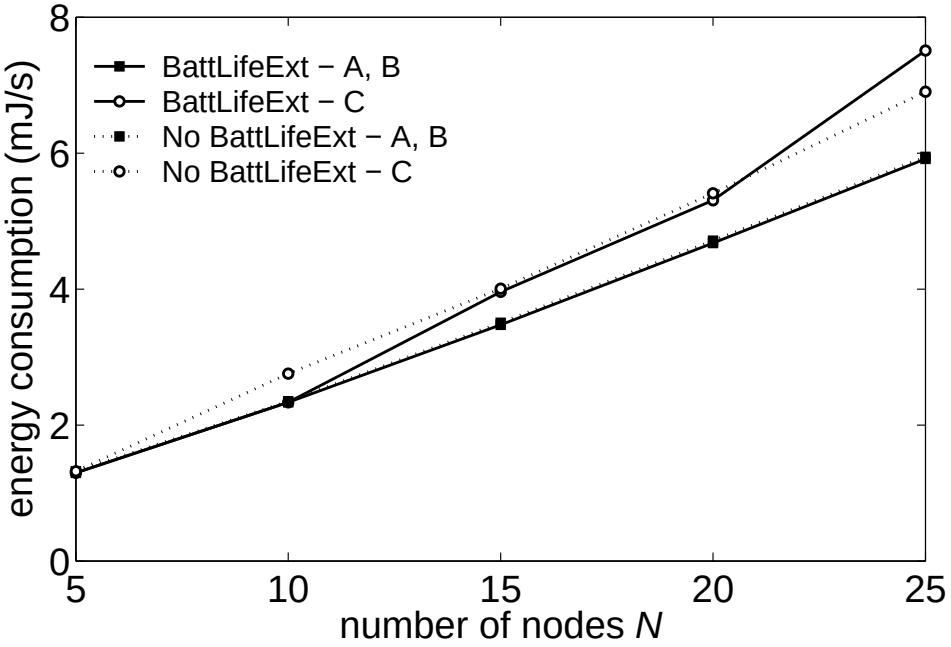

Figure 4.13: Battery life extension mode and regular mode of 802.15.4 in 2.4 GHz frequency band.

Band	N_{all}	Scenario A				Scenario B				Scenario C			
		802.15.4		S&T		802.15.4		S&T		802.15.4		S&T	
		SO	BO	T	T_{bi}	SO	BO	T	T_{bi}	SO	BO	T	T_{bi}
868 MHz	5	0	6	6	492	0	6	30	468	0	6	97	401
	10	0	6	6	492	0	6	30	468	1	6	202	296
	15	0	6	10	448	0	6	34	464	1	6	202	296
	20	0	6	11	487	0	6	41	457	1	6	230	286
	25	0	6	15	483	0	6	47	451	1	6	230	286
915 MHz	5	0	7	6	992	0	7	30	968	0	7	97	901
	10	0	7	6	992	0	7	30	968	1	7	202	796
	15	0	7	10	998	0	7	34	964	1	7	202	796
	20	0	7	11	987	0	7	41	957	1	7	230	768
	25	0	7	15	983	0	7	47	951	1	7	230	768
2.4 GHz	5	0	7	6	4992	0	7	30	4968	0	7	97	4901
	10	0	7	6	4992	0	7	30	4968	1	7	202	4796
	15	0	7	10	4998	0	7	34	4964	1	7	202	4796
	20	0	7	11	4987	0	7	41	4957	1	7	230	4768
	25	0	7	15	4983	0	7	47	4951	1	7	230	4768

Table 4.4: Optimal solutions for 802.15.4 MAC and S&T MAC in different frequency bands and different scenarios.

(GMP) arithmetic library to compute factorials for large numbers [126].

Figure 4.10 - 4.12 illustrate the performance comparisons of the minimal energy consumption for the S&T MAC and the IEEE 802.15.4 MAC in various frequency bands and scenarios. Results for the 915 MHz frequency band are not shown because they are similar to the results for the 868 MHz frequency band.

It can be observed that the energy consumption is significantly reduced when high data rate is used. For relatively small k in Scenario A and B, the energy consumption of the two MAC schemes are comparable. In fact, the S&T MAC has lower energy consumption than the standard in Scenario A when the frequency band is 2.4 GHz.

However, in Scenario C where k is relatively large, the standard can still maintain a low level of energy consumption, while the energy of the S&T MAC increases dramatically, as depicted separately in Figure 4.12. This is because when k is relatively large, the length of CAP, T, needs to be large (and thus the node idle period T_{nip} is greatly increased), as shown in Figure 4.8. The optimal solutions for the two

N_{all}	SO	BO
5	0	7
10	0	7
15	1	7
20	1	7
25	2	7

Table 4.5: Optimal solutions for 802.15.4 MAC with battery life extension in 2.4 GHz frequency band (Scenario C).

MAC schemes are listed in Table 4.4.

We also discovered by simulation that the energy consumption of the 802.15.4 MAC under our proposed energy minimization framework does not benefit from the use of the battery life extension mode. Figure 4.13 compares the energy consumption between the battery life extension mode and the regular mode for the standard operating at 2.4 GHz. Similar results were found for the other frequency bands. The energy consumption remains virtually unchanged when k is small as in Scenario A and B. In Scenario C, while the battery life extension mode shows minor advantage for low traffic load, it performs even worse than the regular mode when the node population becomes large. This is because in the battery life extension mode, the *backoff exponent* BE starts from 2 and thus it has a smaller backoff range than the regular mode, while the maximum number of backoffs, *macMaxCSMABackoffs*, remains the same. When the traffic load increases, there is more contention and more nodes will reach *macMaxCSMABackoffs* and give up transmission. In order to meet the proportion of successful packet transmissions, the SD must be increased, which results in an increase in energy consumption. This is verified by the results in Table 4.5. For example, when N_{all} is equal to 25 in the 2.4 GHz frequency band with Scenario C, the optimal SO becomes 2 ($SO = 1$ is no longer a feasible solution), whereas in the regular mode, the optimal SO remains at 1 (see Table 4.4).

4.6 Summary

In this chapter, we focused on the problem of energy optimization in WSNs. We presented a brief literature review for MAC protocols which use various techniques to reduce energy consumption in WSNs. Given the low energy consumption requirement of sensor networks, simplicity has been an important feature in the design of MAC protocols, including the IEEE 802.15.4 MAC. We considered a simpler protocol, called S&T MAC, in which a sensor node chooses a transmission slot uniformly in an equally slotted period without using carrier sensing. We also derived the probability that at least k out of n nodes successfully transmit their packets under the S&T MAC, which is a new solution to a problem similar to certain occupancy problems.

Sensor networks usually operate with low duty cycles to minimize energy consumption. We presented an energy optimization framework which minimizes energy consumption per unit time of the entire network by optimizing the active and sleep periods, and attains the flexibility to incorporate various QoS requirements, such as packet delivery ratio and maximum packet delay. More specifically, we formulated duty cycle optimization problems that interact with the underlying MAC protocol and energy models when the system parameters such as the traffic models and the user-specific QoS parameters are given.

We then applied the framework to the S&T MAC and IEEE 802.15.4 MAC. Using the same QoS requirements, our results showed that, in most cases, the standard has better performance than the S&T MAC in terms of energy consumption. For scenarios where the packet delivery ratio is low, the S&T MAC has comparable (in some cases even better) performance than the IEEE 802.15.4 MAC. Although the energy efficiency of the S&T MAC has no obvious advantage in most cases compared to the IEEE 802.15.4 MAC, the simplicity of its operations, as discussed in Section 4.3.2, might be an appealing feature for many sensor network applications where the system complexity is desirably kept as low as possible. We have also shown that the battery life extension mode of the standard under our energy minimization framework is no more energy efficient than the regular mode.

Chapter 5

Joint PRMA and Packet Scheduling for Multimedia Cellular Networks

5.1 Introduction

A mobile cellular communication system consists of numerous cells, each of which functions as a basic geographic service unit through a base station (BS). In a cell that may have many mobile terminals accommodated, any activity of communication is centrally controlled by the BS.

Mobile cellular technologies together with the services they provide for subscribers have undergone a tremendous evolution since the first generation (1G) analog cellular networks (e.g., the Advanced Mobile Phone Service (AMPS) [127]) were first deployed in the early 1980s. These cellular systems typically use frequency modulation and frequency division duplex (FDD) for radio transmission and provide data rates of less than 10 kb/s for mobile voice telephone calls.

Subsequently, the second generation (2G) cellular systems that use digital modulation techniques were developed and have significantly outperformed their predecessors in spectrum utilization and security aspects [128]. The Global System for Mobile Communications (GSM) standard has become the most popular 2G cellular system throughout the world. A combination of TDMA and FDMA is employed in GSM. Another widely-used 2G cellular system standard is the Interim Standard 95 (IS-95) [129] which is based on the CDMA technology. In addition to the traditional telephone services, new supplementary data services such as paging, fax and short messaging service (SMS) are provided in the 2G cellular systems.

As an upgrade to the 2G systems, the so-called 2.5G cellular technologies (e.g., the general packet radio service (GPRS) [130] and the enhanced data rates for GSM

Class	Application	Data rate (b/s)	Maximum delay (ms)	Loss rate
CBR	Voice	32 k - 2 M	30-60	10^{-2}
VBR	Videoconference	128 k-6 M	40-90	10^{-3}
UBR	File transfer	1 M-10 M	Large	10^{-8}
ABR	Web browsing	1 M-10 M	Large	10^{-8}

Table 5.1: QoS requirements for different applications (adapted from [7]).

evolution (EDGE) [131]) have been developed in response to the market demand of modern data-centric applications. The 2.5G cellular systems provide substantially increased data transmission capability (for instance, EDGE can provide a raw peak throughput data rate of 547.2 kb/s [132]) to support higher data rate services such as web browsing, e-mail, mobile commerce (m-commerce) and location-based mobile services.

The third generation (3G) cellular networks support multimedia traffic with QoS assurances at peak data rates of 2 Mb/s and provide seamless services across both wired and wireless networks with universal mobility. The CDMA technology has been chosen by 3G standardization groups (3GPP and 3GPP2) [133]. Applications envisioned for 3G networks and their evolutions include voice over Internet Protocol (VoIP), video/audio streaming, video-conferencing, multimedia messaging service, and mobile Internet access, *etc.* Table 5.1 shows four service classes — constant bit rate (CBR), variable bit rate (VBR), unspecified bit rate (UBR) and available bit rate (ABR) [7] — as well as their corresponding QoS requirements and typical applications.

In contrast to 1G and 2G cellular systems, 3G networks are anticipated to carry traffic that is typically a mixture of voice, video, audio and data messages, and need to satisfy diverse QoS targets such as transmission rate, delay bound and maximum tolerable bit error rate (BER). It is believed that traditional voice-based MAC protocols would perform unsatisfactorily in a multimedia environment where the traffic variability is much higher [134]. The coexistence of heterogeneous traffic types in a same cellular network poses new challenges to the design of highly flexible and efficient MAC protocols. Some desirable attributes of a MAC for 3G cellular

networks are

1. spectrum efficiency, in other words, the network can support as many users as possible;

2. satisfying QoS of heterogenous traffic types;

3. low complexity in terms of computation and signaling.

A number of MAC protocols for multimedia CDMA cellular networks have appeared. Akyildiz *et al.* [135] proposed a wireless multimedia access control protocol with BER scheduling (WISPER) where packets with equal or similar BER requirements are allocated in the same slots using an iterative procedure. Huang and Zhuang [136] designed a MAC for time-division duplex (TDD) CDMA networks, in which an optimal packet scheduling algorithm is used to allocate system resources to each user. More recently, Wang [137] introduced a MAC protocol that uses a minimum-power allocation algorithm to minimize the interference (and thus increase the capacity of the network) and exploits both rate- and BER- scheduling to maximize throughput. We shall review the related work in more detail in Section 5.2. These existing MAC protocols are efficient in terms of high data throughput and they meet QoS requirements. However, they may be undesirable in practice due to the high computational complexity of their scheduling algorithms. Moreover, in these protocols, the BS needs to rearrange and broadcast all of the slot assignments to every active terminal before the next uplink frame starts. Consequently, the heavy signaling overhead on the downlink could result in inefficiency and instability, especially when the wireless links are in harsh conditions.

To reduce signaling overhead and at the same mitigate computational requirements, many packet reservation techniques have been proposed for wireless MAC. Packet reservation multiple access (PRMA) has been receiving significant research attention since Goodman *et al.* [138] initially proposed it in 1989. Derived from the reservation-ALOHA (R-ALOHA) [139], PRMA exploits the silent periods of a typical voice conversation to accommodate more users than there are channels available. As a statistical multiplexer, PRMA requires little central coordination from the BS.

Variants of PRMA in CDMA networks, such as CDMA/PRMA [140] and Multidimensional PRMA with prioritized Bayesian broadcast (MDPRMA-BB) [3] have also been proposed. One of the main drawbacks of these PRMA-based MAC protocols for CDMA multimedia networks is that multiple access interference (MAI) significantly degrades the packet transmission success probability when many terminals transmit in a single time slot [141].

In this chapter, we propose a relatively simple yet efficient MAC solution for the uplink in multimedia cellular CDMA networks. In our proposal, the idea of PRMA and packet scheduling techniques are considered jointly to maximize the system throughput, whilst the computational complexity and signaling overhead of the proposed MAC are kept relatively low.

The remainder of the chapter is organized as follows. In Section 5.2, the previous work related to our proposal is reviewed in detail. Our proposal, which we call joint PRMA and packet scheduling (JPPS), is described in Section 5.3. Simulation results and some discussion appear in Section 5.4, followed by a summary in Section 5.5.

5.2 Related Work

5.2.1 The PRMA Protocol Family

Goodman *et al.* [138] proposed the PRMA scheme, which is a TDMA-based protocol to multiplex voice and data traffic in cellular networks. In PRMA, time is divided into frames, each consisting of N fixed-length time slots. The protocol exploits the fact that a typical voice conversation is usually composed of "talking" and "silent" periods. Before the current slot starts, the base station(BS) broadcasts its status, either "available" or "reserved", to all terminals in the cell. The propagation delay is assumed to be negligible and the binary feedback (either available or reserved) is thus available instantaneously prior to the next slot. The PRMA frame structure with an example slot status is shown in Figure 5.1.

When a talkspurt begins, the terminal sends the head-of-line packet to an "available" slot with a certain probability. If only one terminal sends a packet in the slot,

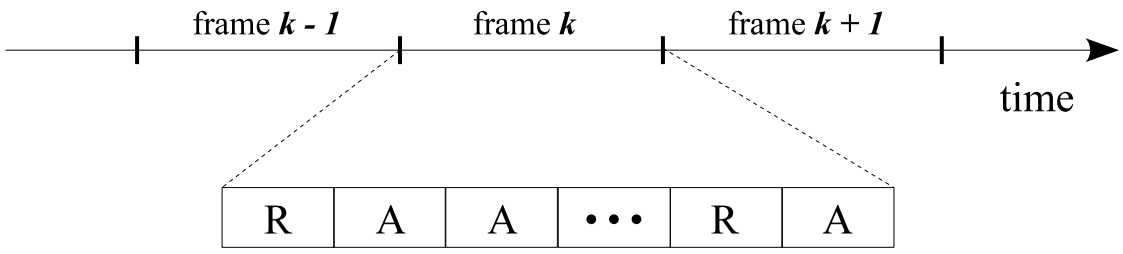

Figure 5.1: Frame structure of PRMA. "A" and "R" denote "available" and "reserved", respectively.

the BS acknowledges the successful reception of the packet and the slot is automatically reserved for the terminal in future frames until the last packet of the talkspurt. If more than one terminal sends packets in a time slot, a collision results and all the contending terminals need to try other free slots. A packet will be dropped if it exceeds the time-out value D_{max}, and the next packet in the spurt will be sent for contention. Data packets are sent in a similar fashion, but no reservation is made for successful packet transmission. Different access probabilities can be used for voice and data terminals to give preference to voice traffic. Performance analysis of the PRMA protocol was presented in [142].

Many variants of PRMA have been proposed. In [143], Narasimhan and Yates introduced a frame reservation multiple access (FRMA) protocol, in which the BS broadcasts an acknowledgement once every frame instead of every slot in PRMA to reduce the receiver activity. Bianchi *et al.* [144] introduced the centralized PRMA (C-PRMA), in which the central role in scheduling transmissions of terminals is assigned to the BS. The QoS requirements of terminals are sent to the BS via random access slots, and the BS employs an earliest due date (EDD) scheduling approach to prioritize the terminals who have the closest deadline. In another variant PRMA++ [145], a few slots in an uplink frame are designated as request slots and the others as information slots. To contend for the medium access, a terminal sends its request in the request slots using the slotted ALOHA protocol, and the BS schedules the terminal's transmission in information slots. The PRMA++ protocol was analyzed in [146].

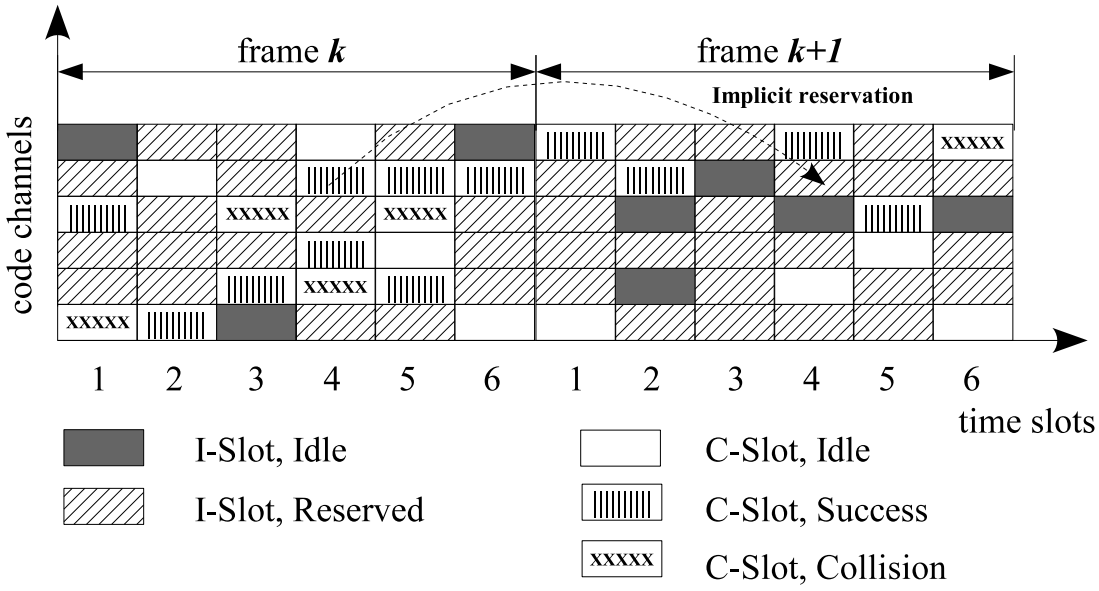

Figure 5.2: Frame structure of MD-PRMA (adapted from [3]).

5.2.2 Joint CDMA and PRMA Protocols

Brand and Aghvami [140] introduced a joint CDMA and PRMA protocol for mixed voice and data transmission. The major differences between CDMA/PRMA and PRMA are as follows. Firstly, a third dimension, namely code channels, is added and thus several terminals can share a single slot by using orthogonal codes. Secondly, instead of the fixed transmission probability p in PRMA, in CDMA/PRMA, p is inversely proportional to the number of accommodated users in the current time slot. As traffic load increases, the performance of CDMA/PRMA suffers from packet corruption and packet dropping due to MAI.

In [3], the MDPRMA-BB MAC protocol was proposed for hybrid TDMA/CDMA systems. The code slots in MDPRMA-BB are either available for contention (C slots) or reserved for information transmission (I slots). As in PRMA, an active terminal will contend in a C slot with a specified access probability. If it receives from the BS a positive acknowledgement indicating the success of the packet transmission, the terminal will implicitly reserve the same slot for future frames until all its buffered packets are transmitted. In downlink frames, the BS broadcasts the access probabilities that were calculated based on the estimated number of the contending terminals and the interference level of the CDMA channels. Figure 5.2 illustrates the frame

structure of the MDPRMA-BB protocol and an example of its implicit reservation mechanism. One of the main drawbacks of the MDPRMA-BB protocol is the lack of support for high-bit-rate services that need multi-slot allocations in each frame. Furthermore, packets of different types with different BER requirements are equally treated in the protocol which is inefficient because the capacity of the slots are in fact limited by the most BER demanding service [134].

In a scheme called joint CDMA/non-collision (NC)-PRMA [141], Wen *et al.* presented a frame structure that is similar to our proposed JPPS protocol. In CDMA/NC-PRMA, all active terminals enjoy the non-collision slot to send their transmission requests through a control slot, and the BS employs slot assignment schemes to accommodate the backlogged terminals into the information slots. The major differences between CDMA/NC-PRMA and our protocol are as follows. First, the non-collision control slot can collect all the transmission requests without contention at the expense of equipping the BS with a specialized n frequency filter bank. In JPPS, on the other hand, a simple optimal channel access scheme is employed to optimize the transmission probabilities and no specialized hardware is necessary. Furthermore, in contrast to the absence of a mechanism to support traffic types other than voice, as proposed in [141], we treat real-time and non-real-time traffic types separately and utilize efficient packet scheduling techniques to maximize throughput.

5.2.3 Packet Scheduling Based MAC protocols

Akyildiz *et al.* [135] proposed a MAC protocol, known as WISPER, for CDMA wireless multimedia networks. In WISPER, one power level for each time slot is used to simplify the system implementation. Assuming all transmission requests are known, the BS first computes the priority levels for all backlogged terminals. By keeping the priority records, the so-called "packet usher procedure" calculates the number of packets of a particular terminal to transmit in the next frame. Then the "packet allocator procedure" assigns time slots for the selected packets based on the BER scheduling rule, which groups the packets with same or similar maximum tolerable BER specifications in the same time slot. The two procedures are iteratively ap-

plied, until all the transmission requests are accommodated or all the time slots are full in the next frame. The numerical results show that WISPER achieves significant improvement in terms of throughput and packet loss ratio over regular slotted CDMA systems that do not use the scheduling techniques.

Based on WISPER, Wang [137] proposed a power minimization algorithm and both rate- and BER- scheduling algorithms were applied. The proposed protocol, which maximizes the slot capacity by allocating the resources using iterative scheduling algorithms and minimizing the power levels at the same time, improves the performance of WISPER, but at the expense of further increased computational complexity.

In [136], Huang and Zhuang introduced a MAC protocol that exploits both time-division and code-division statistical multiplexing for TDD wideband CDMA multimedia networks. An optimal packet scheduling technique for QoS provisioning and high bandwidth utilization was proposed to allocate slots to users with various traffic types such as real-time voice, video and non-real-time bursty data. A heuristic bin-packing algorithm was then considered to solve the packet scheduling problem as a suboptimal but practical solution. The same authors proposed a QoS-oriented MAC protocol with fair packet loss sharing (FPLS) scheduling in [147], where the BER requirements are satisfied by choosing appropriate power levels. Transmission of the multimedia packets is arranged by the FPLS scheduler such that the packet loss is evenly shared by all the admitted users.

5.3 Joint PRMA and Packet Scheduling

5.3.1 System Definition

In January 1998, the European and Japanese 3G standard, Universal Mobile Telecommunications System (UMTS), was ratified by the European Telecommunications Standards Institute (ETSI) [34, 148]. Two modes are included in the UMTS Terrestrial Radio Access (UTRA): an FDD mode and a TDD mode. In this chapter, we propose a MAC protocol for the uplink data transmission by considering PRMA and

Multiple access scheme	TD-CDMA
Chip rate	3.84 Mchips/s
Modulation	QPSK
Bandwidth	5 MHz
Frame Size	10 msec
Number of time slots per frame	15
Number of slots for uplink per frame	7
Spreading factor	16

Table 5.2: UTRA physical layer specifications and JPPS system parameters.

packet scheduling in a joint manner (and thus we name it JPPS). The JPPS protocol is suitable for any multimedia CDMA cellular systems with packetized transmission, but here we restrict its usage to the UTRA TDD mode.

The multiple access scheme time division CDMA (TD-CDMA) which is a combination of TDMA and CDMA is recommended for the UTRA TDD mode [149]. The TDD mode has the flexibility to accommodate asymmetric traffic. This is because the uplink and downlink are multiplexed in time division and the proportion of the uplink and downlink slots (separated by switching points) can be readily configured [150]. In UTRA TDD, each frame is equal to 10 ms in length and divided into 15 equally-sized time slots, each of which may be allocated to either uplink or downlink [149].

Multiple terminals are allowed to transmit within the same time slot in a CDMA system by being assigned unique pseudorandom noise (PN) code sequences. In the UTRA TDD mode, the original information bits are spread using the orthogonal variable spreading factor (OVSF) codes whose lengths vary in the range of 1, 2, 4, 5, and 16 [149]. As in [147], we use a constant spreading factor of 16, and as a result of power control, packets with the same BER will have the same receiver power.

To support high data services, a terminal is able to transmit multiple packets in parallel using the multicode (MC) technology [151]. In the MC operation, multiple code channels can be allocated to a single terminal by deriving orthogonal spreading codes from its primary PN code. The physical layer specifications of the UTRA TDD mode and some system parameters we use for JPPS are summarized in Table 5.2.

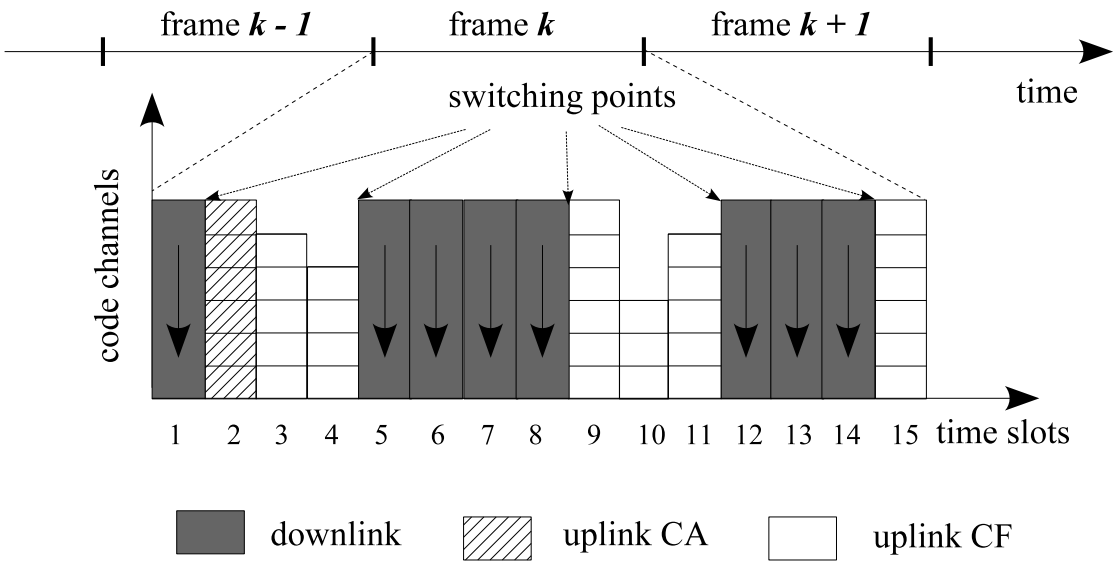

Figure 5.3: JPPS Frame structure. "CA" and "CF" denote "contention access" and"contention free", respectively.

5.3.2 Frame Structure

The frame structure of the JPPS protocol is illustrated in Figure 5.3. We assume an almost symmetric scenario where seven out of the 15 time slots in a UTRA TDD frame are allocated for uplink transmission. In JPPS, the first uplink time slot in a frame is designated as a contention access (CA) slot and other uplink time slots are contention free (CF) slots.

The CA slot is available for contention and thus active terminals can transmit their transmission requests through it. For voice traffic, we use head-of-line packets of talkspurts as transmission requests in order to minimize packet delay. An optimal channel access scheme, which optimizes the transmission probabilities in the CA slot is designed and presented in Section 5.3.5. The BS collects the transmission requests from the CA slot and performs packet scheduling techniques to both real-time and non-real-time traffic types in the CF slots. The first slot of a JPPS frame is always reserved for downlink transmission so that the access probabilities and slot allocation scheme for the current frame can be delivered to the active terminals before they commence data transmission in the uplink.

5.3.3 Packet Transmission

In JPPS, active terminals send transmission requests or head-of-line voice packets through the CA slot to contend for the use of the CF slots. The BS treats real-time traffic and non-real-time traffic with different priorities. Packet scheduling techniques are then applied in order to increase data throughput.

Real-time traffic transmission

As in PRMA, once a real-time traffic flow is admitted into the system, the code channel(s) that guarantees the QoS requirements of the traffic will be reserved for the terminal until its last buffered packet is transmitted. A packet of real-time traffic will be discarded if it has not been transmitted after a usually small pre-defined time-out value.

Unlike the packet scheduling-based MAC protocols, the JPPS protocol performs slot assignments by considering both data throughput maximization and control overhead reduction. At the end of every frame, the BS examines the slot allocation status, and maintains the previous allocation scheme as much as possible and reallocates the reserved terminals only when necessary. Consequently, unless the reserved terminals are informed by the BS of the change of slot allocations, the terminal is able to continue to use the previous slots to transmit. In this way, the downlink signaling overhead can be mitigated.

Non-real-time traffic transmission

In non-real-time traffic, we assume that packets will not be discarded until it exceeds a big time-out value which is usually in the order of a hundred frames. Taking the delay-insensitive nature of the non-real-time traffic into account, JPPS schedules the non-real-time terminals to transmit with lower priority compared to real-time traffic flows. After allocating all the real-time traffic using the packet scheduling algorithm described in the next section, the BS will select a non-real-time terminal j to transmit if there are still available code channels. No reservation applies to non-real-time terminals. This procedure will continue until all the free code channels have

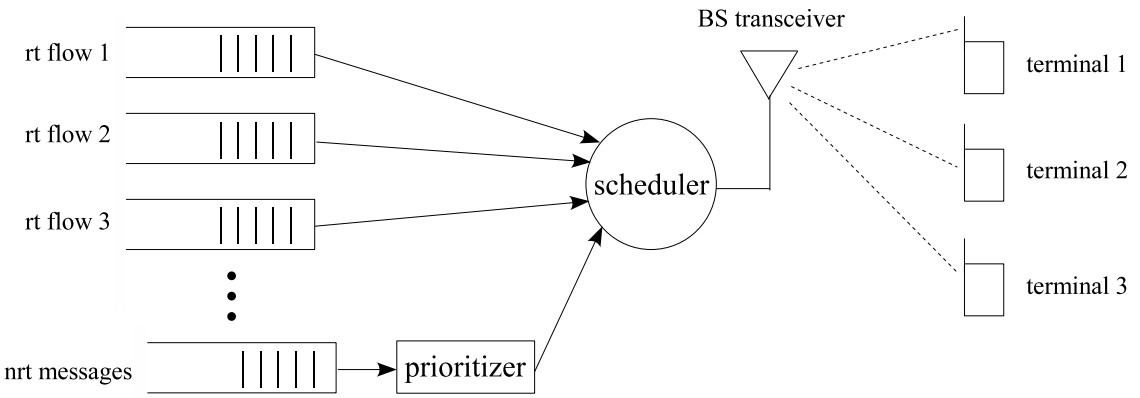

Figure 5.4: Packet scheduler. "rt" and "nrt" denote "real-time" and "non-real-time", respectively.

been filled or no non-real-time packets are outstanding. Terminal j is determined by the following prioritization scheme:

$$j = \arg\max_i w_i S_i \tag{5.1}$$

where w_i and S_i denote the time (measured in frames) that terminal i has waited and its batch size (i.e., number of packets), respectively.

Although the non-real-time terminals need to wait longer when the traffic load is heavy, the real-time terminals benefit, and in turn the overall performance of JPPS is considerably improved, especially when the traffic load is below a certain threshold, as shall be demonstrated by the simulation results.

5.3.4 Packet Scheduling

When both real-time and non-real-time traffic types with diverse QoS and BER requirements, are admitted to the system, an efficient packet scheduling technique with low complexity is required. In JPPS, we assume a power control scheme such that the BS's received power levels from different terminals are uniform in a given slot, as in WISPER [135]. Note that the received power levels for different slots can still be different. In this way, the implementation complexity is minimized. The maximum number of simultaneous transmissions for each traffic type can be determined from the bit-energy-to-noise ratio $\frac{E_b}{N_0}$, provided that the maximum tolerable

BER values for each traffic is known [135].

If traffic types with different BER values are transmitted in the same slot, the capacity of the slot is limited by the traffic type with the most stringent BER requirement [135]. As illustrated in Figure 5.3, the CF slots with different number of blocks indicate the capacity variability caused by BER requirements. Therefore, by grouping the packets with the same or similar BER requirements into the same slot, the overall throughput can be maximized. In JPPS, the basic principle of BER scheduling is adopted as follows.

For every non-empty CF slot, we define M_{BER}, which is the smallest BER value (i.e., the most stringent BER requirement) that the packets in this slot have. In all CF slots, either real-time or non-real-time packets are accommodated according to the following procedure. A packet will be allocated into

1. a CF slot whose M_{BER} is the same as the packet's BER value, otherwise,
2. an empty CF slot, otherwise,
3. a CF slot whose M_{BER} is smaller than the packet's BER value, otherwise,
4. a CF slot whose M_{BER} is greater than the packet's BER value, and then the CF slot's M_{BER} will be updated using the packet's BER value.

5.3.5 Optimal Channel Access

JPPS can support mixed traffic sources of real-time traffic and non-real-time elastic data. All the active terminals can inform the BS of their transmission requests through the CA slot of each frame. For the CF slot, we set a uniform received power level which is sufficient for the BER requirement of voice packets. The capacity of the CA slot is partitioned into two parts: c_{nv} code channels for non-voice traffic transmission and the rest for voice contention. As the other traffic types are usually not as abundant as voice, we assume that the predefined c_{nv} code channels are always sufficient for non-voice terminals to send transmission request packets with probability one. Let

p_v : voice terminal transmission probability.

D_v : voice time-out (frames).

p_{drop} : maximum allowed packet dropping probability.

λ_v: estimated contending voice terminals.

β : available code channels in CF slots.

c_v : pre-defined code channels in CA slot for voice contention.

The transmission permission probability for voice contention is computed by solving an optimization problem as follows:

$$\begin{aligned} \max: \quad & p_v \\ s.t. \quad & 0 \leq p_v \leq 1 \\ & (1-p_v)^{D_v} \leq p_{drop} \\ & \lambda_v \cdot p_v \leq \min(\beta, c_v). \end{aligned} \tag{5.2}$$

We define λ_v as the estimated number of contending voice terminals, and its value is approximated by the average number of the successfully admitted voice terminals in the past 20 frames. The second constraint is equivalent to $p_v \geq 1 - p_{drop}^{\frac{1}{D_v}}$. Thus the problem can be formulated as a simple linear programming (LP) optimization problem by combining the first two constraints as follows:

$$\begin{aligned} \max: \quad & p_v \\ s.t. \quad & 1 - p_{drop}^{\frac{1}{D_v}} \leq p_v \leq 1 \\ & \lambda_v \cdot p_v \leq \min(\beta, c_v). \end{aligned} \tag{5.3}$$

Before each frame starts, the BS will find an optimal p_v by directly solving the LP problem and every active voice terminal can obtain p_v through the downlink broadcasting channel.

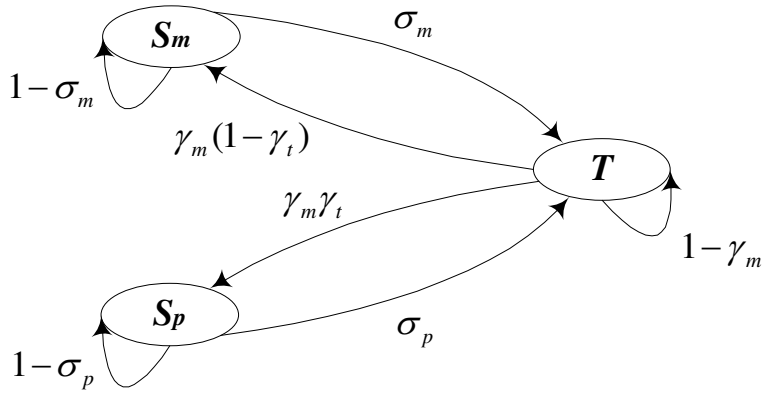

Figure 5.5: Speech model (reproduced from [4]).

5.3.6 Signaling Consideration

We aim to propose a low-complexity MAC protocol for multimedia CDMA networks. Apart from the computational complexity, a heavy signaling overhead reduces the efficiency of a MAC protocol and could even result in instability because of the hostile wireless link environment where packet errors and losses can routinely occur. In our proposed JPPS, as in PRMA, the slot allocation for a reserved terminal will be implicitly used for future frames except in the following circumstances. The BS notifies the nodes of a new allocation scheme when calls arrive or depart and the scheduler finds a new assignment scheme. In contrast to the packet scheduling-based MAC protocols that generate new slot assignment schemes for each frame, our proposed JPPS can save more than 90% percent of the signaling overhead according to our observations from simulation.

5.4 Performance Evaluation

5.4.1 Traffic Models and System Parameters

In the following, we introduce the traffic models used in this work. Four types of traffic (i.e., voice calls, audio streaming, video streaming and elastic data) with diverse QoS requirements are chosen for evaluation.

Voice traffic model

A voice conversation usually consists of talking, pausing and listening patterns. As in [4,135], we consider here a speech model that includes principal spurts, principal gaps, and minispurts and minigaps within a principal spurt that can be identified by sensitive speech activity detectors. The durations of all spurts and gaps are exponentially distributed and statistically independent of one another.

In this model, the mean duration of a principal spurt is assumed to be 1.000 s and the mean duration of a principal gap is 1.350 s. The minispurts and minigaps have mean durations of 0.275 s and 0.050 s, respectively. The length of conversation is also exponentially distributed with a mean duration of 180 s. It is also assumed that the vocoders generate a voice data rate of 16.5 kb/s in minispurts. This speech model can be described by a three-state Markov chain as shown in Figure 5.5, where T represents the talking state, S_p represents the principal silent gap and S_m the minisilent gap. The transmission probabilities of transitions from S_m and S_p to T are represented by σ_m and σ_p, respectively. The probability that a minispurt ends in any time slot is defined by γ_m, and γ_t defines the probability that a minispurt is the final one in its principal talkspurt. These transmission probabilities can be readily calculated using the mean durations of the spurts and gaps [4].

Audio traffic

In the audio traffic model, we assume that a continuous audio bit stream of data rate 32 kb/s is generated. The audio session length is exponentially distributed with a mean duration of 180 s.

Video traffic

The video model represents the generation of a constant bit rate of digital video streaming traffic. The session length is assumed to be exponentially distributed with a mean duration of 180 s and the video data rate is 64 kb/s.

Parameter		Value
Number of (raw) info bits per slot		165
Simulation time		10800 s (3 hours)
Voice	Maximum tolerable BER	10^{-3}
	Maximum number of packets per slot	8
	Time-out (frames)	4
	Maximum transmission rate capability	1 packet/slot
	Traffic percentage	70%
Audio	Maximum tolerable BER	10^{-4}
	Maximum number of packets per slot	5
	Time-out (frames)	6
	Maximum transmission rate capability	3 packets/slot
	Traffic percentage	8%
Video	Maximum tolerable BER	10^{-6}
	Maximum number of packets per slot	4
	Time-out (frames)	5
	Maximum transmission rate capability	6 packets/slot
	Traffic percentage	7%
Data	Maximum tolerable BER	10^{-9}
	Maximum number of packets per slot	6
	Time-out (frames)	(2× total_packets)
	Maximum transmission rate capability	1 packet/slot
	Traffic percentage	15%

Table 5.3: System parameters used in JPPS.

Elastic data traffic

In this simple model, the data message (e.g., an e-mail) length is exponentially distributed with a mean value of 30 kbytes.

In order to evaluate the performance of the JPPS protocol, we simulated a test environment with mixed traffic sources in Matlab. The detailed simulation parameters are outlined in Table 5.3. The maximum transmission rate capability in Table 5.3 describes the maximum number of packets that can be transmitted by a terminal in a single slot. The relative rates of terminal arrivals are fixed in our simulation so that voice accounts for 70% of the overall traffic, audio 8%, video 7% and elastic data 15%. Note that for the data traffic, the value of time-out is set to equal twice the total packets in a data message. For example, if a data message has 50 packets, then if any packet of the message has not been delivered after 100 frames since its

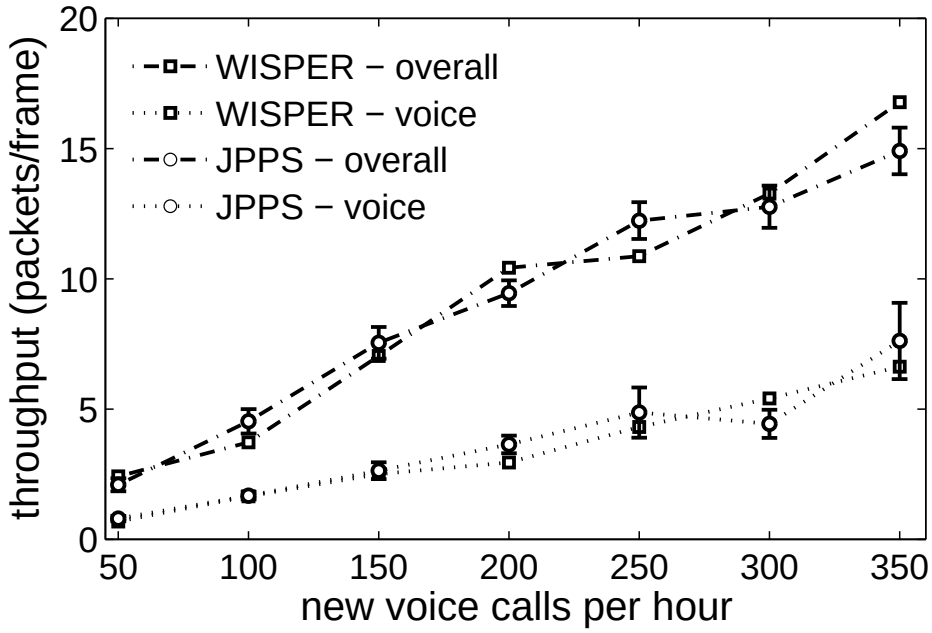

Figure 5.6: Throughput comparison.

arrival, it will be discarded. We adopted this time-out definition from [135] for fair comparisons between our protocol and WISPER.

5.4.2 Simulation Results and Discussion

In this section, the simulation results and the comparisons between JPPS and WISPER are shown. We present the simulation results for JPPS together with their respective 95% confidence intervals based on the Student-t distribution.

Figure 5.6 shows that the throughput of the two protocols are very close. However, JPPS's throughput is slightly lower than WISPER after the traffic load becomes heavier than 250 new voice calls per hour. As depicted in Figure 5.7, in contrast to the gradually increasing packet loss rate of WISPER, JPPS achieves a very low packet loss rate when the traffic load is below some threshold (at about 250 new voice calls per hour in our simulation), and increases rapidly after that. This is because the use of packet reservation guarantees the transmission of a real-time traffic flow when the system is unsaturated, whereas a large number of packets will

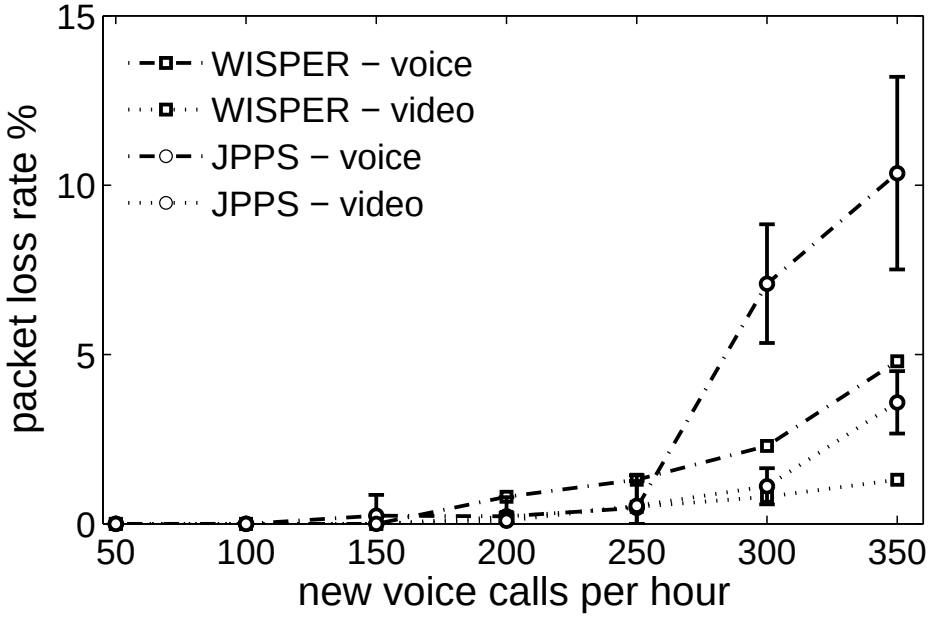

Figure 5.7: Packet loss comparison.

be dropped when the system becomes congested.

Figure 5.8 shows a significant improvement of JPPS over WISPER in terms of the average packet delay for real-time traffic flows, which again is due to the packet reservation mechanism. The results of audio traffic are omitted in Figure 5.7 because of its similar performance to video; for the same reason, the average packet delay of video in 5.8 is not shown. The performance improvements of real-time traffic is due to the sacrifice of packet delay of non-real-time data, as depicted in Figure 5.9. Thanks to the non-real-time data prioritizer described, no non-real-time packet loss is observed when the traffic load is lower than 350 new voice calls per hour.

5.5 Summary

We proposed the JPPS – a new MAC protocol for multimedia CDMA cellular networks with low-complexity. JPPS incorporates PRMA with packet scheduling techniques to give a simple yet efficient MAC solution. In JPPS, real-time and non-real-

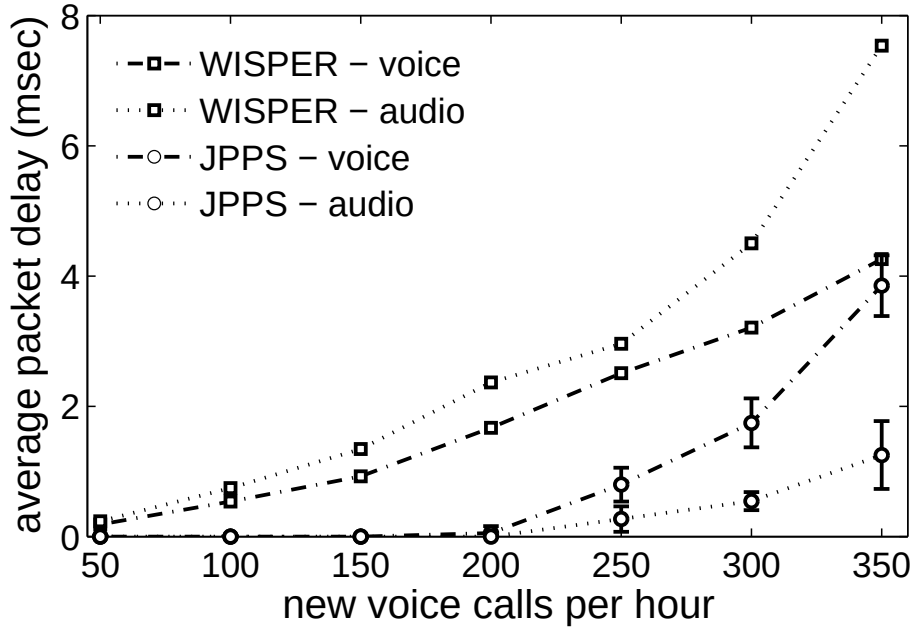

Figure 5.8: Average packet delay (voice and audio packets) comparison.

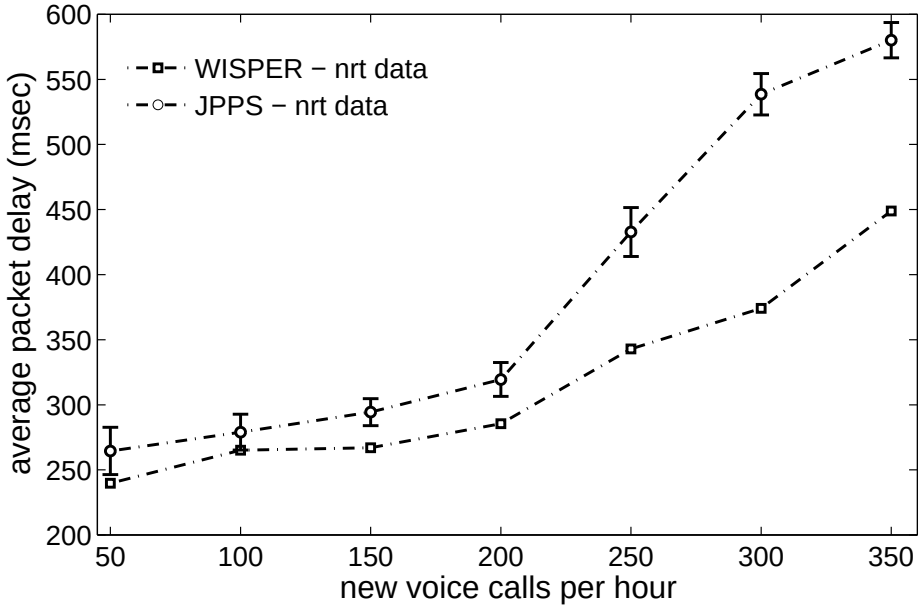

Figure 5.9: Average packet delay (non-real-time data packets) comparison.

time traffic are prioritized differently. Once a real-time traffic flow is admitted to the system, its code channel(s) are implicitly reserved until its last packet is transmitted, as in PRMA. We also prioritize within various non-real-time messages and do not apply reservations for non-real-time terminals. Packet scheduling techniques are then used to schedule all the real-time and non-real-time packets to increase data throughput. Finally, an optimal channel access scheme is proposed for active terminals to transmit transmission requests through channel contention.

Our simulation results show that the throughput of JPPS is comparable with that of WISPER, however, the performance of real-time traffic is significantly improved in terms of average packet delay over WISPER. The packet loss rate of JPPS also outperforms that of WISPER below some traffic load threshold (about 250 new voice calls per hour). Although the performance of average packet delay of non-real-time packets is degraded compared to WISPER, no packet loss is observed when the traffic load is lower than 350 new voice calls per hour, owing to the use of a non-real-time data prioritizer.

Chapter 6

Conclusion

This thesis has been focused on the performance analysis, evaluation and optimization of MAC protocols for wireless networks. The proposed methodologies with the main results are summarized in the following. We firstly identified the new energy saving features introduced in the MAC of the recently ratified IEEE 802.15.4, and defined an energy conserving CSMA-CA protocol. We then analyzed and optimized this new CSMA-CA protocol under both saturation and nonsaturation traffic conditions by proposing a novel analytical model that is based on a one-dimensional Markov chain and a simple fixed-point formulation. For the saturation condition, we also presented explicit optimization results to maximize throughput, performed asymptotic analysis and investigated unfairness issues of the energy conserving CSMA-CA protocol. The accuracy of our model and the effectiveness of our optimization results were then verified with extensive simulations. Our model is quite flexible and it could be put to other uses than those shown in Chapter 2, such as the study of packet delay statistics or the study of the performance of different backoff algorithms.

Secondly, we proposed a new non-stationary three-dimensional Markov chain model to analyze the packet delivery performance of the IEEE 802.15.4 MAC under the OSD traffic type where nodes periodically get backlogged at the same time. The OSD traffic is problematic for CSMA due to high collision rates. However, this type of workload is anticipated in many IEEE 802.15.4 applications. Our Markov chain model is able to capture the qualitative behavior of the non-stationary system under the OSD traffic condition and accurately approximates the packet delivery statistics. The accuracy of the model has been verified by *ns*-2 simulations. It was discovered that the performance of the packet delivery in such networks can be very low. Our

results suggest that the cluster size and message length need to be carefully chosen for satisfactory performance. A new backoff strategy with a large initial backoff window and decreasing backoff windows for subsequent backoffs was considered to improve the performance of the standard.

In an attempt to minimize energy consumption of wireless sensor networks, we considered a simple S&T MAC protocol, where sensor nodes choose transmission slots uniformly in an equally slotted period without sensing the carrier. The S&T MAC entails only a small number of operations which may facilitate the reduction of energy consumption for computation, and it is most likely to be a competitive MAC solution for scenarios where only a small proportion of the packets are needed to report some event (e.g., event-driven workload). We also derived the probability that at least k out of n nodes successfully transmit their packets under the S&T MAC, which is a new solution to a problem similar to a certain birthday problem. Furthermore, we propose a new framework to minimize energy consumption by optimally choosing duty cycles for wireless sensor networks. In this framework, the expected energy consumption per unit time of the entire network is minimized by satisfying various QoS requirements, such as packet delivery ratio and maximum packet delay. The S&T MAC and IEEE 802.15.4 MAC were then examined under our energy optimization framework as case studies. Our results showed that the IEEE 802.15.4 MAC has better energy performance than the S&T MAC in most cases. The S&T MAC has comparable (in some cases even better) performance than the IEEE 802.15.4 MAC when the packet delivery ratio is low. It was also shown that the battery life extension mode of the standard under our energy minimization framework is no more energy efficient than the regular mode.

We also introduced a MAC protocol for wireless multimedia cellular networks which support a wide range of services such as video/audio streaming, video-conferencing, multimedia messaging service, *etc.* In the proposed protocol, we jointly considered the techniques of packet reservation and packet scheduling to accommodate multimedia traffic types by meeting the diverse QoS requirements such as transmission rate, delay bound and maximum tolerable bit error rate for various traffic types. We also proposed a simple optimal channel access scheme

for active terminals to transmit transmission requests through channel contention. Simulation results show that the performance of real-time traffic is significantly improved in terms of packet loss rate and average packet delay over WISPER, while the throughput of JPPS is comparable with that of WISPER. A possible direction to further improve the performance of the JPPS is that the packet scheduling method can be further improved to increase the data throughput using power minimization algorithms. Moreover, a call admission control algorithm can be added on top of JPPS to guarantee the QoS of the admitted terminals.

Bibliography

[1] IEEE 802.15.4, "Wireless medium access control (MAC) and physical layer (PHY) specifications for low rate wireless personal area networks (LR-WPANS)," Standard, IEEE, 2003.

[2] G. Lu, B. Krishnamachari, and C. S. Raghavendra, "An adaptive energy-efficient and low-latency MAC for data gathering in wireless sensor networks," in *Proc. International Parallel and Distributed Processing Symposium (IPDPS)*, 2004, pp. 224–231.

[3] A. E. Brand and A. H. Aghvami, "Multidimensional PRMA with prioritized bayesian broadcast – a MAC strategy for multiservice traffic over UMTS," *IEEE Trans. Vehic. Technol.*, vol. 47, no. 4, pp. 1148–1161, Nov. 1998.

[4] D. J. Goodman and S. X. Wei, "Efficiency of packet reservation multiple access," *IEEE Trans. Vehic. Technol.*, vol. 40, no. 1, pp. 170–176, Feb. 1991.

[5] F. Tobagi and V. B. Hunt, "Performance analysis of carrier sense multiple access with collision detection," *Computer Networks*, vol. 4, pp. 245–259, Oct./Nov. 1980.

[6] J. A. Gutierrez, M. Naeve, E. Callaway, M. Bourgeois, V. Mitter, and B. Heile, "IEEE 802.15.4: a developing standard for low-power low-cost wireless personal area networks," *IEEE Network*, vol. 15, no. 5, pp. 12–19, 2001.

[7] H. Fattah and C. Leung, "An overview of scheduling algorithms in wireless multimedia networks," *IEEE Wireless Communications*, vol. 9, no. 5, pp. 76–83, Oct. 2002.

[8] A. J. Paulraj, D. A. Gore, R. U. Nabar, and H. Bolcskei, "An overview of MIMO communications - a key to gigabit wireless," *Proc. IEEE*, vol. 92, no. 2, pp. 198–218, 2004.

[9] R. van Nee and R. Prasad, *OFDM for Wireless Multimedia Communications*, Artech House, Inc. Norwood, MA, USA, 2000.

[10] C. Berrou and A. Glavieux, "Near optimum error correcting coding and decoding: turbo-codes," *IEEE Trans. Commun.*, vol. 44, no. 10, pp. 1261–1271, 1996.

[11] A. S. Tanenbaum, *Computer Networks*, Prentice Hall, 2003, Thrid Edition.

[12] F. Tobagi, "Multiaccess protocols in packet communication systems," *IEEE Trans. Commun.*, vol. 28, no. 4, pp. 468–488, 1980.

[13] N. Abramson, "The ALOHA system – another alternative for computer communications," in *Proc. 1970 Fall Joint Conput. conf. AFIPS Conf.*, Montvale, New Jersey, USA, 1970, AFIPS Press, vol. 37, pp. 281–285.

[14] L. Kleinrock and F. Tobagi, "Packet switching in radio channels: Part I–carrier sense multiple-access modes and their throughput-delay characteristics," *IEEE Trans. Commun.*, vol. 23, no. 12, pp. 1400–1416, 1975.

[15] I. Rubin, "Group random-access disciplines for multi-access broadcast channels," *IEEE Trans. Inform. Theory*, vol. 24, no. 5, pp. 578–592, 1978.

[16] J. Martin, *System analysis for data transmission*, Englewood New Jersey: Prentice Hall, 1972.

[17] F. Tobagi and L. Kleinrock, "Packet switching in radio channels: Part III–polling and (dynamic) split-channel reservation multiple access," *IEEE Trans. Commun.*, vol. 24, no. 8, pp. 832–845, 1976.

[18] S. S. Lam, "Packet broadcast networks – a performance analysis of the R-ALOHA protocol," *IEEE Trans. Computers*, vol. C-29, no. 7, pp. 596–603, 1980.

[19] L. Kleinrock and Y. Yemini, "An optimal adaptive scheme for multiple access broadcast communication," in *Proc. IEEE International Conference on Communications (ICC)*, June 1978, pp. 721–725.

[20] S. M. Cherry, "The wireless last mile," *IEEE Spectrum*, vol. 40, no. 9, pp. 18–22, 2003.

[21] C. Eklund, R. B. Marks, K. L. Stanwood, and S. Wang, "IEEE standard 802.16: a technical overview of the WirelessMAN air interface for broadband wireless access," *IEEE Communications Magazine*, vol. 40, no. 6, pp. 98–107, 2002.

[22] IEEE 802.16, "Air interface for fixed broadband wireless access," IEEE standard for local and metropolitan area networks, IEEE, Nov. 2004.

[23] ETSI, "P802.16/D5c-2002, HIPERMAN Draft," Standard, July 2002.

[24] "IEEE 802.11 working group for wireless LANs," available at http://www.ieee802.org/11/ .

[25] IEEE 802.11, "Wireless LAN medium access control (MAC) and physical layer (PHY) specifications," Standard, IEEE, Nov. 1997.

[26] ESTI, "Broadband radio access networks (BRAN); HIPERLAN type 2; data link control (DLC) layer; part 1: Basic transport functions," Standard, Dec. 1999.

[27] J. Khun-Jush, G. Malmgrem, P. Scbramm, and J. Torsner, "HiperLAN type 2 for broadband wireless communication," *Ericsson Review*, , no. 2, 2000.

[28] K. Mandke, H. Nam, L. Yerramneni, C. Zuniga, and T. Rappaport, "The evolution of ultra wide band radio for wireless personal area networks," *High Frequency Electron.*, pp. 22–32, Sept. 2003.

[29] IEEE 802.15 Working Group, http://www.ieee802.org/15/.

[30] B. Chatschik, "An overview of the bluetooth wireless technology," *IEEE Communications Magazine*, vol. 39, no. 12, pp. 86–94, 2001.

[31] P. McDermott-Wells, "What is bluetooth?," *IEEE Potentials*, vol. 23, no. 5, pp. 33–35, 2005.

[32] M. Tubaishat and S. Madria, "Sensor networks: an overview," *IEEE Potentials*, vol. 22, no. 2, pp. 20–23, Apr.-May 2003.

[33] I. F. Akyildiz, S. Weilian, Y. Sankarasubramaniam, and E. Cayirci, "A survey on sensor networks," *IEEE Communications Magazine*, vol. 40, no. 8, pp. 102–114, Aug. 2002.

[34] H. Holma and A. Toskala, *WCDMA for UMTS*, John Wiley & Sons Ltd, 2004, Thrid Edition.

[35] V. K. Garg and T. S. Rappaport, *Wireless Network Evolution: 2G to 3G*, Prentice Hall PTR, Upper Saddle River, NJ, USA, 2001.

[36] K. Pahlavan and A. Levesque, *Wireless Information networks*, John Wiley & Sons, Inc., Hoboken, New Jersey, 2005, Second Edition.

[37] A. Nasipuri, J. Zhuang, and S. R. Das, "A multichannel CSMA MAC protocol for multihop wireless networks," in *Proc. IEEE Wireless Communications and Networking Conference (WCNC)*, 1999, vol. 3, pp. 1402–1406.

[38] T.-S. Yum and K.-W. K.-W. Hung, "Design algorithms for multihop packet radio networks with multiple directional antennas stations," *IEEE Trans. Commun.*, vol. 40, no. 11, pp. 1716–1724, 1992.

[39] Y. Onozato, J. Liu, and S. Noguchi, "Stability of a slotted ALOHA system with capture effect," *IEEE Trans. Vehic. Technol.*, vol. 38, no. 1, pp. 31–36, 1989.

[40] D. J. Goodman and A. A. M. Saleh, "The near/far effect in local ALOHA radio communications," *IEEE Trans. Vehic. Technol.*, vol. 36, no. 1, pp. 19–27, 1987.

[41] N. Abramson, "The ALOHA system," in *Computer Communication Networks*, pp. 501–518. Engel Cliff, New Jersey: Prentice Hall, 1973.

[42] L. Roberts, "ALOHA packet system with and without slots and capture," *Comput. Commun. Rev.*, vol. 5, no. 2, pp. 28–42, Apr. 1975.

[43] G. S. Sidhu, R. F. Andrews, and A. B. OppenHeimer, "Inside AppleTalk," available at: http://developer.apple.com/MacOs/opentransport/docs/dev/Inside_AppleTalk.pdf.

[44] T. R. Park, T. H. Kim, J. Y. Choi, S. Choi, and W. H. Kwon, "Throughput and energy consumption analysis of IEEE 802.15.4 slotted CSMA/CA," *Electron. Lett.*, vol. 41, no. 18, pp. 1017–1019, 2005.

[45] S. Pollin, M. Ergen, and S. C. Ergen et al., "Performance analysis of slotted carrier sense IEEE 802.15.4 medium access layer," in *Proc. IEEE GLOBECOM.*, 2006.

[46] F. Tobagi and L. Kleinrock, "Packet switching in radio channels: Part II–the hidden terminal problem in carrier sense multiple-access and the busy-tone solution," *IEEE Trans. Commun.*, vol. 23, no. 12, pp. 1417–1433, 1975.

[47] P. Karn, "MACA – a new channel access method for packet radio," in *Proc. ARRL/CRRL Amateur Radio 9th Computer Networking Conference*, 1990, pp. 134–140.

[48] V. Bharghavan, A. Demers, S. Shenker, and L. Zhang, "MACAW: a media access protocol for wireless LAN's," in *Proc. The Conference on Communications Architectures, Protocols and Applications (SIGCOMM)*, New York, NY, USA, 1994, pp. 212–225, ACM Press.

[49] J. S. J. Chen and V. O. K. Li, "Reservation CSMA/CD: a multiple access protocol for LAN's," *IEEE J. Select. Areas Commun.*, vol. 7, no. 2, pp. 202–210, 1989.

[50] I. Chlamtac, W. Franta, and K. Levin, "BRAM: The broadcast recognizing access method," *IEEE Trans. Commun.*, vol. 27, no. 8, pp. 1183–1190, 1979.

[51] C. H. Foh and M. Zukerman, "CSMA with reservations by interruptions (CSMA/RI): a novel approach to reduce collisions in CSMA/CD," *IEEE J. Select. Areas Commun.*, vol. 18, no. 9, pp. 1572–1580, 2000.

[52] C. Wu and V. Li, "Receiver-initiated busy-tone multiple access in packet radio networks," in *Proc. ACM SIGCOMM*, 1987, pp. 336–342.

[53] D. Saha and S. E. Kay, "Cellular digital packet data network," *IEEE Trans. Vehic. Technol.*, vol. 46, no. 3, pp. 697–706, 1997.

[54] M. Sreetharan and R. Kumar, *Cellular Digital Packet Data*, Artech House, 1996.

[55] J. L. Haine, P. M. Martin, and R. L. A. Goodings, "A european standard for packet-mode mobile data," in *Proc. IEEE International Symposium on Personal, Indoor and Mobile Radio Communications (PIMRC)*, 1992, pp. 513–519.

[56] Z. J. Haas and J. Deng, "Dual busy tone multiple access (DBTMA)-a multiple access control scheme for ad hoc networks," *IEEE Trans. Commun.*, vol. 50, no. 6, pp. 975–985, 2002.

[57] Y. Yang, F. Huang, X. Gu, M. Guizani, and H. H. Chen, "Double sense multiple access for wireless ad hoc networks," in *Proc. The International Conference on Quality of Service in Heterogeneous Wired/Wireless Networks (QShine)*, 2006.

[58] S. Tasaka, *Performance analysis of Multiple Access Protocols*, MIT Press, Cambridge, Mass., 1986.

[59] L. Kleinrock and S. Lam, "Packet switching in a multiaccess broadcast channel: Performance evaluation," *IEEE Trans. Commun.*, vol. 23, no. 4, pp. 410–423, 1975.

[60] J. Meditch and C. T. Lea, "Stability and optimization of the CSMA and CSMA/CD channels," *IEEE Trans. Commun.*, vol. 31, no. 6, pp. 763–774, 1983.

[61] S. Tasaka, "Dynamic behavior of a CSMA-CD system with a finite population of buffered users," *IEEE Trans. Commun.*, vol. 34, no. 6, pp. 576–586, 1986.

[62] G. Bianchi, "Performance analysis of the IEEE 802.11 distributed coordination function," *IEEE J. Select. Areas Commun.*, vol. 18, no. 3, pp. 535–547, Mar. 2000.

[63] "Network Simulator ns-2," available at http://www.isi.edu/nsnam/ns/.

[64] Y. Zheng, K. Lu, and D.W. Fang, "Performance analysis of IEEE 802.11 DCF in imperfect channels," *IEEE Trans. Vehic. Technol.*, vol. 55, no. 5, pp. 1648–1656, 2006.

[65] D. Malone, K. Duffy, and D. Leith, "Modeling the 802.11 distributed coordination function in nonsaturated heterogeneous conditions," *IEEE/ACM Trans. Networking*, vol. 15, no. 1, pp. 159–172, 2007.

[66] J. W. Robinson and T. S. Randhawa, "Saturation throughput analysis of IEEE 802.11e enhanced distributed coordination function," *IEEE J. Select. Areas Commun.*, vol. 22, no. 5, pp. 917–928, 2004.

[67] Z. Kong, D. H. K. Tsang, B. Bensaou, and D. Gao, "Performance analysis of IEEE 802.11e contention-based channel access," *IEEE J. Select. Areas Commun.*, vol. 22, no. 10, pp. 2095–2106, 2004.

[68] H. Samelson, "On the brouwer fixed point theorem," *Portugal. Math.*, vol. 22, pp. 189–191, 1963.

[69] B. J. Kwak, N. O. Song, and L. E. Miller, "Performance analysis of exponential backoff," *IEEE/ACM Trans. Networking*, vol. 13, no. 2, pp. 343–355, 2005.

[70] V. Ramaiyan, A. Kumar, and E. Altman, "Fixed point analysis of single cell IEEE 802.11e WLANs: uniqueness, multistability and throughput differentiation," in *Proc. of The ACM international Conference on Measurement and Modeling of Computer Systems (SIGMETRICS)*, 2005, pp. 109–120.

[71] "Zigbee alliance," available at http://www.zigbee.org .

[72] J. Zheng and M.J. Lee, "Will IEEE 802.15.4 make ubiquitous networking a reality?: a discussion on a potential low power, low bit rate standard," *IEEE Communications Magazine*, vol. 42, no. 6, pp. 140–146, June 2004.

[73] J. Zheng and M.J. Lee, "A comprehensive performance study of IEEE 802.15.4," in *Sensor Network Operations*, pp. 218–237. IEEE Press, Wiley Interscience, 2006.

[74] G. Lu, B. Krishnamachari, and C. S. Raghavendra, "Performance evaluation of the IEEE 802.15.4 MAC for low-rate low-power wireless networks," in *Proc. IEEE International Conference on Performance, Computing, and Communications (ICPCC)*, 2004, pp. 701–706.

[75] N. Golmie, D. Cypher, and O. Rebala, "Performance analysis of low rate wireless technologies for medical applications," *Computer Communications*, vol. 28, no. 10, pp. 1266–1275, 2005.

[76] N. F. Timmons and W. G. Scanlon, "Analysis of the performance of IEEE 802.15.4 for medical sensor body area networking," in *Proc. IEEE Conference on Sensor and Ad Hoc Communications and Networks (SECON)*, Oct. 2004, pp. 16–24.

[77] B. Bougard, F. Catthoor, D. C. Daly, A. Chandrakasan, and W. Dehaene, "Energy efficiency of the IEEE 802.15.4 standard in dense wireless microsensor networks: modeling and improvement perspectives," in *Proc. Design, Automation and Test in Europe*, 2005, vol. 1, pp. 196–201.

[78] J. Misic, S. Shafi, and V. B. Misic, "Performance of a beacon enabled IEEE 802.15.4 cluster with downlink and uplink traffic," *IEEE Transactions on Parallel and Distributed Systems*, vol. 17, no. 4, pp. 361–376, 2006.

[79] J. Misic, S. Shafi, and V. B. Misic, "Maintaining reliability through activity management in an 802.15.4 sensor cluster," *IEEE Trans. Vehic. Technol.*, vol. 55, no. 3, pp. 779–788, 2006.

[80] J. Misic, S. Shafi, and V. B. Misic, "The impact of MAC parameters on the performance of 802.15.4 PAN," *Ad Hoc Networks*, vol. 3, no. 5, pp. 509–528, 2005.

[81] I. Ramachandran, A. Das, and S. Roy, "Analysis of contention access part of IEEE 802.15.4 MAC," *ACM Trans. Sen. Netw.*, vol. 3, no. 1, 2007.

[82] C. K. Singh and A. Kumar, *Performance Evaluation of an IEEE 802.15.4 Sensor Network with a star topology*, Submitted for publication, avaiable at http://ece.iisc.ernet.in/~anurag/papers/anurag/singh-kumar05submitted-detailed.pdf .

[83] K. Leibnitz, N. Wakamiya, and M. Murata, "Modeling of IEEE 802.15.4 in a cluster of synchronized sensor nodes," in *Proc. International Teletraffic Congress (ITC)*, Aug. 2005, pp. 1345–1354.

[84] K. Yedavalli and B. Krishnamachari, "Enhancement of the IEEE 802.15.4 MAC protocol for scalable data collection in dense sensor networks," Technical report CENG-2006-14, University of Southern California, Computer Engineering, Nov. 2006.

[85] A. Woo and D. E. Culler, "A transmission control scheme for media access in sensor networks," in *Proc. International Conference on Mobile Computing and Networking (MobiCom)*, 2001, pp. 221–235.

[86] Y. C. Tay, K. Jamieson, and H. Balakrishnan, "Collision-minimizing CSMA and its applications to wireless sensor networks," *IEEE J. Select. Areas Commun.*, vol. 22, no. 6, pp. 1048–1057, Aug. 2004.

[87] A. Jayasuriya, S. Perreau, A. Dadej, and S. Gordon, "Hidden vs. exposed terminal problem in ad hoc networks," in *Proc. of the Australian Telecommunication Networks and Applications Conference (ATNAC)*, Dec. 2004.

[88] M. A. Bender, M. Farach-Colton, S. He, B. C. Kuszmaul, and C. E. Leiserson, "Adversarial contention resolution for simple channels," in *Proc. ACM*

symposium on Parallelism in Algorithms and Architectures (SPAA), 2005, pp. 325–332.

[89] C. Foh and M. Zukerman, "Performance evaluation of IEEE 802.11," in *Proc. of IEEE Vehicular Technology Conference (VTC), Spring*, 2001, vol. 2, pp. 841–845.

[90] R. Szewczyk, E. Osterweil, J. Polastre, M. Hamilton, A. Mainwaring, and D. Estrin, "Habitat monitoring with sensor networks," *ACM Commun.*, vol. 47, no. 6, pp. 34–40, 2004.

[91] Y. Wu, S. Fahmy, and N. B. Shroff, "Optimal sleep/wake scheduling for time-synchronized sensor networks with QoS guarantees," in *Proc. IEEE International Workshop on Quality of Service (IWQoS)*, 2006.

[92] M. Molle, "A new binary logarithmic arbitration method for Ethernet," Technical Report CSRI-298, Computer Systems Research Institute, University of Toronto, Canada, 1994.

[93] C. S. Raghavendra, Krishna Sivalingam, and Taieb Znati, *Wireless Sensor Networks*, Kluwer Academic Publishers, 2004.

[94] C. Y. Chong and S. P. Kumar, "Sensor networks: evolution, opportunities, and challenges," *Proc. IEEE*, vol. 91, no. 8, pp. 1247–1256, Aug. 2003.

[95] "21 ideas for the 21st century," *Business Week*, pp. 78–167, Aug. 30 1999.

[96] N. Bulusu and S. Jha, *Wireless Sensor Networks: A Systems Perspective*, Artech House, 2005.

[97] J. M. Kahn, R. H. Katz, and K. S. J. Pister, "Next century challenges: mobile networking for "smart dust"," in *Proc. Annual ACM/IEEE international conference on Mobile computing and networking (MobiCom)*, New York, NY, USA, 1999, pp. 271–278, ACM Press.

[98] J. M. Rabaey, M. J. Ammer, J. L. da Silva, D. Patel, and S. Roundy, "PicoRadio supports ad hoc ultra-low power wireless networking," *IEEE Computer*, vol. 33, no. 7, pp. 42–48, July 2000.

[99] C. C. Enz, A. El-Hoiydi, J. D. Decotignie, and V. Peiris, "WiseNET: an ultralow-power wireless sensor network solution," *IEEE Computer*, vol. 37, no. 8, pp. 62–70, Aug. 2004.

[100] W. Heinzelman, A. Chandrakasan, and H. Balakrishnan, "An application-specific protocol architecture for wireless microsensor networks," *IEEE Transactions on Wireless Communications*, vol. 1, no. 4, pp. 660–670, Oct. 2002.

[101] D. Estrin, R. Govindan, J. Heidemann, and S. Kumar, "Next century challenges: Scalable coordination in sensor networks," in *Proc. of the ACM/IEEE International Conference on Mobile Computing and Networking (MobiCom)*, Seattle, Washington, USA, Aug. 1999, pp. 263–270, ACM.

[102] C. Intanagonwiwat, R. Govindan, D. Estrin, J. Heidemann, and F. Silva, "Directed diffusion for wireless sensor networking," *IEEE/ACM Trans. Networking*, vol. 11, no. 1, pp. 2–16, 2003.

[103] J. N. Al-Karaki and A. E. Kamal, "Routing techniques in wireless sensor networks: a survey," *IEEE Wireless Communications*, vol. 11, no. 6, pp. 6–28, 2004.

[104] W. Ye, J. Heidemann, and D. Estrin, "Medium access control with coordinated adaptive sleeping for wireless sensor networks," *IEEE/ACM Trans. Networking*, vol. 12, no. 3, pp. 493–506, June 2004.

[105] L. Krishnamachari, D. Estrin, and S. Wicker, "The impact of data aggregation in wireless sensor networks," in *Proc. of International Conference on Distributed Computing Systems (ICDCS)*, July 2002, pp. 575–578.

[106] K. Dasgupta, K. Kalpakis, and P. Namjoshi, "An efficient clustering-based heuristic for data gathering and aggregation in sensor networks," in *Proc.*

of IEEE Wireless Communications and Networking (WCNC), Mar. 2003, pp. 1948–1953.

[107] A. Kansal and M. B. Srivastava, "An environmental energy harvesting framework for sensor networks," in *Proc. of the International Symposium on Low Power Electronics and Design (ISLPED)*, Aug. 2003, pp. 481–486.

[108] M. Ali, U. Saif, A. Dunkels, T. Voigt, K. Romer, K. Langendoen, J. Polastre, and Z. A. Uzmi, "Medium access control issues in sensor networks," *ACM SIGCOMM Computer Communication Review*, vol. 36, no. 2, pp. 33–36, 2006.

[109] I. Demirkol, C. Ersoy, and F. Alagoz, "MAC protocols for wireless sensor networks: a survey," *IEEE Communications Magazine*, vol. 44, no. 4, pp. 115–121, 2006.

[110] K. Sohrabi, J. Gao, V. Ailawadhi, and G. J. Pottie, "Protocols for self-organization of a wireless sensor network," *IEEE Personal Commun.*, vol. 7, no. 5, pp. 16–27, 2000.

[111] G. Pei and C. Chien, "Low power TDMA in large wireless sensor networks," in *Proc. of IEEE Military Communications Conference (MILCOM)*, 2001, vol. 1, pp. 347–351.

[112] S. Chatterjea, L. F. W. van Hoesel, and P. J. M. Havinga, "AI-LMAC: an adaptive, information-centric and lightweight mac protocol for wireless sensor networks," in *Proc. of Intelligent Sensors, Sensor Networks and Information Processing Conference (ISSNIP)*, 2004, pp. 381–388.

[113] L. F. W. van Hoesel, T. Nieberg, H. J. Kip, and P. J. M. Havinga, "Advantages of a TDMA based, energy-efficient, self-organizing MAC protocol for WSNs," in *Proc. of IEEE Vehicular Technology Conference (VTC), Spring*, 2004, vol. 3, pp. 1598–1602.

[114] J. Li and G. Y. Lazarou, "A bit-map-assisted energy-efficient MAC scheme for wireless sensor networks," in *Proc. of the international symposium on Information processing in sensor networks (IPSN)*, 2004, pp. 55–60.

[115] T. van Dam and K. Langendoen, "An adaptive energy-efficient MAC protocol for wireless sensor networks," in *Proc. of ACM Conference on Embedded Networked Sensor Systems (SenSys)*, Nov. 2003, pp. 171–180.

[116] P. Lin, C. Qiao, and X. Wang, "Medium access control with a dynamic duty cycle for sensor networks," in *Proc. IEEE Wireless Communications and Networking Conference (WCNC)*, 2004, vol. 3, pp. 1534–1539.

[117] J. Polastre, J. Hill, and D. Culler, "Versatile low power media access for wireless sensor networks," in *Proc. ACM Conference on Embedded Networked Sensor Systems (SenSys)*, Nov. 2004, pp. 95–107.

[118] A. El-Hoiydi and J.-D. Decotignie, "WiseMAC: an ultra low power MAC protocol for the downlink of infrastructure wireless sensor networks," in *Proc. International Symposium on Computers and Communications (ISCC)*, June 2004, vol. 1, pp. 244–251.

[119] V. Rajendran, K. Obraczka, and J. J. Garcia-Luna-Aceves, "Energy-efficient, collision-free medium access control for wireless sensor networks," *Wireless Networking*, vol. 12, no. 1, pp. 63–78, 2006.

[120] I. Rhee, A. Warrier, M. Aia, and J. Min, "Z-MAC: a hybrid MAC for wireless sensor networks," in *Proc. the 3rd international conference on Embedded networked sensor systems (SenSys)*, 2005, pp. 90–101.

[121] C. Schurgers, V. Tsiatsis, S. Ganeriwal, and M. Srivastava, "Optimizing sensor networks in the energy-latency-density design space," *IEEE Transactions on Mobile Computing*, vol. 1, no. 1, pp. 70–80, 2002.

[122] K. Jamieson, H. Balakrishnan, and Y.C. Tay, "Sift: A MAC protocol for event-driven wireless sensor networks," Technical Report Tech. Rep. 894, MIT Lab Comput. Sci., [Online]. Avaiable: http://www.chipcon.com/.

[123] W. Feller, *An Introduction to Probability Theory and Its Applications*, John Wiley & Sons Inc., 1968, Thrid Edition, Volume I.

[124] N. L. Johnson and S. Kotz, *Urn Models and Their Application*, John Wiley & Sons, Inc., 1977.

[125] Chipcon, 2004, Chipcon Transceiver CC1000 Data Sheet v2.2. [Online]. Avaiable: http://www.chipcon.com/.

[126] The GNU Multiple Precision Arithmetic Library. [Online]. Avaiable: http://www.swox.com/gmp/.

[127] W. R. Young, "Advanced mobile phone service: Introduction, background, and objectives," *Bell Syst. Tech. Journal*, vol. 58, pp. 1–14, Jan. 1979.

[128] K. Raith and J. Uddenfeldt, "Capacity of digital cellular TDMA systems," *IEEE Trans. Vehic. Technol.*, vol. 40, no. 2, pp. 323–331, May 1991.

[129] TIA/EIA Iterim Standard-95, "Mobile station – base station compatibility standard for dual-mode wideband spread spectrum cellular system," Tech. Rep., July 1993.

[130] J. Cai and D. J. Goodman, "General packet radio service in GSM," *IEEE Communications Magazine*, vol. 35, no. 10, pp. 122–131, Oct. 1997.

[131] A. Furuskar, S. Mazur, F. Muller, and H. Olofsson, "EDGE: enhanced data rates for GSM and TDMA/136 evolution," *IEEE Personal Commun.*, vol. 6, no. 3, pp. 56–66, June 1999.

[132] T. S. Rappaport, *Wireless Communications: Principles and Practice*, Prentice Hall, 2002, Second Edition.

[133] T. Ojanpera and R. Prasad, "An overview of air interface multiple access for IMT-2000/UMTS," *IEEE Communications Magazine*, vol. 36, no. 9, pp. 82–86, Sep. 1998.

[134] I. F. Akyildiz, J. McNair, L. C. Martorell, R. Puigjaner, and Y. Yesha, "Medium access control protocols for multimedia traffic in wireless networks," *IEEE Network*, vol. 13, no. 4, pp. 39–47, July-Aug. 1999.

[135] I. F. Akyildiz, D. A Levine, and I. Joe, "A slotted CDMA protocol with BER scheduling for wireless multimedia networks," *IEEE/ACM Trans. Networking*, vol. 7, no. 2, pp. 146–158, Apr. 1999.

[136] V. Huang and W. Zhuang, "Optimal resource management in packet-switching TDD CDMA systems," *IEEE Personal Commun.*, vol. 7, no. 6, pp. 26–31, Dec. 2000.

[137] X. Wang, "Wide-band TD-CDMA MAC with minimum-power allocation and rate- and BER-scheduling for wireless multimedia networks," *IEEE/ACM Trans. Networking*, vol. 12, no. 1, pp. 103–116, Feb. 2004.

[138] D. J. Goodman, R. A. Valenzuela, K. T. Gayliard, and B. Ramamurthi, "Packet reservation multiple access for local wireless communications," *IEEE Trans. Commun.*, vol. 37, no. 8, pp. 885–890, Aug. 1989.

[139] S. Tasaka, "Stability and performance of the R-ALOHA packet broadcast system," *IEEE Trans. Computers*, vol. C-32, pp. 717–726, Aug. 1983.

[140] A. E. Brand and A. H. Aghvami, "Performance of a joint CDMA/PRMA protocol for mixed voice/data transmission for third generation mobile communication," *IEEE J. Select. Areas Commun.*, vol. 14, no. 9, pp. 1698–1707, Dec. 1996.

[141] J. H. Wen, J. K. Lain, and Y. W. Lai, "Performance evaluation of a joint CDMA/NC-PRMA protocol for wireless multimedia communications," *IEEE J. Select. Areas Commun.*, vol. 19, no. 1, pp. 95–106, Jan. 2001.

[142] S. Nanda, D. J. Goodman, and U. Timor, "Performance of PRMA: a packet voice protocol for cellular systems," *IEEE Trans. Vehic. Technol.*, vol. 40, no. 3, pp. 584–598, Aug. 1991.

[143] P. Narasimhan and R. D. Yates, "A new protocol for the integration of voice and data over PRMA," *IEEE J. Select. Areas Commun.*, vol. 14, no. 4, pp. 623–631, May 1996.

[144] G. Bianchi, F. Borgonovo, L. Fratta, L. Musumeci, and M. Zorzi, "C-PRMA: a centralized packet reservation multiple access for local wireless communications," *IEEE Trans. Vehic. Technol.*, vol. 46, no. 2, pp. 422–436, May 1997.

[145] J. Dunlop, J. Irvine, D. Robertson, and P. Cosimini, "Performance of a statistically multiplexed access mechanism for a tdma radio interface," *IEEE Personal Commun.*, vol. 2, no. 3, pp. 56–64, June 1995.

[146] L. Lenzini, B. Meini, and E. Mingozzi, "An efficient numerical method for performance analysis of contention MAC protocols: a case study (PRMA++)," *IEEE J. Select. Areas Commun.*, vol. 16, no. 5, pp. 653–667, June 1998.

[147] V. Huang and W. Zhuang, "QoS-oriented packet scheduling for wireless multimedia CDMA communications," *IEEE Transactions on Mobile Computing*, vol. 3, no. 1, pp. 73–85, Jan.-Mar. 2004.

[148] E. Dahlman, P. Beming, J. Knutsson, F. Ovesjo, M. Persson, and C. Roobol, "WCDMA – the radio interface for future mobile multimedia communications," *IEEE Trans. Vehic. Technol.*, vol. 47, no. 4, pp. 1105–1118, Nov. 1998.

[149] M. Haardt, A. Klein, R. Koehn, S. Oestreich, M. Purat, V. Sommer, and T. Ulrich, "The TD-CDMA based UTRA TDD mode," *IEEE J. Select. Areas Commun.*, vol. 18, no. 8, pp. 1375–1385, Aug. 2000.

[150] 3GPP, "UTRA (UE) TDD: radio transmission and reception (release 1999)," Technical Report 3G TR 25.102 v 3.5.0, 3G Partnership Project, Dec. 2000.

[151] C.-L. I and R. D. Gitlin, "Multi-code cdma wireless personal communications networks," in *Proc. of the IEEE International Conference on Communications (ICC)*, June 1995, vol. 2, pp. 1060–1064.

Appendix A

Proof of Lemma 1 in Chapter 4

We now restate and prove Lemma 1.

Lemma 1. (a) If $n \leq T$,

$$P_n = \frac{T!}{T^n (T-n)!} \tag{1}$$

(b) If $0 \leq k \leq n-2$ and $k < T$,

$$P_k = \frac{1}{T^N} \times \sum_{w=k}^{\min(N,T)} \binom{N}{w} \binom{T}{w} \binom{w}{k} w! \, (-1)^{w-k} (T-w)^{N-w}. \tag{2}$$

Proof. It is clear that the total number of possible ways in which n nodes can be allocated to T slots is T^n. Result (1) follows by noting that the number of different permutations of T slots taken n at a time without repetitions is $T!/(T-n)!$.

To derive (2), we first consider the allocation of the successful nodes to slots. The number of ways B_k in which k nodes can be allocated to k different slots is

$$B_k = \binom{n}{k} \frac{T!}{(T-k)!}. \tag{3}$$

Once the successful nodes have been allocated, the remaining $n-k$ nodes must be assigned to the remaining $T-k$ slots in such a way that no slot is left with only one node. From elementary combinatorial theory, if $n-k$ objects are assigned to $T-k$ classes (slots) such that the order of objects in each class is unimportant, then the number of permutations of these objects taken all at a time is

$$(n-k)! \, \psi(\mathbf{r}), \quad \text{s.t.} \quad \sum_{i=1}^{T-k} r_i = n-k$$

where

$$\psi(\mathbf{r}) = \frac{1}{r_1!\, r_2! \ldots r_{T-k}!} \tag{4}$$

and r_j is the number of objects in the jth class, and the vector $\mathbf{r} = (r_1, \ldots, r_{T-k})$ uniquely defines the assignment. For our problem, the set S of valid assignment vectors $\mathbf{r}$ is given by

$$S = \{\mathbf{r} : r_i = 0 \text{ or } r_i \geq 2, 1 \leq i \leq T-k\,; \sum_{i=1}^{T-k} r_i = n-k\}. \tag{5}$$

Therefore, the number of ways C_{n-k} in which $n-k$ unsuccessful nodes can be allocated to $T-k$ slots is given by

$$C_{n-k} = (n-k)! \sum_{\mathbf{r}\in S} \psi(\mathbf{r}). \tag{6}$$

Furthermore, it is easy to see that

$$P_k = \frac{B_k C_{n-k}}{T^n}. \tag{7}$$

In the remaining steps, we re-express the factor $\sum_{\mathbf{r}\in S} \psi(\mathbf{r})$ that appears in (6) in a form more amenable to computation. We derive the expression by using a generating function approach. The idea is to start by considering the case where the number of nodes is unrestricted, and then later to impose the restriction $n-k$.

We consider an arbitrary slot amongst the $T-k$ slots, and define the sequence

$$a_j = \begin{cases} 1/j! & \text{if } j = 0 \text{ or } j = 2, 3, \ldots \\ 0 & \text{if } j = 1. \end{cases} \tag{8}$$

The term a_j has the following interpretation: the reciprocal of the possible permutations if j nodes have been allocated to the slot. Since we are concerned with the unsuccessful nodes, we exclude allocations of a single node to the slot.

Referring back to (4) and (5), we see that $\sum_{\mathbf{r}\in S} \psi(\mathbf{r})$ has the form of a term of the convolution of sequences of type (8), which suggests a generating function

approach. In fact, $\sum_{\mathbf{r}\in S}\psi(\mathbf{r})$ is the $(n-k)$th term of the convolution of $T-k$ sequences of type (8). The generating function of (8) is

$$A(z)=\sum_{\substack{j=0\\ j\neq 1}}^{\infty} a_j z^j = e^z - z.$$

To aggregate the $T-k$ sequences corresponding to the $T-k$ slots, we form the $(T-k)$-fold convolution. The generating function $H(z)$ of the convolution is

$$\begin{aligned} H(z) &= (e^z - z)^{T-k} \\ &= \sum_{j=0}^{T-k} \binom{T-k}{j} (-1)^{T-k-j} z^{T-k-j} e^{jz}. \end{aligned} \tag{9}$$

Also, by definition, we can express $H(z)$ in the form $H(z)=\sum_{j=0}^{\infty} h_j z^j$. Since we have the restriction $n-k$ on the total number of nodes, we are only interested in the coefficient h_{n-k} of the generating function; this coefficient is exactly equal to the factor $\sum_{\mathbf{r}\in S}\psi(\mathbf{r})$. To find h_{n-k}, we expand e^{jz} in (9) in its Taylor series to obtain

$$H(z)=\sum_{j=0}^{T-k}\binom{T-k}{j}(-1)^{T-k-j}\sum_{m=0}^{\infty}\frac{j^m}{m!}z^{m+T-k-j}. \tag{10}$$

Equating the power of z in (10) to $n-k$ yields

$$m = n - T + j \tag{11}$$

and since $m \geq 0$, we must have

$$j \geq \max(T-n, 0) \tag{12}$$

where we introduce the max function to deal with the possibility that $n > T$. From (10), (11) and (12) we obtain

$$h_{n-k}=\sum_{j=\max(T-n,0)}^{T-k}\binom{T-k}{j}(-1)^{T-k-j}\frac{j^{n-T+j}}{(n-T+j)!}. \tag{13}$$

Making the substitution $w = T - j$ in (13) yields,

$$h_{n-k} = \sum_{w=k}^{\min(n,T)} \binom{T-k}{T-w} (-1)^{w-k} \frac{(T-w)^{n-w}}{(n-w)!}. \tag{14}$$

Finally, substituting h_{n-k} for $\sum_{\mathbf{r}\in S} \psi(\mathbf{r})$ in (6), and using (7) leads, after some rearrangement, to (2). □

University Library

A gateway to Melbourne's research publications

Minerva Access is the Institutional Repository of The University of Melbourne

Author/s:
Shu, Feng

Title:
Analysis and optimization of MAC protocols for wireless networks

Date:
2007-06

Citation:
Shu, F. (2007). Analysis and optimization of MAC protocols for wireless networks. PhD thesis, Department of Electrical and Electronic Engineering, The University of Melbourne.

Publication Status:
Unpublished

Persistent Link:
http://hdl.handle.net/11343/39319

File Description:
Analysis and optimization of MAC protocols for wireless networks

Terms and Conditions:
Terms and Conditions: Copyright in works deposited in Minerva Access is retained by the copyright owner. The work may not be altered without permission from the copyright owner. Readers may only download, print and save electronic copies of whole works for their own personal non-commercial use. Any use that exceeds these limits requires permission from the copyright owner. Attribution is essential when quoting or paraphrasing from these works.